U.S. DEPARTMENT OF COMMERCE
National Technical Information Service

PB-271 979

On the Safety Provided by Alternate Seismic Design Methods

Massachusetts Inst of Tech, Cambridge Dept of Civil Eng.

Prepared for

National Science Foundation, Washington, D C

Jul 77

Massachusetts Institute of Technology
Department of Civil Engineering
Constructed Facilities Division
Cambridge, Massachusetts 02139

Evaluation of Seismic Safety of Buildings

Report No. 9

ON THE SAFETY PROVIDED BY ALTERNATE SEISMIC DESIGN METHODS

by

Dario A. Gasparini

Supervised by

Erik H. Vanmarcke
and
John M. Biggs

July 1977

Sponsored by National Science Foundation
Division of Advanced Environmental Research
and Technology
Grants ATA 74-06935 and ENV 76-19021

Publication No.R77-22 Order No. 573

ABSTRACT

A method is developed herein for obtaining distributions of responses of elastic multi-degree-of-freedom systems subject to earthquake excitation. Uncertainty in both dynamic model and earthquake excitation parameters is accounted for. Random vibration theory and an approximate first-passage problem solution are utilized. Distributions of responses are computed for two 4-DOF dynamic models. Sensitivity of such distributions to earthquake and dynamic model parameters is quantified.

Factors contributing to uncertainty in the strength measures used for rigid frame buildings are examined. A simple frame is designed by elastic criteria and a second moment description of the story strength measures is given.

Probabilities of exceeding limit-elastic response levels are computed for three models by utilizing the derived load effect and strength distributions. Probabilities conditional on peak ground accelerations are first obtained; then seismic risk information is incorporated to arrive at unconditional failure probabilities. Sensitivity of such safety estimates to seismic risk information and strength distribution parameters is examined. Comparisons with the safety assessments of other investigators are also made.

Alternate elastic seismic design strategies are reviewed and their interrelationships are clarified. The relative conservatism of resultant designs is compared by using the methodology developed in the report.

BIBLIOGRAPHIC DATA SHEET | MIT-CE-R77-22

4. Title and Subtitle

ON THE SAFETY PROVIDED BY ALTERNATE SEISMIC DESIGN METHODS
(Evaluation of Seismic Safety of Buildings)

5. Report Date: July 1977

6.

7. Author(s): Dario A. Gasparini, Supervised by Prof. J. M. Biggs and Erik H. Vanmarcke

8. Performing Organization Rept. No. R77-22; No. [illegible]

9. Performing Organization Name and Address

Massachusetts Institute of Technology
Dept. of Civil Engineering
77 Massachusetts Avenue
Cambridge, Massachusetts 02139

10. Project/Task/Work Unit No.

11. Contract/Grant No. NSF ATA 74-06935 & ENV 76-

12. Sponsoring Organization Name and Address

National Science Foundation
1800 "G" St., N.W.
Washington, D.C. [illegible]

13. Type of Report & Period Covered: Research 10/76 to pres

14.

15. Supplementary Notes

This is report No. 9 in a series begun under Grant ATA 74-06935 and continued under Grant ENV 76-19021

16. Abstracts

Utilizing random vibration theory and an approximate first passage problem solution, a method is developed for obtaining distributions of responses of elastic multi-degree-of-freedom systems to earthquake excitation. Uncertainty in both dynamic model and earthquake excitation parameters is accounted for.

Factors contributing to uncertainty in the strength measures used for rigid frame buildings are examined. A simple frame is designed by elastic criteria and a second moment description of the story strength measures is given.

Utilizing the desired load effect and strength distributions and by incorporating seismic risk information, the probability of failure is computed.

Alternate elastic seismic design strategies are reviewed and their interrelationships are clarified.

17. Key Words and Document Analysis. 17a. Descriptors

structural dynamics
elastic response
seismic design
failure probability

17b. Identifiers/Open-Ended Terms

17c. COSATI Field/Group 13 02 Civil Engineering 13 13 Structural Engineering

18. Availability Statement

Release unlimited

19. Security Class (This Report) UNCLASSIFIED

20. Security Class (This Page) UNCLASSIFIED

21. No. of Pages 216

22. Price PC A10 MF A01

FORM NTIS-35 (REV. 10-73)

THIS FORM MAY BE REPRODUCED

PREFACE

This is the ninth report prepared under the research project entitled "Evaluation of Seismic Safety of Buildings," supported by National Science Foundation Grant ATA 74-06935 and its continuation Grant ENV 76-19021. This report is derived from a thesis written by Dario A. Gasparini in partial fulfillment of the requirements for the degree of Doctor of Philosophy in the Department of Civil Engineering at the Massachusetts Institute of Technology.

The purpose of the supporting project is to evaluate the effectiveness of the total seismic design process, which consists of steps beginning with seismic risk analysis through dynamic analysis and the design of structural components. The project seeks to answer the question: "Given a set of procedures for these steps, what is the actual degree of protection against earthquake damage provided?" Alternative methods of analysis and design are being considered. Specifically, these alternatives are built around three methods of dynamic analysis: (1) time-history analysis, (2) response spectrum modal analysis, and (3) random vibration analysis.

The formal reports produced thus far are:

1. Arnold, Peter, Vanmarcke, Erik H., and Gazetas, George, "Frequency Content of Ground Motions during the 1971 San Fernando Earthquake," M.I.T. Department of Civil Engineering Research Report R76-3, Order No. 526, January 1976.

2. Gasparini, Dario, and Vanmarcke, Erik H., "Simulated Earthquake Motion Compatible with Prescribed Response Spectra," M.I.T. Department of Civil Engineering Research Report R76-4, Order No. 527, January 1976.

3. Vanmarcke, Erik H., Biggs, J.M., Frank, Robert, Gazetas, George, Arnold, Peter, Gasparini, Dario A., and Luyties, William, "Comparison of Seismic Analysis Procedures for Elastic Multi-degree Systems," M.I.T. Department of Civil Engineering Research Report R76-5, Order No. 528, January 1976.

4. Frank, Robert, Anagnostopoulos, Stavros, Biggs, J.M., and Vanmarcke, Erik H., "Variability of Inelastic Structural Response Due to Real and Artificial Ground Motions," M.I.T. Department of Civil Engineering Research Report R76-6, Order No. 529, January 1976.

5. Haviland, Richard, "A Study of the Uncertainties in the Fundamental Translational Periods and Damping Values for Real Buildings," Supervised by Professors J. M. Biggs and Erik H. Vanmarcke, M.I.T. Department of Civil Engineering Research Report R76-12, Order No. 531, February 1976.

6. Luyties, William H. III, Anagnostopoulos, Stavros, and Biggs, John M., "Studies on the Inelastic Dynamic Analysis and Design of Multi-Story Frames," M.I.T. Department of Civil Engineering Research Report R76-29, Order No. 548, July 1976.

7. Gazetas, George, "Random Vibration Analysis of Inelastic Multi-Degree-of-Freedom Systems Subjected to Earthquake Ground Motions," Supervised by Professor Erik H. Vanmarcke, M.I.T. Department of Civil Engineering Research Report R76-39, Order No. 556, August 1976.

8. Haviland, Richard W., Biggs, John M., and Anagnostopoulos, Stavros A., "Inelastic Response Spectrum Design Procedures for Steel Frames," M.I.T. Department of Civil Engineering Research Report R76-40, Order No. 557, September 1976.

The project is supervised by Professors John M. Biggs and Erik H. Vanmarcke of the Civil Engineering Department. They have been assisted by Dr. Stavros Anagnostopoulos, A Research Associate in the Department. Research assistants , in addition to Dr. Gasparini, who contributed to the work reported herein were Peter Arnold, Robert Frank, William Luyties, and Richard Haviland.

TABLE OF CONTENTS

TABLE OF CONTENTS
(continued)

TABLE OF CONTENTS
(continued)

TABLE OF CONTENTS
(continued)

LIST OF FIGURES

LIST OF FIGURES
(continued)

LIST OF FIGURES
(continued)

LIST OF FIGURES
(continued)

LIST OF TABLES

LIST OF TABLES
(continued)

LIST OF TABLES
(continued)

CHAPTER 1

INTRODUCTION AND SCOPE OF RESEARCH

1.1 OBJECTIVES

The research reported herein is based on two broad objectives. The first is the development of a methodology to compute probabilities of exceeding specified performance parameters in a structure due to seismic forces. The second is the comparison of alternate methods of seismic analysis and design by utilizing such a methodology.

This introduction seeks to outline the breadth of studies possible within such broad objectives and hence define and place in perspective the work reported in subsequent chapters.

1.2 SEISMIC SAFETY

It is clear that the term "seismic safety" may have a variety of meanings which depend on the specific critical response of interest and the performance criteria used. Further, to quantify "safety" several approaches may, in practice, be used. This section attempts to classify definitions and alternative approaches and to identify the specific ones used throughout this study.

1.2.1 Definition of Safety and Critical Response Parameter

Elastic - Inelastic

Probability of failure computations require that a distribution or moments (e.g., mean and variance) of the critical load effect(s) be obtained. For inelastic load effects (e.g., ductility levels) such statistical descriptions can presently only be arrived at through multiple time history analyses. Such analyses, however, require extensive modeling and computational efforts and are therefore impractical. More useful random vibration methodologies are only now being developed for shear-beam type dynamic models [32].

It appears that for the present, if derived load effect distributions or moments are to be used, one is limited to defining failure in terms of elastic criteria; that is, defining failure as exceeding random, limit-elastic levels of peak accelerations, displacements, shears, moments, axial forces, etc.

Individual Member - "Floor" Response

Load effects at the individual member level are generally not obtained directly from dynamic analyses which utilize lumped mass models. In a typical analysis, a lumped mass model is first formulated, the corresponding eigenvalue problem is solved, and the time history of each modal response is calculated. A static problem must then be solved for each of the modal deflected shapes to obtain normalized modal contributions to each member load effect. Only then may modal contributions be combined either exactly or in an approximate fashion (SRSS).

A state-space random vibration formulation differs from the above modal time history analysis only in that the time histories of modal RMS responses are calculated (of course the form of the input is also different.) A distribution of any response may then be obtained by an approximate first passage problem (see Chapter 2) solution, either at the member or at the floor level.

In summary, obtaining distributions of load effects for individual members generally requires detailed static models, and static analysis capabilities; i.e., capabilities equal to those of the program APPLE PIE [53]. Assuming a random vibration approach, and assuming dynamic model parameters as deterministic, a sequence of steps which may lead to distributions of <u>member</u> load effects is depicted in Figure 1.1.

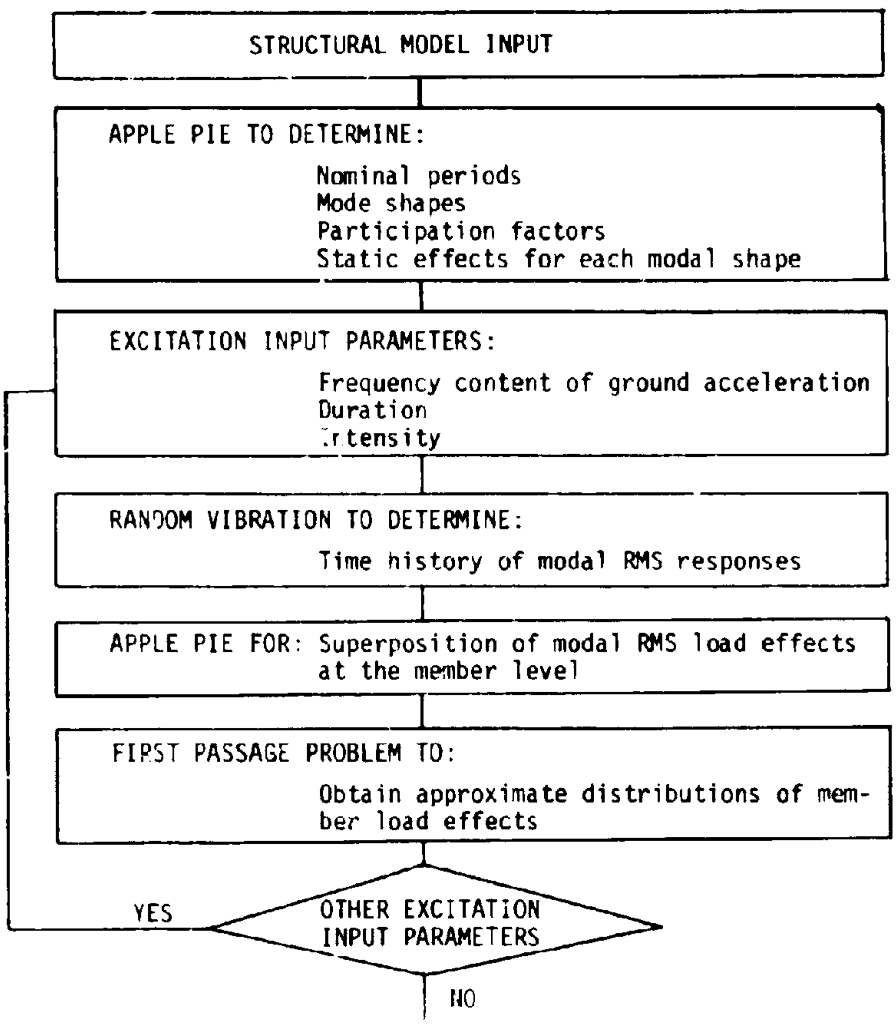

FIGURE 1.1 - METHODOLOGY FOR OBTAINING DISTRIBUTIONS OF ELASTIC LOAD EFFECTS AT THE MEMBER LEVEL

Cumulative-Non-cumulative

Tang [76] and Yao [77], among others, have noted that low cycle fatigue failures are possible during earthquakes. The implication is that very large (inelastic) strains occur during the dynamic response of structures. Typically, to assess probabilities of such failures, a random process of strain is assumed; the relationship between the earthquake load and the load effect (strain) is not explored in detail. Such cumulative failure criteria are not explicitly considered herein.

Multiple Correlated Earthquake Events

Multiple earthquakes at a site may have correlated properties (frequency content, duration, intensity, etc.); hence Shinozuka [50], for one, has stated that joint statistical distributions of such parameters are to be considered if the safety of a structure in time is to be quantified. McGuire [42] recently examined three types of correlation among earthquakes. correlation between records of motion made at the same site during different earthquakes (site effect correlation); correlation between records made at different sites during the same earthquake (source effect correlation); and correlation between the two components of motion of the same record (component correlation). His conclusions were that "successive observations of different earthquakes at the same site (for the sites used in this study) can be assumed to be uncorrelated" although source effect and component correlations were found significant.

As an approximation, then, the assumption is made herein that the parameters which define the earthquake for the random vitration analysis, i.e., frequency content, intensity and duration, are uncorrelated.

Load Combinations

It is recognized that earthquake loads occur or act simultaneously with dead, live and perhaps even wind loads. Such loads should theoretically be statistically described in space and time and combined to define both loading and resistance [33]. It is assumed herein that load effects at the "floor" level, e.g., interstory distortions, are caused solely by earthquake forces. Only to arrive at estimates of story strength measures are nominal (or deterministic) values of dead and live loads considered (see Chapter 3).

System Reliability

The thrust of the work here is not to develop system reliability formulations, but rather marginal, modal reliabilities for dynamic systems. Chapter 4 does discuss in a limited sense the question: "What is the probability that yielding will not occur anywhere in the structure?" No attempt is made there, however, to establish correlations among modal strength measures or among modal safety margins [63].

Summary

Safety is herein defined in terms of elastic, non-cumulative failure criteria at the dynamic model response level. It means not exceeding random, limit-elastic responses (r ative displacement, accelerations) at a story in the structure. Such criteria may not be meaningful for ordinary civil structures; rather it is more consistent with design and performance criteria used for nuclear power plants.

1.2.2 Alternate Formulations for Determining Reliability

Second Moment - Full Distribution

To arrive at reliability assessments, perhaps the first choice to be made is between a second moment reliability formulation and a full distribution approach. The former establishes bounds on reliability given only second moments (e.g., means and variances) of random variables: Veneziano [62] has recently summarized the theory and made contributions to it. The full distribution approach seeks to define probability distributions for both random capacity and demand measures and to calculate failure probabilities through evaluations of the convolution integral:

$$P_F = \int_0^\infty (1 - F_D(c)) f_C(c)\, dc \qquad (1.1)$$

where $F_D(c)$ = Cumulative distribution function of demand (LOAD EFFECT)

$f_C(c)$ = Probability distribution function of capacity (STRENGTH)

Statistical vs. Probabilistic Models

Statistical reliability models may generally be defined as those which include considerations of uncertainty in the distributions $f_C(c)$ and $f_D(d)$ (and their parameters) to arrive at overall reliability estimates. Conversely, probabilistic models assume the distributions and their parameters are "correct." It is intuitively apparent that the available data regarding seismic risk, for example, do not exclusively support one probabilistic model or one set of parameters. Hence statistical models for seismic risk are logical. Indeed, Veneziano [65] has recently quantified the effects of statistical uncertainty on reliability estimates.

The approach followed herein is probabilistic; however, sensitivity to alternate capacity and demand distributions may be evaluated numerically for any one structure by repeated analyses.

Studies in Seismic Safety

Shinozuka [50] (1974) in a state-of-the-art paper has stated that "much more work must be done before realistic safety assessments and assurance can be made with the aid of the stochastic approach." Indeed research in structural dynamics has focused on developing more detailed inelastic models to be used in conjunction with time history analyses in an effort to gain understanding and control of inelastic behavior [12]. In recognition of the uncertainty in earthquake excitation, generally multiple analyses are recommended. Such studies are only tangential to reliability assessments; authors more directly concerned with reliability have generally assumed various probability distributions (and their parameters) for demand and capacity and presented corresponding ranges in reliability estimates. For example, Ferry-Borges [33] assumed a type II (or a Type I) distribution for seismic demand and a normal strength distribution to arrive at failure probabilities as functions of the factor of safety γ^* (defined as the ratio between the lower 5% fractile of $f_C(c)$ and the upper 5% fractile of $f_D(d)$) and of assumed coefficients of variation.

Similarly, Newmark [44] assumed lognormally distributed demand and capacity measures, and focused on defining factors of safety (ratios of median capacities to median demands) and coefficients of variation for the distributions. Newmarks' methodology as well as those of Veneziano [65] and WASH 1400 [47] are discussed in Chapter 4.

1.2.3 Approach Followed Herein

Full distributions for both capacity and demand measures are used herein. Chapter 2 is devoted to deriving, through a random vibration methodology, the analytical distribution $f_D(d)$. Uncertainties in both the structural model and the forcing function are accounted for, although the dynamic model is assumed linear and invariant in time. The distributions derived are conditional on the intensity measure a_{max}. Chapter 3 derives second moments of the resistance measures for a specific example and presents arguments for the use of alternate probability distributions. Chapter 4 then, computes conditional failure probabilities by means of Equation (1.1) and combines such conditional probabilities with seismic risk analyses (in terms of peak ground acceleration) to arrive at overall modal reliability estimates.

1.3 METHODS OF SEISMIC DESIGN AND ANALYSIS

1.3.1 Alternate Performance Criteria

It is recognized herein that ordinary buildings are designed on the basis of much different performance criteria than, say, nuclear power plants. The performance of critical systems in nuclear power plants is deemed uncertain under gross inelastic structural behavior and hence limit-elastic performance criteria are presently used [51] even for the load effects due to the Safe Shutdown Earthquake [51]. On the other hand, performance criteria for conventional buildings, as promulgated by the UBC [69], SEAOC [54], ATC [20], or the Massachusetts Building Code, accept that inelastic behavior will occur during a major earthquake and have as their main objective prevention of collapse and major loss of life. As such, inelastic analysis and design procedures should consistently be used. Intense research efforts are currently aimed at developing such procedures [79,48,16], but none are presently in use. Rather, elastic analyses are generally used with pseudo-static earthquake loads significantly smaller than those expected to occur about once during the life of the structure.

The intention herein is not to compare analysis and design methods consistent with UBC performance criteria, but rather methods consistent with NRC-like performance criteria.

1.3.2 Alternate Analysis and Design Methods

The implication of NRC-like performance criteria is that earthquake dynamic analysis procedures, at least for the structure if not the underlying soil, are generally linearly elastic. Elastic analysis procedures may, in turn, be classified as response spectrum, time history (real or artificial motions), or random vibration methods. Chapter 5, then, classifies alternatives within the three methods, explores their interrelationships and compares their relative merits in terms of the reliability of corresponding designs.

1.3.3 Dynamic Models

Given a deterministic input, there remains uncertainty in the response of a structure because of the mathematical modeling necessary for the dynamic analysis. Generally how complex a model one chooses for analysis is determined by weighing the reduction in uncertainty with the additional analytical costs. Models may be two or three dimensional, use lumped masses or consistent mass finite elements, may or may not include the local soil, and be linear or nonlinear. Herein only linear two-dimensional lumped mass models are considered. They are widely used, and statistical data exists regarding their accuracy in modeling actual observed behavior. The two key dynamic properties of such models, natural period and damping, are considered random variables.

1.4 SUMMARY

Probability-of-failure estimates are derived herein for limit-elastic performance criteria. Chapter 2 develops a method to compute distribution of responses considering uncertainty in both the seismic input and the dynamic model. Sensitivity studies are reported regarding the effects of random parameters on such load effect distributions. Chapter 3 examines uncertainty in strength measures and partially quantifies such uncertainty for an example structure. Chapter 4 presents resultant probability of failure estimates and quantifies their sensitivity to seismic risk assumptions, strength distributions and their parameters and the assumed design damping value. Chapter 5 then evaluates alternative elastic seismic analysis procedures utilizing the capabilities developed.

CHAPTER 2

OBTAINING DISTRIBUTIONS OF ELASTIC SEISMIC LOAD EFFECTS

2.1 SOURCES OF UNCERTAINTY

Prediction of structural response requires mathematical models for both the loading (excitation) and for the structure. Such models are approximate, and hence the predicted responses are uncertain. A statistical prediction of responses is, therefore, logical. Qualitatively, one may separate the total response uncertainty: one component arising from the structural model given a deterministic excitation and the other arising from the uncertain excitation. Structural and excitation models are interrelated in the sense that a structural model may dictate the type of description given to the excitation and vice versa. Mathematical analytical methods further define the scope of information required for the two models. Alternative analysis formulations and excitation and structure models must then be examined together.

2.2 ALTERNATE FORMULATIONS FOR OBTAINING LOAD EFFECTS

As mentioned in the introduction, alternate dynamic analysis formulations can be generally classified as random vibration, time history, and response spectrum methods. No individual single analysis yields distributions of responses which account for all the apparent uncertainty in response. Multiple analyses must be performed unless some assumptions are made regarding the analytical form of the distribution of the response and its parameters.

It is evident that time history analyses require a level of information regarding future earthquake motion which we can never hope to achieve: i.e., the exact details of the ground motions. Further, multiple time history analyses (for MDOF systems) to arrive at load effect distributions are impractical (expensive). One can, alternatively, analyze a set of historical response spectra and obtain estimated probability distributions for individual response spectrum ordinates. With this in mind, McGuire [43] computed directly m and m + σ response spectrum ordinates using a seismic risk analysis methodology [24] and assumed the ordinates to be lognormally distributed. Subsequent response spectrum analyses give load effect levels and approximate associated probabilities of non-exceedance. They are only approximate because the combination of, say, two or more m + σ modal responses does not usually imply that the total response will also be m + σ. Moreover, one must then further account for uncertainty in structural model parameters and intensity measures of the motion.

Alternatively, if the earthquake is modeled as a random process described by a power spectral density function (PSDF) [1] and a duration, random vibration methods may be used to predict load effects. Such analyses yield distributions of peak responses which account for the random phasing of possible motions. Generally, in a random vibration analysis, the structural model as well as the ordinates of the PSDF and the duration are assumed deterministic. Given that all the above parameters are, in reality, non-deterministic for a site, distributions of load effects obtained through conventional random vibration methods do not represent the possible total uncertainty in behavior. Nonetheless, the latter approach is believed to be the most rational way to arrive at load effect distributions. The singular disadvantage is that it is presently applicable only to linear systems. Random vibration methods are only now being developed for inelastic, multi-degree-of-freedom (MDOF) shear-beam dynamic models [32].

Given the choice of random vibration as the analytical tool and the associated (random process) model for the earthquake, there remains to choose the type of dynamic model for the structure. It is apparent, however, that one is limited to considering linear elastic lumped mass models, since statistics assessing their reliability and accuracy in predicting important observed dynamic structural properties are available [34,22].

2.3 RANDOM VIBRATION

2.3.1 Alternate Formulations

The intent here is not to present in detail random vibration theory, but simply to place in perspective the particular random vibration formulation used and to clarify some of its major assumptions. To do this, alternative formulations and assumptions will be briefly reviewed.

The three basic approaches associated with stationary random vibration are identified as follows:

1. Classical time domain approach
2. Frequency domain approach
3. State space approach.

The time domain approach describes a random process by the mean $m(t)$ and the autocorrelation function $B(t_1,t_2)$ [1]. If these descriptors are considered invariant with respect to a shift in the time axis, the process is said to be stationary with mean m and $B(t_1,t_2) = B(t_2-t_1)$. For a one-degree-of-freedom (1-DOF) system, the time domain result relating stationary input X (earthquake random process) to stationary output Y (response random process) is [1]:

$$B_{yy}(t_2- t_1) = \iint_{-\infty}^{\infty} B_{xx}(\tau_1- \tau_2)h(t_1- \tau_1)h(t_2-\tau_2)d\tau_1 d\tau_2 \qquad (2\text{-}1)$$

where $h(t)$ = impulse response function . It can be seen that the double convolution integral required to evaluate $B_{yy}(t_2- t_1)$ makes such a formulation difficult.

Alternatively, in the frequency domain, a random process is described by the power spectral density function $G(\omega)$ (the Fourier transform of the autocorrelation function [1]). The frequency domain result analogous to that given by Equation (2-1) is:

$$G_Y(\omega) = |H^2(\omega)|\ G_X(\omega) \qquad (2\text{-}2)$$

where $H(\omega)$ is the transfer function [1] of the system. Such a formulation is simpler and hence more desirable to use than the time domain result. Non-stationarity in the processes may be modeled using the concept of time dependent spectral density function, $G(\omega,t)$ [7].

The state-space formulation [5] yields, as a direct result, the evolution of the variance of the response process (for MDOF systems the evolutionary modal variance values may be computed and combined exactly in time to obtain the total evolutionary response variance). A limitation of such a formulation is that the excitation must be an uncorrelated or white process [5]. One must therefore use "filters," for example, augment the dynamic model with a rough model for the soil underlying a structure, in order to obtain spectral density functions at the ground level which resemble those observed from real earthquakes.

2.3.2 Random Vibration Formulation Used

The random vibration methodology used herein and specifically the solution of the first passage problem are those described and developed by Vanmarcke et al. [4, 7, 61] and summarized in Reference 64. It is a frequency domain formulation. The input (ground acceleration) process is assumed to have a zero mean with a time invariant or stationary spectral density function. Non-stationarity in the response process, Y, is considered. Briefly, the time dependent $G_Y(\omega,t)$ (of a 1-DOF relative displacement response) is obtained by:

$$G_Y(\omega,t) = |H(\omega,t)|^2 G(\omega) \tag{2.3}$$

where $H(\omega,t)$ is a time dependent transfer function [4].

The distribution of the maximum responses is obtained through an approximate solution of the first passage problem [2]. The solution utilizes the first and second moments of the response spectral density function (see section 2.4.1) and an additional spectral parameter which is a measure of the bandwidth of the frequency content (see Equation (2.12). The inherent assumption of the solution is that the excitation process (earthquake) is Gaussian and stationary for an equivalent strong motion duration, S'. The non-stationarity of the response is accounted for by introducing the concept of an "equivalent stationary response" duration, which is estimated from the ratio of the response variance values at S'/2 and S' [64].

It must be noted that ground motion models which account for the time varying nature of the relative frequency content have also been proposed [38]. However, stationary models appear to be sufficiently accurate for the purpose of seismic response prediction.

Accepting the described earthquake model and analysis procedure, then, implies that the relative frequency content, i.e., $G(\omega)$, its intensity, and the strong motion duration S' are the key input parameters. Statistics of such parameters derived from historical earthquakes and the current state of earthquake prediction, indicate that these parameters are, in fact, random for any one site.

Frequency Content

The relative frequency content of earthquake motion may be described directly through random $G(\omega)$ ordinates or alternatively, through $G(\omega)$ given by an analytical expression having random coefficients. The simplest relative frequency model for $G(\omega)$ is band-limited white noise as shown in Figure 2.1, with the intensity parameter G_o and a maximum frequency component in the motion corresponding to ω_o. Computed $G(\omega)$'s for

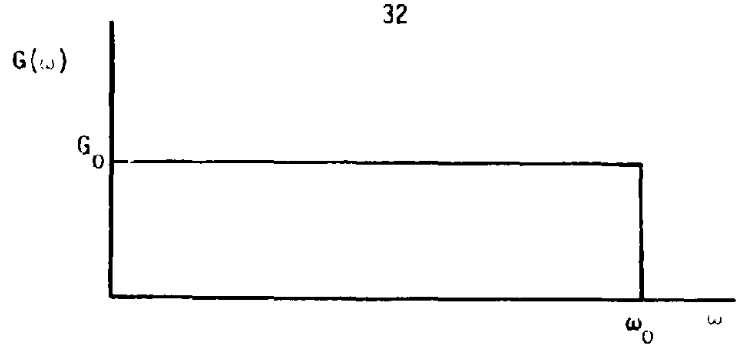

FIGURE 2.1 - BAND LIMITED WHITE NOISE

real earthquakes, however, do not support such a model. Alternately, Kanai-Tajimi (K-T) [39] proposed the following form for the spectral density function of ground acceleration during an earthquake:

$$G(\omega) = \frac{[1 + 4\zeta_g^2\ (\omega/\omega_g)^2]\ G_0}{[1 - (\omega/\omega_g)^2]^2 + 4\zeta_g^2\ (\omega/\omega_g)^2} \tag{2.4}$$

Such an expression represents, in fact, the stationary frequency content of the acceleration response of a 1-DOF oscillator (having natural frequency ω_g and viscous damping ζ_g) when excited by white noise excitation. It can be noted that the two key parameters are ω_g and ζ_g; G_0 is again a measure of intensity. Adopting such a model, then, implies that the <u>variability in relative frequency content can be described by variability in ω_g and ζ_g</u>.

The problem of defining the seismic input has now been cast into one of providing (probabilistic) information on ω_g, ζ_g, S' and G_0. It is considered in detail in the following section.

2.4 PROBABILISTIC DESCRIPTION OF EARTHQUAKE LOADING

2.4.1 Spectral Moments

To understand how earthquake realizations may be used to obtain statistics for the parameters of the random process model, some important interpretations of the moments of the spectral density function must be stated. These interpretations are summarized by Vanmarcke [74] and are only briefly reviewed herein.

Moments of any PSDF $G(\omega)$ may generally be defined as

$$\lambda_i = \int_0^\infty \omega^i G(\omega) d\omega \qquad (2\text{-}5)$$

or, alternatively, by defining the normalized power spectral density function as:

$$G^*(\omega) = \frac{G(\omega)}{\int_0^\infty G(\omega)\, d\omega} \qquad (2\text{-}6)$$

The moments become:

$$\lambda_i^* = \int_0^\infty \omega^i\, G^*(\omega)\, d\omega \qquad (2\text{-}7)$$

The integral over frequency of $G(\omega)$ equals the average total power, or the variance σ^2 for processes which fluctuate about a zero mean value, i.e.:

$$\sigma^2 = \int_0^\infty G(\omega)\, d\omega \qquad (2\text{-}8)$$

and $$\int_0^{\infty} G^*(\omega)\, d\omega = 1 = \sigma^2 \qquad (2\text{-}9)$$

A measure of where the spectral mass is concentrated along the frequency axis is given by [74]:

$$\Omega = \sqrt{\lambda_2/\lambda_0} = \sqrt{\lambda_2^*/\lambda_0^*} = \sqrt{\lambda_2^*} \qquad (2\text{-}10)$$

The time domain interpretation of the latter parameter is that, for Gaussian processes, [74]

$$\Omega = \nu_0 \, 2\pi \qquad (2\text{-}11)$$

where ν_0 is the mean rate of upcrossings of the zero level by the process.

A measure of the dispersion of the spectral density function about its center frequency is [74]:

$$q = \sqrt{1 - \lambda_1^2/\lambda_0\lambda_2} = \sqrt{1 - \lambda_1^{*2}/\lambda_2^*} \qquad (2\text{-}12)$$

2.4.2 The Parameter ζ_g

ζ_g controls the peakedness or, conversely, the dispersion of the K-T $G(\omega)$, hence it can be expected to be related to the parameter q. For real earthquakes Sixsmith and Roesset [55] present statistics for q as summarized in Table 2.1. It can be noted that q is fairly constant and approximately equal to 0.65. For simplicity, then, one may assume that, correspondingly, the variation of ζ_g is small and that its value may be

	Ω	q
Band-Limited White Noise Spectral Density	$\frac{1}{3}\,\omega_0 = 0.58$	0.5
Kanai Tajimi Spectral Density for $\omega \lesssim \omega_0 = 4\omega_g$ and $\zeta_g = 0.6$	$\sim 2.1\,\omega_g$	0.67

TABLE 2.1a - APPROXIMATE VALUES FOR PARAMETERS OF RELATIVE FREQUENCY CONTENT

	Ω (rad/sec)	q
El Centro 1940 NS	31.35	0.73
El Centro 1940 EW	25.51	0.64
Olympia N 10 W	36.07	0.65
Olympia N 80 E	30.85	0.62
Taft N 69 W	27.71	0.66
Taft S 21 W	27.46	0.64

TABLE 2.1b - SPECTRAL PARAMETERS COMPUTED FROM SQUARED FOURIER AMPLITUDES $|f(\omega)|^2$ of EARTHQUAKES (Sixsmith and Roesset, 1970)

assumed to be that which gives a $q = 0.65$ for the Kanai-Tajimi $G(\omega)$. In fact, $q_{K-T} \approx 0.67$ for $\zeta_g = 0.6$. In summary, it is assumed that ζ_g may be treated as a constant equal to 0.6.

2.4.3 The Parameter ω_g

For the K-T $G(\omega)$ the parameter Ω, as defined by Equation (2-11) is

$$\Omega = 2\pi\nu_o \approx 2.1\ \omega_g \qquad (2.13)$$

One may then, in the time domain, obtain statistics for the mean rate of upcrossings of the zero level for a set of real earthquakes, and directly interpret them as ω_g statistics for the assumed K-T $G(\omega)$. For the set of earthquakes listed in Table 2.2, Figure 2.2 shows the corresponding histogram of Ω values, the mean, $\bar{\Omega}$, and the coefficient of variation. Figure 2.3 shows the variation of the Kanai-Tajimi $G^*(\omega)$ with changing ω_g.

2.4.4 The Parameter S'

To arrive at statistics of strong motion duration S' the 39 earthquakes listed in Table 2.2 were analyzed as follows. The integral

$$\int_0^t a^2(t)\,dt \qquad (2\text{-}14)$$

a measure of the evolution of the total power of the motion, was computed and plotted for each of the motions. Figure 2.4 shows a typical resultant plot. The region of rapid, linear growth of the integral was visually chosen to be the "strong motion duration" of the earthquake.

Earthquake Number	Name	Max. Acceleration in in/sec²	No. of Points Δt = 0.02 sec.
1	N08E VERNON 33	52.930	1505
2	S82E VERNON 33	74.227	1507
3	N S EL CENTRO 34	101.400	1516
4	E W EL CENTRO 34	70.136	1252
5	N45E FERNDALE 38	62.900	998
6	S45E FERNDALE 38	36.477	998
7	N S EL CENTRO 40	112.866	1457
8	E W EL CENTRO 40	82.797	1490
9	S W STA BARBARA 41	91.250	998
10	N W STA BARBARA 41	93.566	998
11	N45E FERNDALE 41	44.158	998
12	S45E FERNDALE 41	47.212	997
13	N89W HOLLISTER 49	87.643	998
14	S01W HOLLISTER 49	50.836	998
15	S44W FERNDALE 51	47.650	998
16	N46W FERNDALE 51	45.779	999
17	S69E TAFT 52	60.602	1497
18	N21E TAFT 52	68.393	3032
19	N79E EUREKA 54	101.672	998
20	S11E EUREKA 54	68.476	998
21	N46W FERNDALE 54	76.917	994
22	S44W FERNDALE 54	62.339	999
23	N S PORTHUENEME 57	58.015	267
24	E W PORTHUENEME 57	33.551	266
25	N10E GOLDEN GATE 57	40.800	631
26	S80E GOLDEN GATE	49.641	662
27	N S NIIGATA 64	51.994	1875
28	E W NIIGATA 64	60.411	1890
29	N65E PARKFIELD-2 66	189.294	933
30	N85E PARKFIELD-5 66	166.674	916
31	N5W PARKFIELD-5 66	154.245	775
32	N50E PARKFIELD-8 66	98.546	919
33	N40W PARKFIELD-8 66	93.759	928
34	N50E PARKFIELD-12 66	22.503	698
35	N40W PARKFIELD-12 66	27.213	529
36	S25W TEMBLOR 66	154.708	503
37	N65W TEMBLOR 66	103.641	495
38	TRAN KOYNA-SAINI 67	163.500	555
39	LONG KOYNA-SAINI 67	223.546	533

TABLE 2.2 - 39 REAL EARTHQUAKE RECORDS

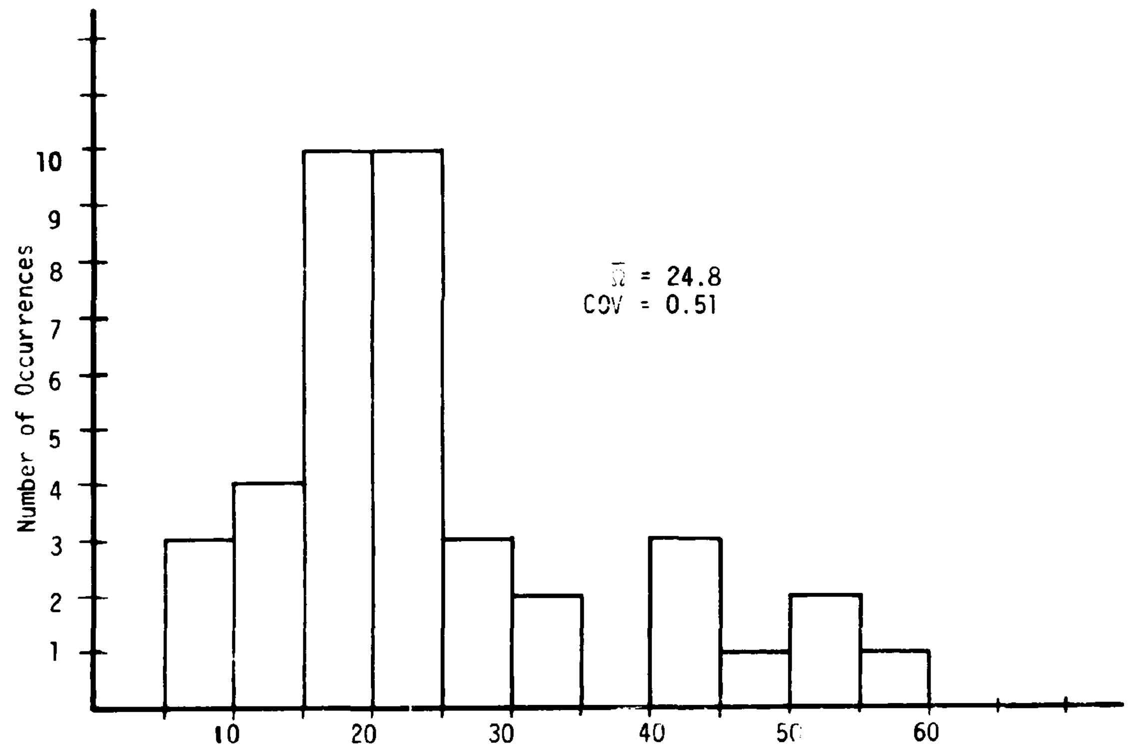

FIGURE 2.2 - HISTOGRAM OF CENTRAL FREQUENCY (Ω) VALUES FROM 39 REAL EARTHQUAKES

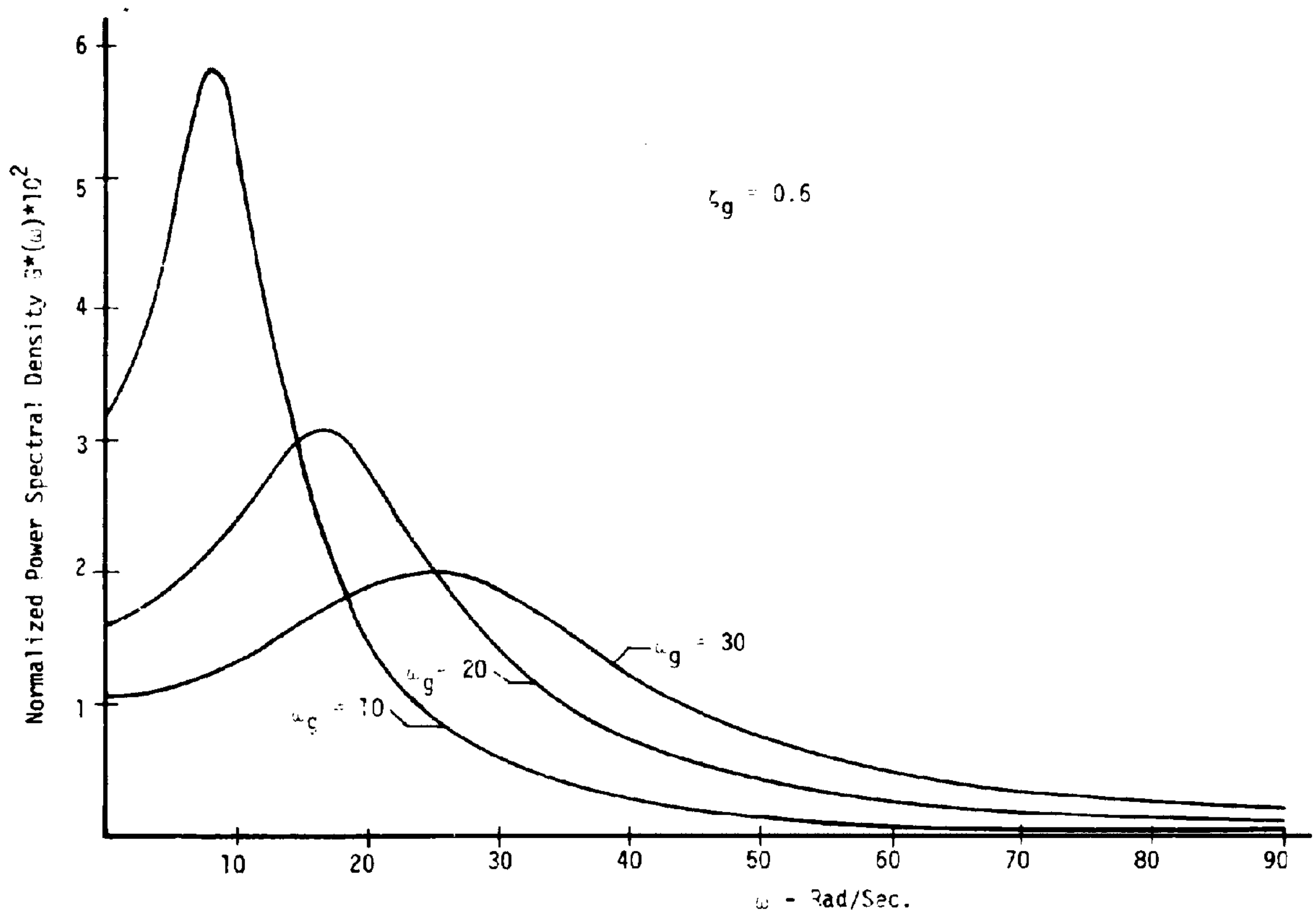

FIGURE 2.3 - KANAI-TAJIMI $S^*(\omega)$ FOR VARIOUS ω_g VALUES

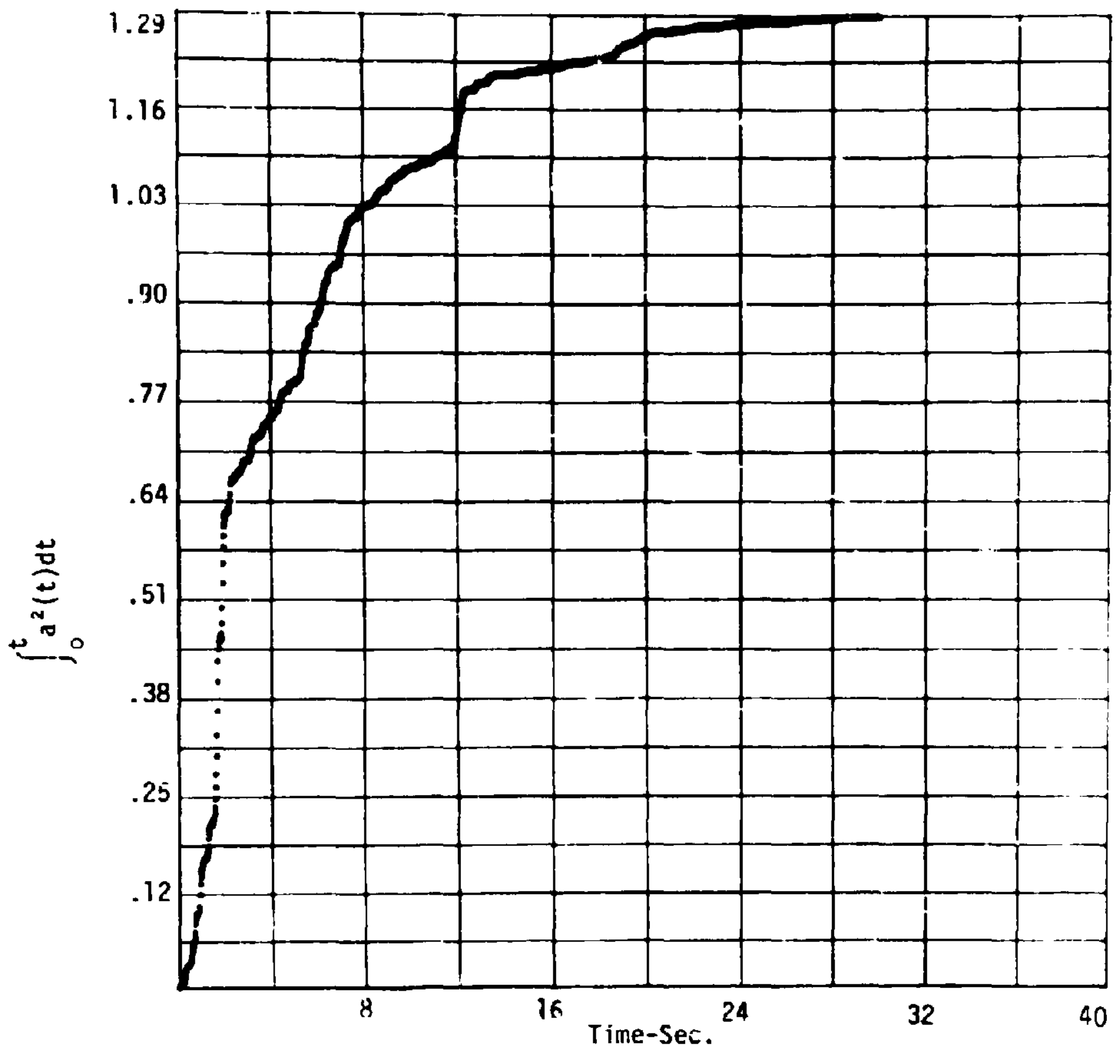

FIGURE 2.4 - EVOLUTION OF INTEGRAL $\int_0^t a^2(t)dt$ FOR A TYPICAL REAL EARTHQUAKE

Figure 2.5 shows the resultant histogram for S', with $m_{S'} = 8.0$ sec. and $V_{S'} = 0.76$.

The procedure used is essentially that of Trifunac and Brady [66] who defined the strong motion duration as the fraction of the total duration necessary for the integral to evolve from 5% to 95% of its ultimate value. With a data set of 363 horizontal components of records associated with Modified Mercalli Intensities (MMI) ranging from V to VIII, they reported $m_{S'} = 21$ sec. and $V_{S'} \simeq 0.55$. Hence their mean strong motion duration is significantly higher than that obtained herein; indeed, it is higher than the mean of the total durations ($m_S \simeq 20.8$ sec.) of the earthquakes in Table 2.2. Such differences indicate the level of statistical or "inductive" uncertainty [65] which exists with an assumed probability model and its parameters.

2.4.5 Model Uncertainty and Correlations Among Parameters

The above assumptions that ζ_g is deterministic and that ω_g and S' may be described by distributions estimated from the statistics of an arbitrary set of earthquakes, provide sufficient information to model the character of the seismic input and arrive at distributions of responses conditional on actual intensity of the motion. Three general immediate questions arise. What is the statistical uncertainty in both the probability distribution models and their parameters for a given site? Are ω_g and S' correlated, thus requiring estimates of their joint probability distribution? Are ω_g and S' correlated to the intensity of the motion?

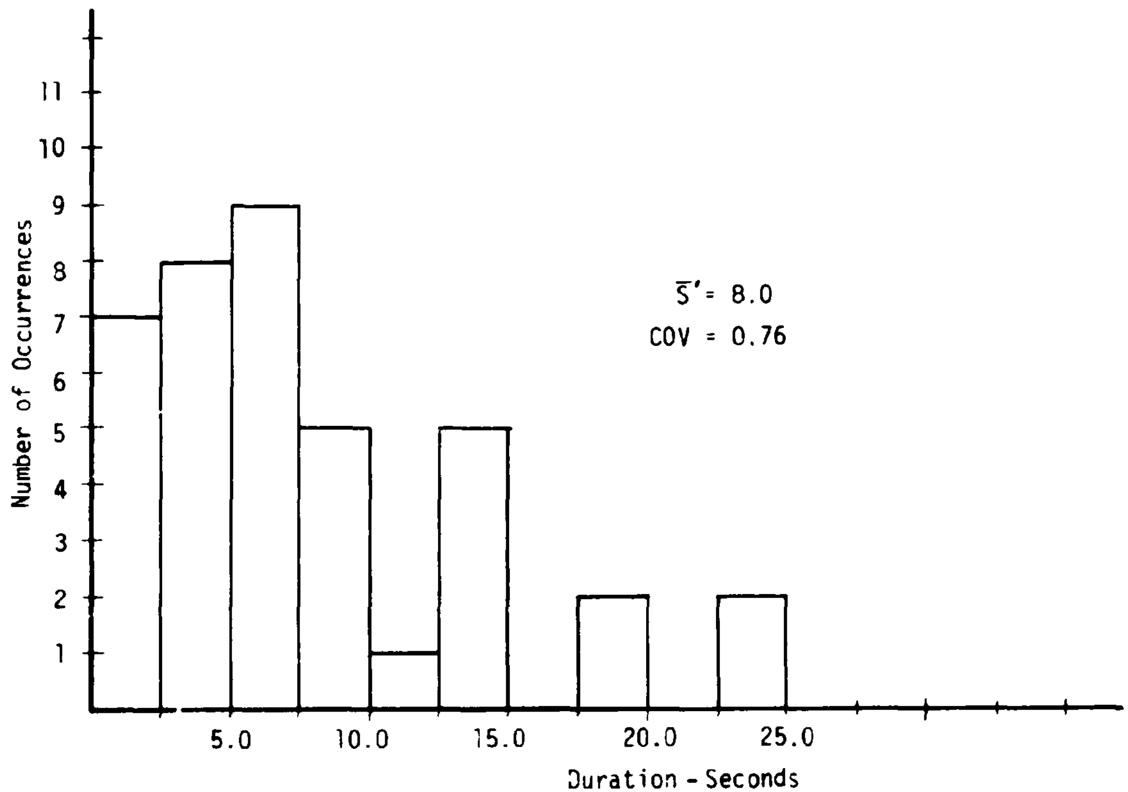

FIGURE 2.5 - HISTOGRAM OF STRONG MOTION DURATION BASED ON 39 REAL EARTHQUAKES

Regarding the first question, and the customary assumption of neglecting uncertainties in both the model and in the parameters as secon -order variations, Veneziano [65] has stated:

> "The arbitrariness of this assumption discredits the claim that a probabilistic approach to safety is more rational than a non-probabilistic approach."

Indeed the arbitrary set of earthquakes of Table 2.2 was chosen for a site where no information exists to definitely exclude any type of motion. For any one site, available geophysical information and predictions could be examined by experts or groups of experts to select an "appropriate" subset of realizable earthquakes chosen from a large population of recorded earthquakes. Bayesian techniques [15] may subsequently be used to obtain a better distribution model and its parameters.

Even with such a procedure, significant statistical uncertainty is likely. Veneziano [65] has developed theoretical methods to quantify the effects of such uncertainty on seismic risk predictions and probability of failure assessments. Herein, numerical studies are performed to show the sensitivity of load effect distributions and failure probabilities to alternate assumptions regarding the distribution models and their parameters.

Regarding the second question, the dependence of S' on intensity, site classification, magnitude, and epicentral distance has most recently been examined by Trifunac and Brady [66]. Their findings, based on a set of 106 Western earthquakes, may be summarized as follows. Mean durations decrease with increasing MMI. Mean durations of strong ground motion are about twice as long on "soft" alluvium as on "hard" base rock.

No "simple and obvious" trend with distance or magnitude is apparent to the authors, although they nonetheless stipulate a linear predictive equation, perform a regression analysis, and state:

> "For each magnitude unit the (acceleration) duration increases by 2 (sec).... while for every 10 km. of distance it increases by about 1 to 1.5 sec."

The intensity of large magnitude earthquakes, however, decays more rapidly with distance [14]. This phenomenon is related to the inelastic behavior of rock and soil at high strain levels [14].

The dependence of Ω on the above parameters has not been quantified. Qualitatively, it is known [66] that high frequency components decay most rapidly with epicentral distance, therefore Ω may be expected to decrease with distance. Also, it has been observed [14] that spectral composition shifts to the long period end of the spectrum with increase in magnitude.

Such trends may imply some degree of correlation between Ω and S', but certainly do not definitely exclude the assumption of independence. For the specific 39 earthquakes considered herein, the scattergram of Figure 2.6 also indicates no clear correlation.

Similarly, a correlation of either Ω or S' with the intensity measure a_{max} has not been established. Figure 2.7a,b, scattergrams of Ω vs. a_{max} and S' vs. a_{max} for the 39 earthquakes, show no clear trend. It must be noted that stationary random vibration theory and first passage problem solutions do, in fact, predict dependence of a_{max} (assuming that it is a peak statistic of a stationary random process) on the square root of the logarithm of the product $\Omega S'$ (see Equation 2.16). Such

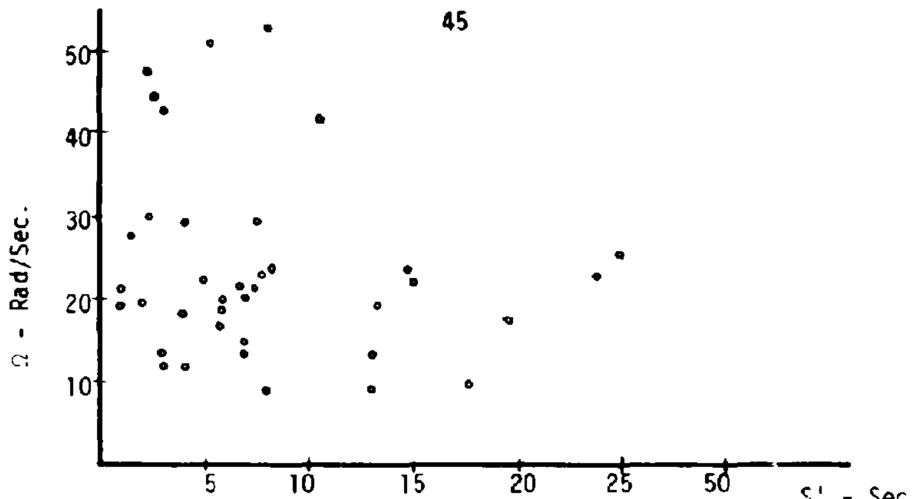

FIGURE 2.6 - SCATTERGRAM OF Ω vs. S'

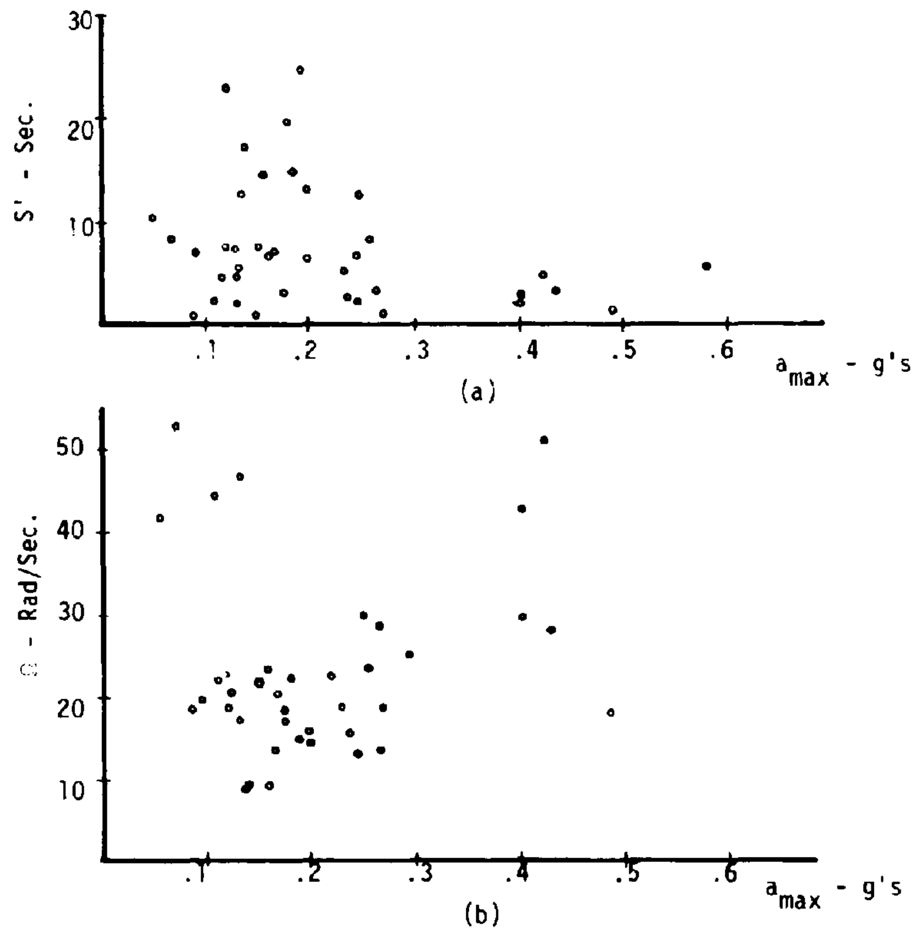

FIGURE 2.7 - SCATTERGRAMS OF Ω and S' vs. INTENSITY a_{max}.

predicted a_{max} values, however, grossly underestimate a_{max} observed in earthquakes having corresponding Ω and S' values.

In summary, the simplest assumptions can initially be made, i.e., no correlation between Ω and S' and no intensity dependence of their distribution.

2.4.6 Intensity Parameter

Having defined the relative frequency content and duration of the random process model of the earthquake, there remains to quantify its intensity. It is clear that geophysical models which directly predict Fourier amplitude spectra or $G(\omega)$ ordinates for a strong motion earthquake at a site are ideally suited to be used in conjunction with random vibration analysis. Indeed, much research has focused on this problem [8,21,52]. Berrill, for one, has recently formulated such a model using the 1971 San Fernando earthquake as his data base. The method uses a simple two-parameter source model to estimate the source excitation strength in terms of Fourier amplitudes and then uses an amplitude decay expression and scatter statistics to obtain Fourier amplitudes of ground acceleration at a site. For the San Fernando earthquake, agreement was found between model prediction and independent observations of $|f(\omega)|$ to within a factor of two or three [8]. Ordinarily, however, site ground motion is not predicted in terms of either $G(\omega)$ ordinates or $|f(\omega)|$ spectra.

Another intensity parameter which may be directly related to $G(\omega)$ ordinates is the variance or mean square value of ground acceleration, since:

$$\int_0^\infty G_a(\omega)\, d\omega = \sigma_a^2 \tag{2.15}$$

Again, seismic risk analyses are not customarily performed for such an intensity parameter. Trifunac and Brady [66], however, have begun to consider correlations between such a parameter and Modified Mercalli Intensity, Richter Magnitude and source distance.

The most commonly used intensity parameter is peak ground acceleration a_{max}. The merits of such an intensity parameter for describing system performance have been considered before and will not be discussed herein. From a random process viewpoint, prediction of such a quantity is indeed difficult. It requires consideration of the first passage problem [2,60]. Existing solutions for the problem generally assume (or are applicable for) Gaussian, stationary and white processes. The latter two assumptions are clearly not applicable to the earthquake case, and hence a suitable solution relating a_{max} and, for example, σ_a does not exist. If one applies the solution which is used to predict peak values of structural response (as used herein and given in [64]) the predicted median peak acceleration is expressed as:

$$\hat{a}_{max} = \sigma_a \sqrt{2 \, \ln \left(\frac{\Omega S' \cdot 2.8}{2\pi}\right)} \tag{2.16}$$

Such a relationship, however, if used to arrive at σ_a and $G(\omega)$ ordinates from $\hat{a}_{max}$, overestimates intensities significantly: i.e., the resultant distributions of load effects from random vibration analyses have significantly higher means than those obtained through multiple time history analyses utilizing real earthquakes normalized to the same peak acceleration.

There remains then to assume a probabilistic model (based on observed statistics) for the relationship between a_{max} and σ_a. What has been done is as follows. A time domain estimate for the variance of the motion was calculated by:

$$\sigma_a^2 = \frac{1}{S'} \int_{\tau_1}^{\tau_2} a^2(t)dt \qquad (2.17)$$

for the set of earthquakes given in Table 2.2. τ_1 and τ_2 define the start and end of the strong motion duration S'. The (39) a_{max}/σ_a ratios were subsequently computed and Figure 2.8 shows the corresponding histogram.

The ratio has, in fact, much larger values than those predicted by random vibration. The implication is that for real earthquakes, the peak ground acceleration is a result of transient bursts of high ground intensity. The histogram of Figure 2.8 is subsequently used to estimate probabilistically the motion intensity parameter σ_a (and hence ordinates of $G(\omega)$) given a peak ground acceleration. This format then allows conventional seismic risk information on acceleration to be used to define the "total" earthquake threat at the site. A more detailed explanation of the entire procedure will be given in Chapter 4.

The previous section presented a method to arrive at a probabilistic description of the seismic loading. As described in the introduction, the other main source of uncertainty which affects the likely load effect distribution is the modeling of the structure. The following sections summarize alternatives available to account for such uncertainty and describe the actual methodology used.

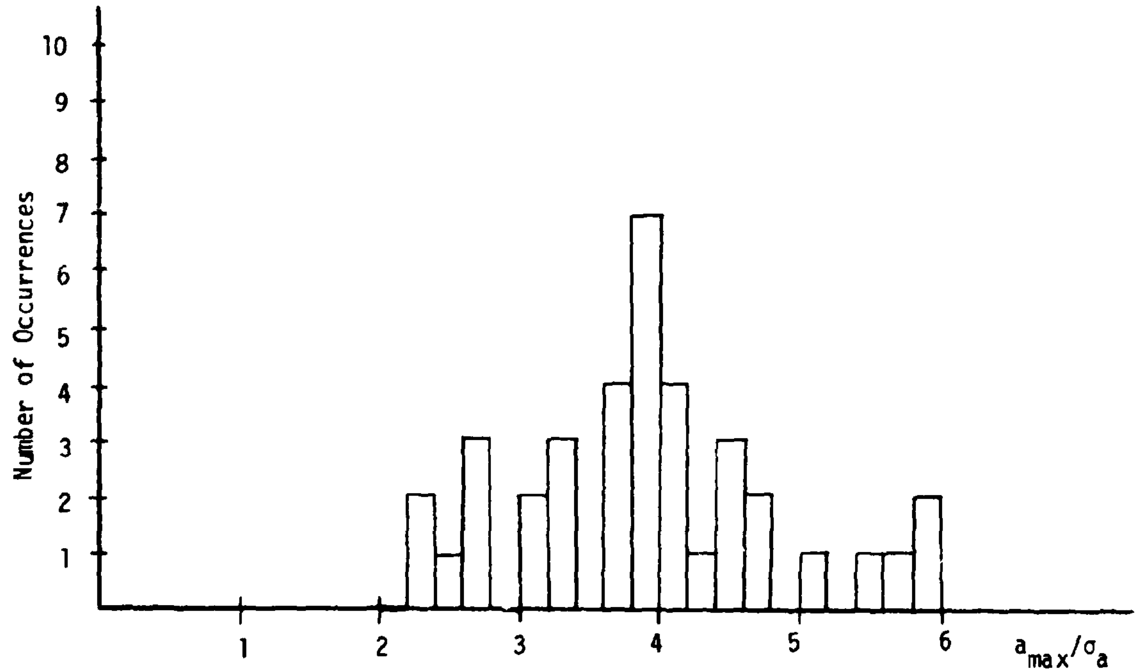

FIGURE 2.8 - HISTOGRAM OF $a_{max.}/\sigma_a$ VALUES BASED on 39 REAL EARTHQUAKES

2.5 PROBABILISTIC MODEL OF STRUCTURE

The introduction summarized the type of models which are generally used for dynamic analyses of structures. It is noted there that by far the most common are elastic lumped mass models and that a data base exists for evaluating their reliability. The focus will then be on them. In essence such models are mathematically described (for input to random vibration analysis) by natural periods T_i, modal damping values ζ_i, modal shapes and modal participation factors Γ_i. The use of empirical formulae to determine T_i and assumed mode shapes is excluded; therefore we are concerned with model parameters derived from an eigenvalue problem solution. The above parameters, T_i, ζ_i, and Γ_i, are all random, given the uncertainty in the factors which determine their value, i.e., mass, stiffness, energy absorption characteristics, etc. The most important parameters which influence structural response are, in fact, T_i and ζ_i; therefore an initial assumption will be made herein that treating only the latter two probabilistically will adequately represent the uncertainty arising from the structural model. For T_i (as well as for mode shapes and participation factors), it appears that a logical way to quantify uncertainty is to utilize a random eigenvalue solution [35]; i.e., input second moment (m, σ^2) statistics for the stiffnesses and masses and compute second moments of the properties of the dynamic model. The drawback of the methodology is the amount of data which is required for the analysis (also it gives no information on ζ_i).

Alternately, statistics assessing the reliability and accuracy of deterministic eigenvalue solutions and ζ_i assumptions may be used. Extensive data evaluation and analysis by Haviland [34] was, in fact, performed for providing such statistics. His work and its limitations are summarized next for both T_i and ζ_i.

2.5.1 The Parameter T_i

First, it must be noted that a sufficient data set of period observations exists only for the fundamental period of structures. Therefore, the necessary assumption is made that all other modal periods have the same uncertainty and are perfectly (statistically) dependent on the fundamental mode period. Secondly, most period observations are for structures designed by UBC-like design criteria, which allow inelastic action during a large earthquake. Our design failure criteria, as discussed in Chapter 3, resemble those of the NRC; hence an additional assumption must be made that the statistics are equally applicable to both design criteria or philosophies.

Within the above restrictions, Haviland [34] considered several important points regarding period determination. He quantified the motion-intensity dependence of periods as well as the permanent variation of period in the pre- , during- and post-earthquake stages of a structure's life. Clearly such effects may be mostly explained by inelastic behavior of the structure and hence, given our severe limitation of considering elastic behavior only, they will not be considered herein. Of primary interest for our purposes are histograms of $T_{OBSERVED}/T_{COMPUTED}$ (T_O/T_C), where T_C is obtained using an eigenvalue solution. Figure 2.9 is such a histogram derived by Haviland [34] for small amplitude (nuclear blasts, eccentric mass excitation, man-induced, wind-induced or ambient vibration) motion.

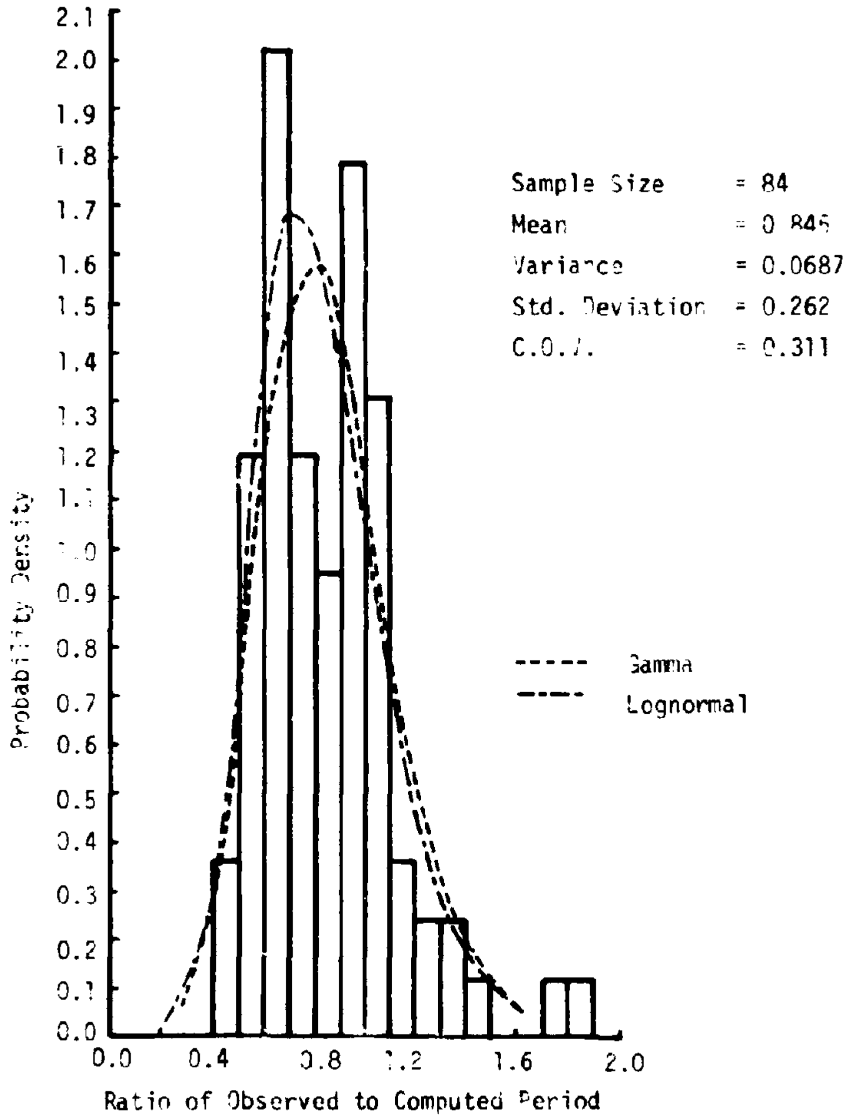

FIGURE 2.9 - HISTOGRAM OF RATIOS OF OBSERVED TO COMPUTED PERIOD DETERMINATIONS FOR SMALL AMPLITUDE VIBRATIONS OF ALL BUILDING TYPES

(From Haviland [34])

Statistics for this ratio for small amplitude motion, large amplitude motion and for the combined data set are given in Table 2.3a,b.

Histograms similar to Figure 2.9 give a direct estimate of the reliability of the eigenvalue prediction. Both the histogram and the deterministic eigenvalue solution may then be used to quantify the uncertainty in the period of the structure. A cautionary note is [34] that models included in the data set may have been biased in the sense that the likely objective was to model the inelastic behavior of the building during an earthquake.

2.5.2 The Parameter ζ_i

No accepted analytical method exists to predict (deterministically or stochastically) the modal damping values for a structure. Hence use of the statistics of observed values of ζ_i as presented by Haviland [34] is the only option available. Similar restrictions as those discussed for period observations are applicable here for the data set of ζ_i values.

Table 2.4, taken from Haviland [34], is a valuable summary of the statistics of histograms of observed ζ_i values for several categories of motion and structural material type. Figure 2.10 is the histogram of values which is most pertinent under the assumption of elastic behavior.

2.5.3 Correlations among Parameters and Model Uncertainty

The three questions raised regarding the ground motion parameters (see section 2.4.5) must also be raised for the parameters T_i and ζ_i. What is the statistical uncertainty in both the distribution models and

STRUCTURAL TYPE	AMPLITUDE														
	SMALL					LARGE					ALL				
	n	$\bar{x}$	s^2	s	c.o.v.	n	$\bar{x}$	s	s	c.o.v.	n	$\bar{x}$	s^2	s	c.o.v.
ALL	84	0.845	0.0687	0.262	0.311	22	1.150	0.119	0.344	0.300	106	0.908	0.0935	0.306	0.336

TABLE 2.3a - SUMMARY OF STATISTICS FOR HISTOGRAMS OF RATIOS OF OBSERVED TO COMPUTED PERIOD DETERMINATIONS

STRUCTURAL TYPE	AMPLITUDE											
	SMALL				LARGE				ALL			
	α	β	m_x	σ_x	α	β	m_x	σ_x	α	β	m_x	σ_x
ALL	9.43	.081	-0.215	.304	10.18	0.103	.0966	.294	7.80	0.103	-.150	.327

TABLE 2.3b - SUMMARY OF PARAMETERS FOR GAMMA AND LOGNORMAL DISTRIBUTIONS [34]

	AMPLITUDE														
	SMALL					LARGE					ALL				
STRUCTURAL TYPE	n	$\bar{x}$	s^2	s	c.o.v.	n	$\bar{x}$	s^2	s	c.o.v.	n	$\bar{x}$	s^2	s	c.o.v.
REINFORCED CONCRETE	104	4.26	10.49	3.23	0.76	17	6.63	17.99	4.24	0.64	121	4.60	12.06	3.47	0.76
STEEL	41	1.68	1.18	1.08	0.65	12	5.65	6.47	2.54	0.45	53	2.58	5.09	2.26	0.87
COMPOSITE CONSTRUC-TION	47	2.72	1.31	1.14	0.42	23	3.23	3.08	1.76	0.54	70	2.89	1.91	1.38	0.48
ALL	192	3.33	7.36	2.71	0.81	52	4.91	10.71	3.27	0.67	244	3.67	8.45	2.91	0.79

TABLE 2.4 - SUMMARY OF STATISTICS FOR HISTOGRAMS OF DAMPING DETERMINATIONS [34]

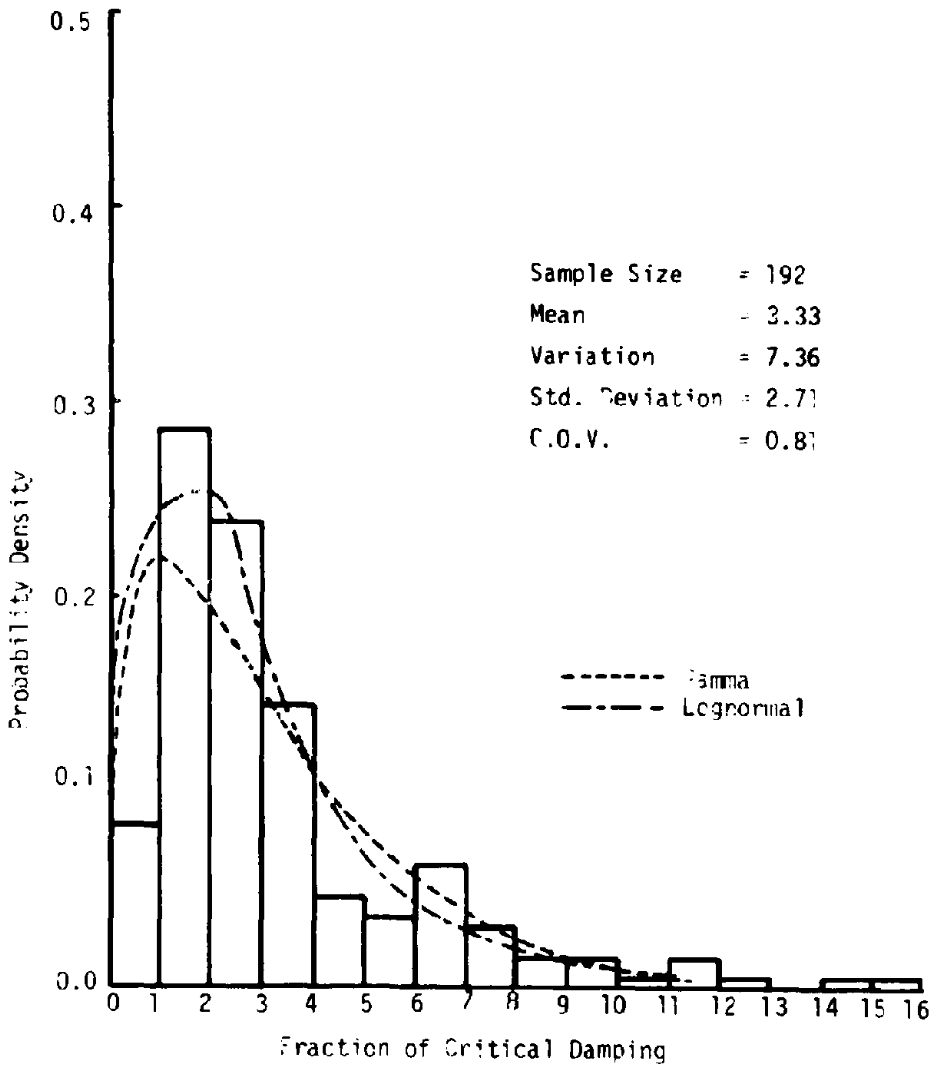

FIGURE 2.10 - HISTOGRAM OF DAMPING DETERMINATIONS FOR SMALL AMPLITUDE VIBRATIONS OF REINFORCED CONCRETE, STEEL, AND COMPOSITE BUILDINGS

(From Haviland [34])

their parameters? Are T_i and ζ_i correlated, given a_{max}? Are T_i and ζ_i correlated with the intensity of the motion?

Again, (as for ω_g and S') uncertainty in the ζ_i and T_0/T_c probabilistic models and their parameters will be examined numerically herein. That is, computed load effect distributions will be obtained for different probabilistic models and variations in their moments will be noted.

Haviland [34] addressed the questions of correlation between T_i and ζ_i. In fact, after plotting several scattergrams of T_i vs. ζ_i, no evident correlation trend was found. There was, however, the singular tendency of very tall steel buildings to be associated with small damping values. Herein the assumption of independence is initially made.

As noted previously, periods generally lengthen with increasing intensity, and damping values become larger. The former fact will be assumed to be mostly a result of inelastic action, and hence assumed negligible in the linear elastic range. The latter trend, however, is recognized to occur even <u>within</u> the linear range. Notably, the NRC Regulatory Guide 1.61 allows for two different assumptions of damping values depending on whether the structure is performing "below 1/2 yield" or "at or near yield." Obtaining one conditional (on intensity) load effect distribution and then scaling it by an entire range of intensities (predicted, say, by seismic risk analyses on acceleration) ignores such dependence. Using the "small amplitude" ζ_i distribution to predict load effects due to earthquakes close to the design earthquake likely introduces significant conservatism. Again, the <u>relative</u> importance of this effect (basically a shift in the mean value of ζ_i) may and will be studied numerically by sensitivity analyses using the overall methodology developed herein.

Summary

The probabilistic model of the earthquake excitation has two random parameters ω_g and S' and an intensity derived from a seismic risk analysis on acceleration. The probabilistic model of the structure treats T_i and ζ_i (and similarly all other periods and damping values)as random. The assumption of independence among the parameters and independence of each of the parameters from intensity (in the linear elastic range) is initially made.

2.6 PROGRAMMED PROCEDURES

The basic steps implemented in a computer program to compute load effect distributions are as follows:

1) Read appropriate data.
2) Perform multiple random vibration analyses using normalized (σ_a=1.0) K-T G(ω) for all discrete combinations of parameters ω_g, S', T_o/T_c, ζ.
3) Derive response distributions unconditional on parameters ω_g, S', T_o/T_c, ζ, but conditional on σ_a = 1.0.
4) Derive response distributions conditional on a_{max} by incorporating probabilistic a_{max} to σ_a relationship.

A brief explanation of each step follows.

2.6.1 Data

For purposes of arriving at conditional (on a_{max}) load effect distributions, the data required may be grouped as follows.

Seismic Loading - Probabilistic descriptions of ω_g, S' and a_{max}/σ_a must be given. Second moments may be given and the probability model specified (normal, lognormal) together with the desired discrete values of the parameter. The model is then discretized and appropriate probabilities are assigned at each of the desired values. Alternatively, discrete probability mass functions may be read in directly.

Dynamic Model - Deterministic values of periods, participation factors, and mode shapes of the structural model must first be specified. Probabilistic models for ζ and T_o/T_c are then specified as for ω_g and S'.

2.6.2 Multiple Random Vibration Analyses

As stated previously, the programmed analysis procedures are for the random vibration formulation described and developed by Vanmarcke [64]. The specific routines were initially implemented by Arnold [28], although important modifications have been implemented. It is to be noted that a random vibration analysis is done for each discrete combination of parameters ω_g, S', T_o/T_c and ζ_i. Having made the assumption of independence, the probability of each parameter combination is given by:

$$P[c] = P[\omega_{gi} \cap S_j' \cap (T_o/T_c)_k \cap \zeta_\ell]$$

$$P[c] = P[\omega_{g,i}]\, P[S_j']\, P[(T_o/T_c)_k] P[\zeta_\ell] \qquad (2\text{-}18)$$

The number of combinations is the product of the number of values in each of the discretized parameter distributions, i.e.,

NUMBER OF COMBINATIONS = NZETA * NS * NWG * NTOTC

Each of the analyses is performed utilizing a normalized (i.e., having a unit variance) K-T spectral density function. A set of cumulative distributions for a desired load effect (acceleration, relative displacement or interstory distortion) results for each point of interest in the model. Each distribution is defined by a set of previously specified probabilities of non-exceedance. Figure 2.11 represents the resultant output.

2.6.3 Remove Conditionality on Parameters

To remove the conditionality on a parameter combination, it is necessary to define a new range of response values. What has been done is as follows. The weighted (by the probability of occurrence of that parameter combination) median and extreme values of the set of distributions are computed. Intermediate values are then chosen (the vector of values and their corresponding probabilities of non-exceedance are augmented to better define the cumulative distribution) and their corresponding probabilities of non-exceedance are calculated. That is, computations of the form given by Equation 2.20 are carried out. Y_{NO} represents, in general, a normalized response value.

$$P[Y_N \leq Y_{NO}] = \sum_{All\ 'c'} P[Y_N \leq Y_{NO}\ |c]\ P\ [c] \qquad (2.20)$$

The resultant distribution for each point of interest remains conditional on an excitation random process having a unit variance.

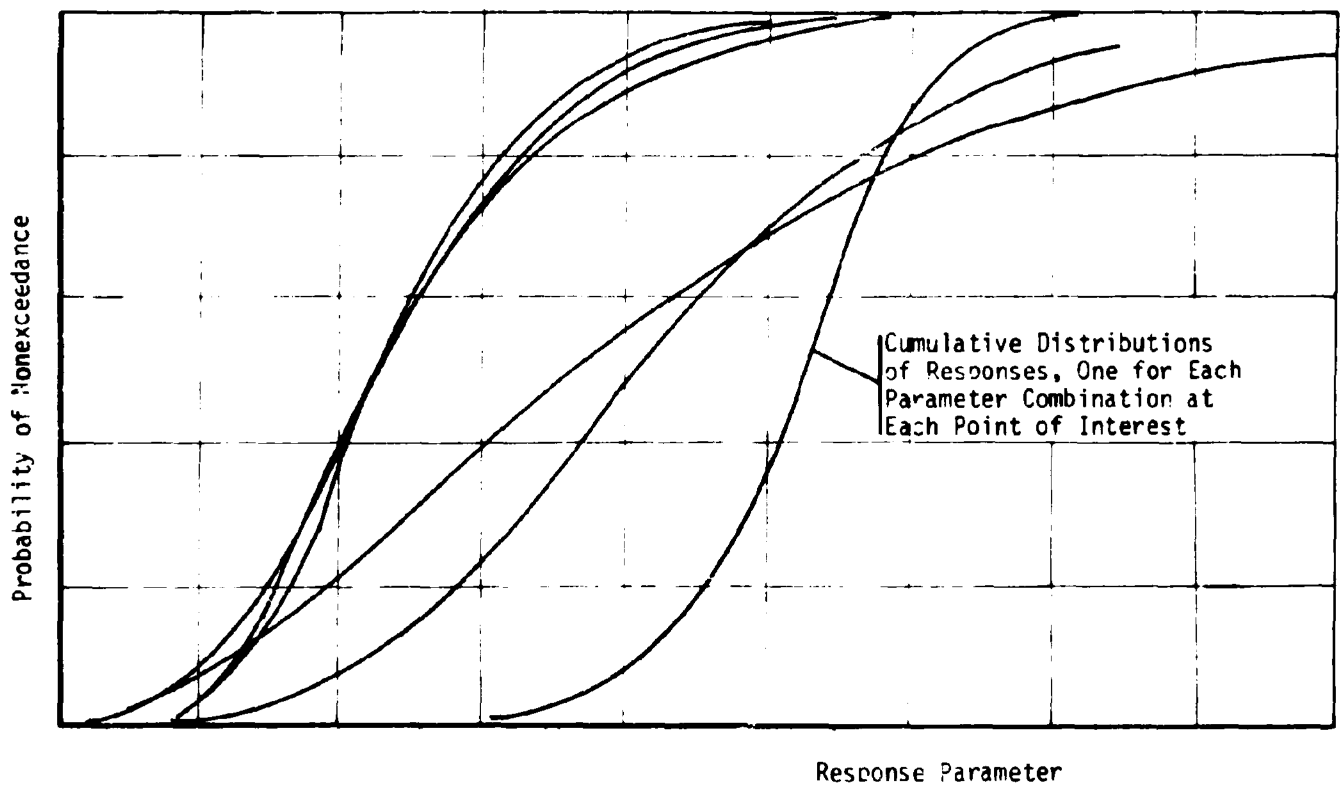

FIGURE 2.11 - TYPICAL OUTPUT FROM A SET OF RANDOM VIBRATION ANALYSES USING ALTERNATE EARTHQUAKE AND DYNAMIC MODEL PARAMETERS

2.6.4 Change Conditionality on Unit Variance to Conditionality on a_{max}

Having an array of Y_{NO} values and their associated probabilities, a new response array conditional on another value of σ_a is:

$$Y_o = Y_{NO} * \sigma_a \tag{2.21}$$

defining

$$r' = a_{max}/\sigma_a \tag{2.22}$$

then

$$P[Y \leq Y_o|\sigma_a] = P[Y \leq Y_o|a_{max}, r'] \tag{2.23}$$

and

$$P[Y \leq Y_o|a_{max}] = \sum_{All\ r'} P[Y \leq Y_o|a_{max}, r'] \; P\,[r'] \tag{2.24}$$

A procedure similar to that described in section 2.6.3 is, therefore, followed. Given an a_{max}, a set of distributions of Y_o results for all values of r', since each a_{max}/r' defines a σ_a. A new array of response values must then be defined as in section 2.6.3 and, using Equation (2.24), corresponding probabilities of non-exceedance computed.

The expression (2.24) above then yields the desired distributions of responses which can, in turn, be combined with seismic risk analyses to obtain overall response distributions. The latter may be used (in conjunction with strength distributions) in a reliability analysis to obtain estimates of probability of failure. Chapter 4 will directly concern itself with such evaluations. At the present, effects of uncertainty in the ω_g, S', ζ, T_o/T_c models and their parameters on the conditional load effect distributions may be evaluated. First, however, it is important to relate distributions obtained by the methodology described to those obtained through multiple, conventional time history analyses.

2.7 COMPUTED LOAD EFFECT DISTRIBUTIONS

For purposes of comparison, the models described in Table 2.5 will be used. They are the same as those used in Reference [72], and they have been chosen because multiple time history analyses with the set of earthquakes shown in Table 2.2 were performed for those structures. All the earthquakes were normalized to a peak ground acceleration equal to 0.3g, and deterministic models were used with modal damping $\zeta_i = 0.02$ in all the modes. For comparison purposes, then, the random vibration analysis described herein was used with the ω_g and S' distribution moments derived from the 39 earthquakes, and shown in Table 2.6. Both parameters were assumed to be lognormally distributed. For purposes of analysis, the distributions were subsequently discretized.

	$\omega_g - \frac{1}{\text{sec}}$	S' - Sec.
m	12.	8.
COV	0.5	0.75

TABLE 2.6 - MOMENTS OF ω_g AND S' DISTRIBUTIONS

The parameters T_o/T_c and ζ were considered deterministic and equal to, respectively, 1.0 and 0.02. Figures 2.12 through 2.19 compare distributions of the first and fourth floor interstory distortion and acceleration responses obtained by the two methods for the two structures. Further, Table 2.7 summarizes the moments of the resultant distributions. The table typifies the accuracy of the proposed methodology. Mean values match most closely. Agreement in the mean may be expected to be better for shorter period structures whose responses for a given excitation dura-

STRUCTURE	MODE	PERIOD	FREQUENCY rad/sec.	PARTICIPATION FACTOR Γ	NORMALIZED MODAL SHAPES Floor 1	Floor 2	Floor 3	Floor 4
1	1	0.3773	16.64	1.3365	0.3219	0.6058	0.8165	0.9288
	2	0.1311	47.94	-0.4087	-0.8159	-0.8171	-0.0008	0.8164
	3	0.0855	73.49	-0.1982	-0.9288	0.3213	0.8168	-0.6057
	4	0.0697	90.19	0.0860	0.6067	-0.9285	0.8161	0.3222
2	1	1.1310	5.565					
	2	0.3298	15.996					
	3	0.2564	24.510					
	4	0.2090	30.067					

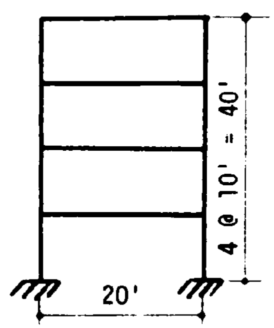

Mass Floor = 0.5 $k\text{-}sec^2/ft$

I_{girder} = 11.5 ft (∞)

A_{column} = 10.0 ft (∞)

I_{column}

Structure 1 = 0.0115 ft^4

Structure 2 = 0.001277 ft^4

TABLE 2.5 - PROPERTIES OF MODEL STRUCTURES

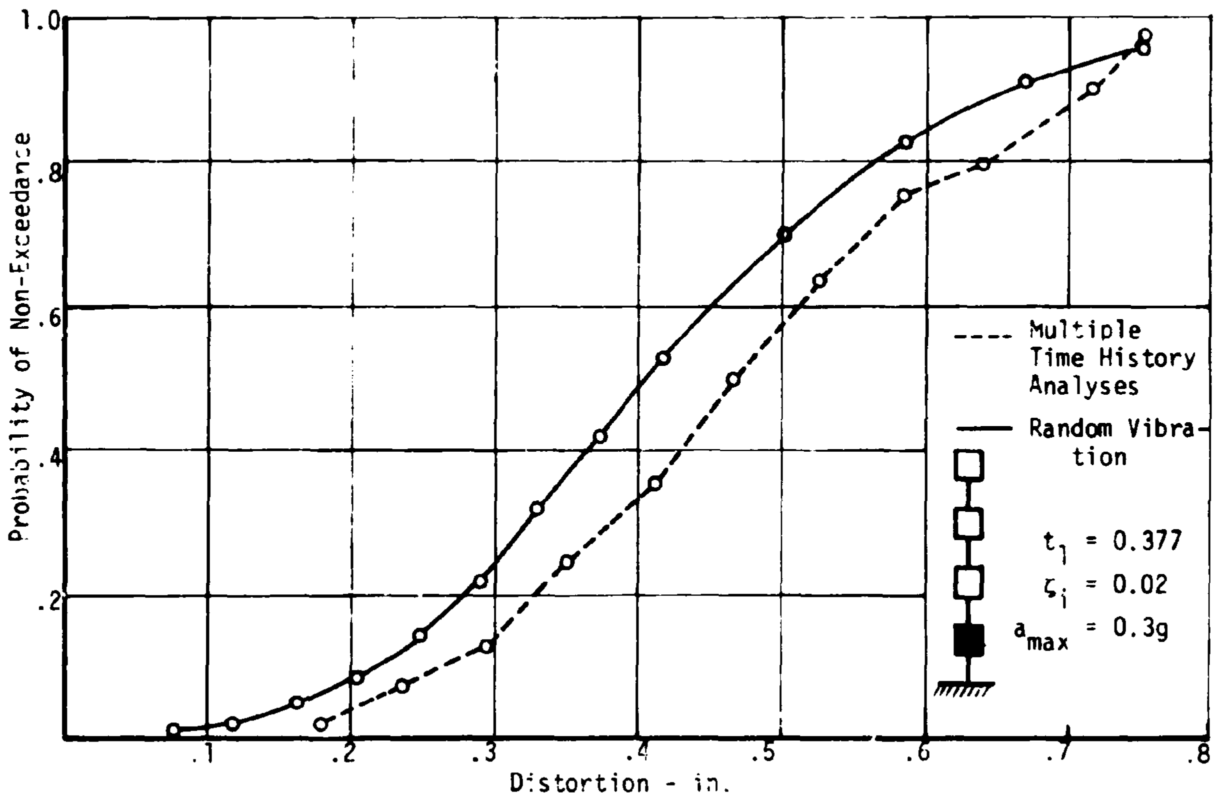

FIGURE 2.12 - CUMULATIVE DISTRIBUTION OF 1ST FLOOR DISTORTION CONDITIONAL ON a_{max} = 0.3g

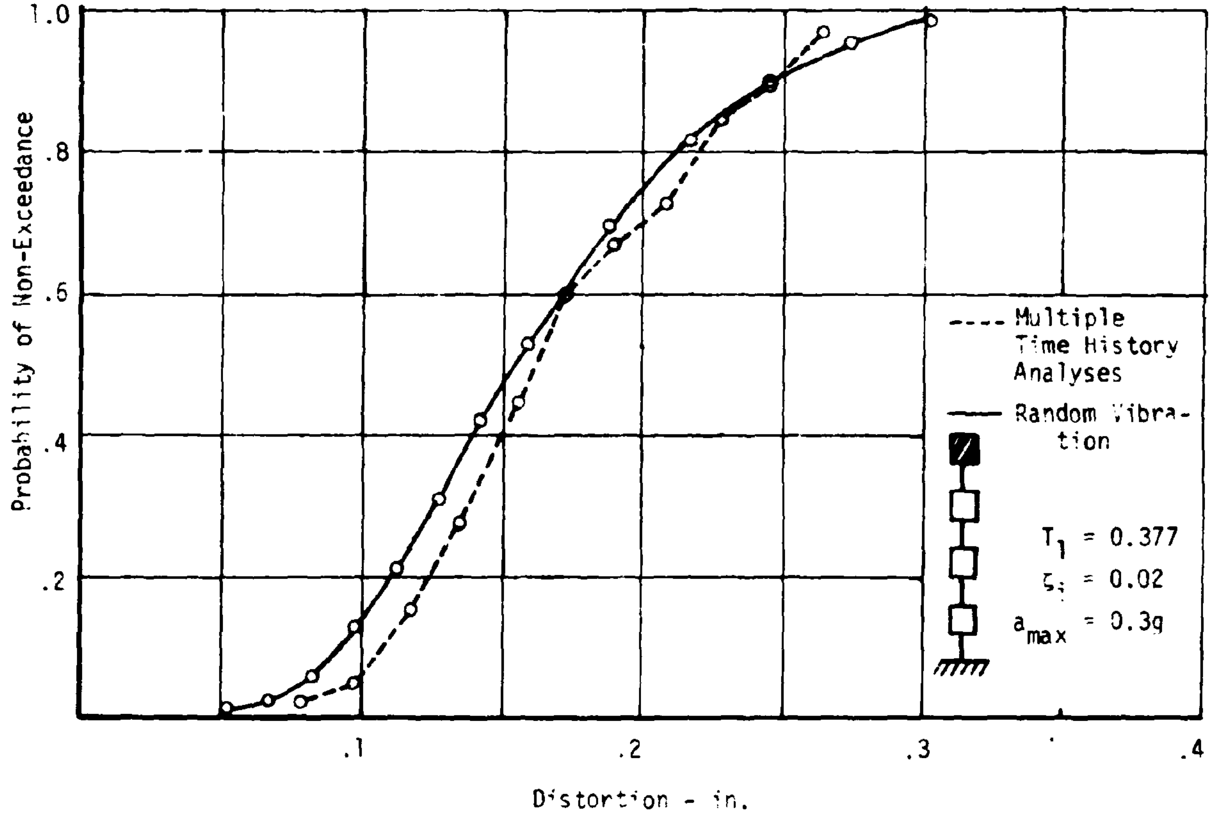

FIGURE 2.13 - CUMULATIVE DISTRIBUTION OF 4TH FLOOR DISTORTION CONDITIONAL ON a_{max} = 0.3g

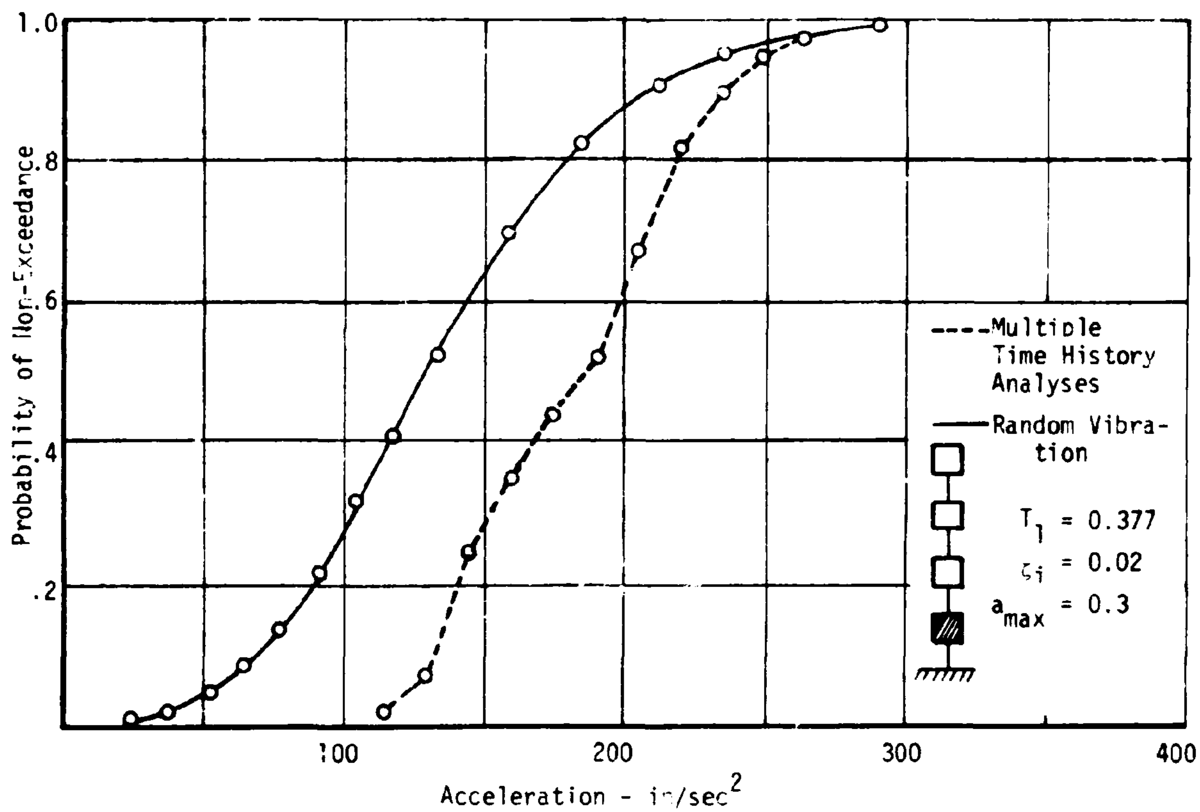

FIGURE 2.14 - CUMULATIVE DISTRIBUTION OF 1ST FLOOR ACCELERATION CONDITIONAL ON a_{max} = 0.3g

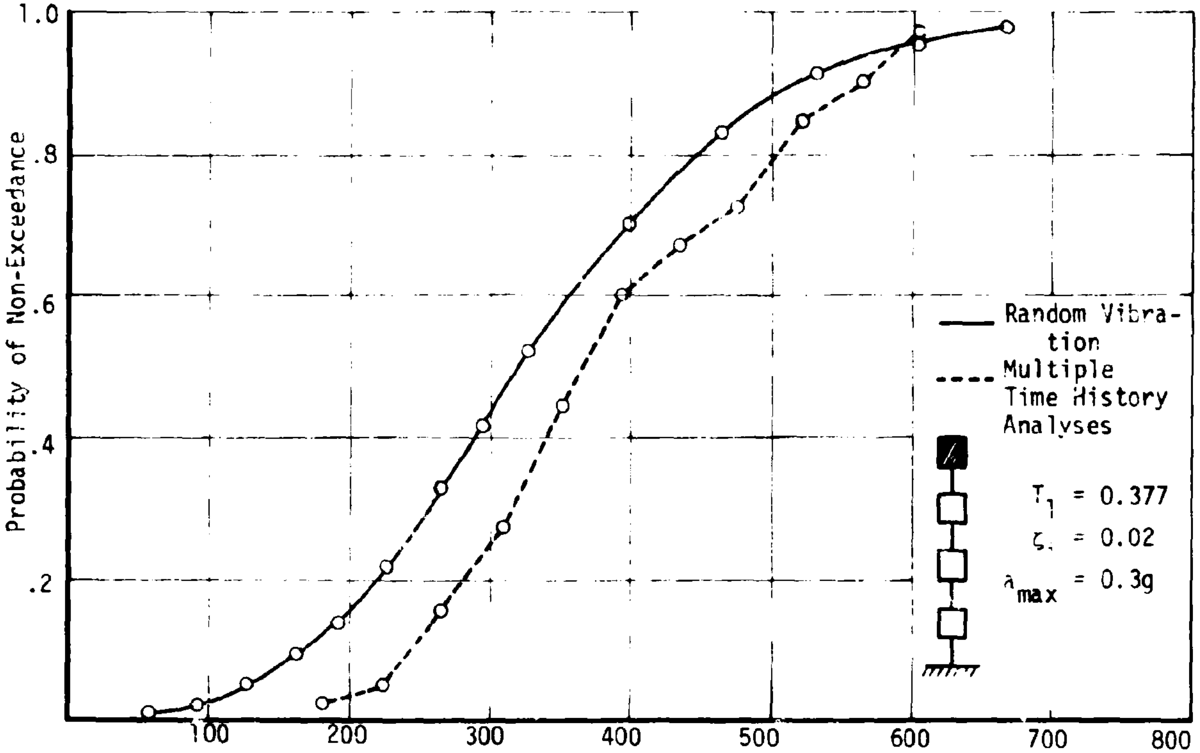

FIGURE 2.15 - CUMULATIVE DISTRIBUTIONS OF 4TH FLOOR ACCELERATION CONDITIONAL ON a_{max} = 0.3g

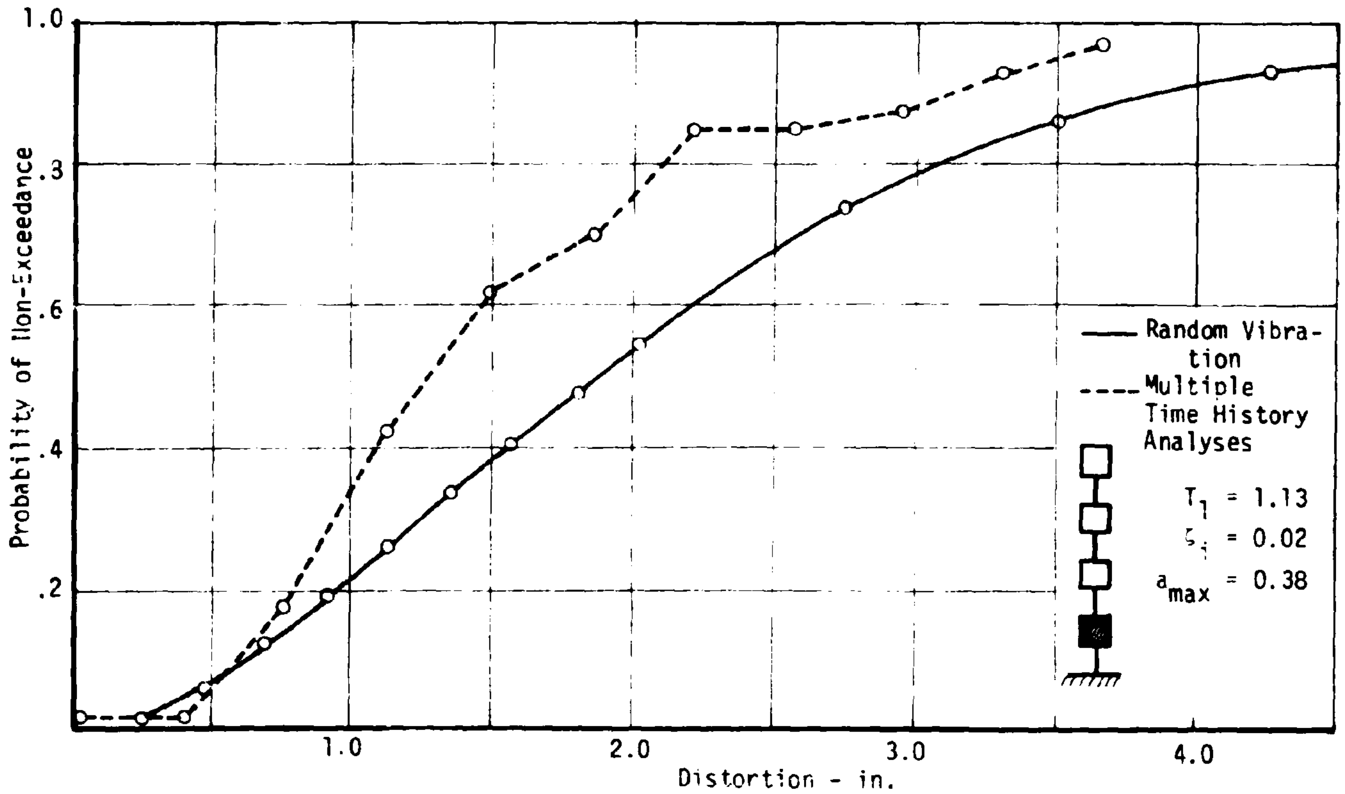

FIGURE 2.16 - CUMULATIVE DISTRIBUTION OF 1ST FLOOR DISTORTION CONDITIONAL ON a_{max} = 0.3g

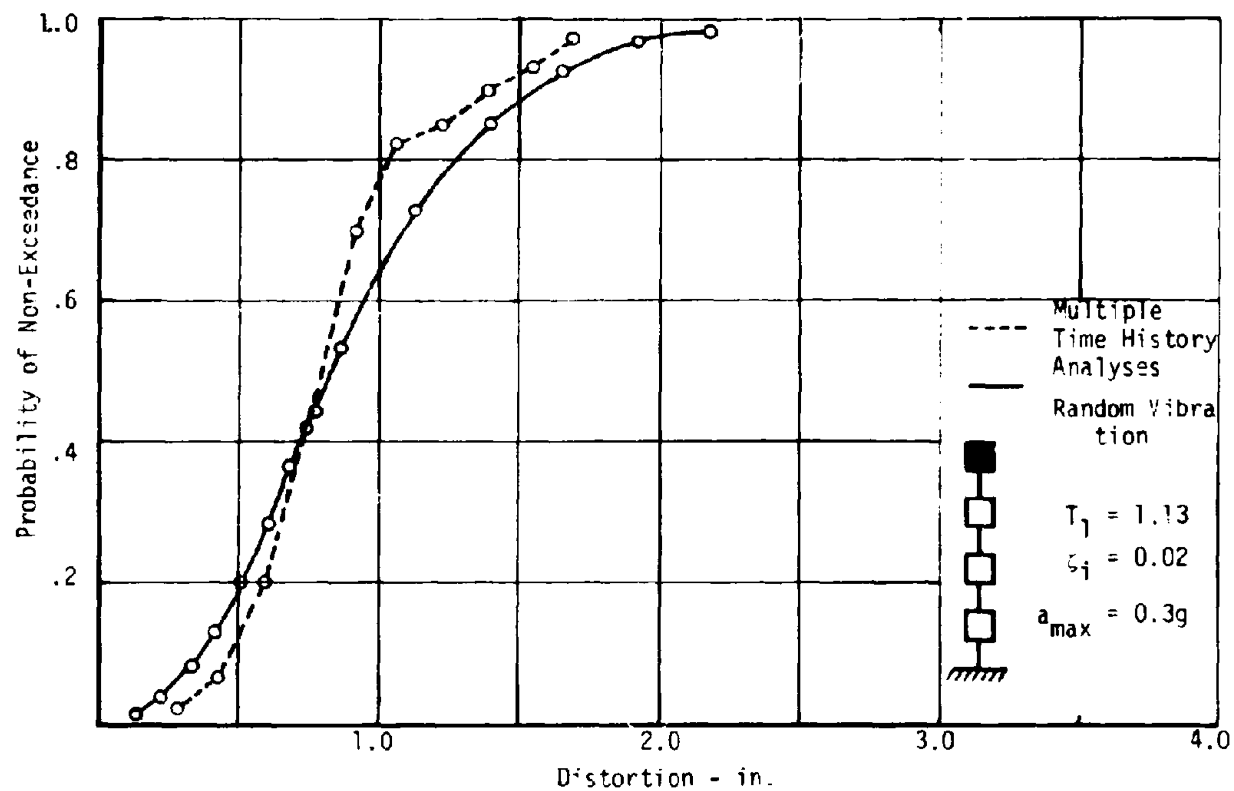

FIGURE 2.17 - CUMULATIVE DISTRIBUTION OF 4^{TH} FLOOR DISTORTION CONDITIONAL ON a_{max} = 0.3g

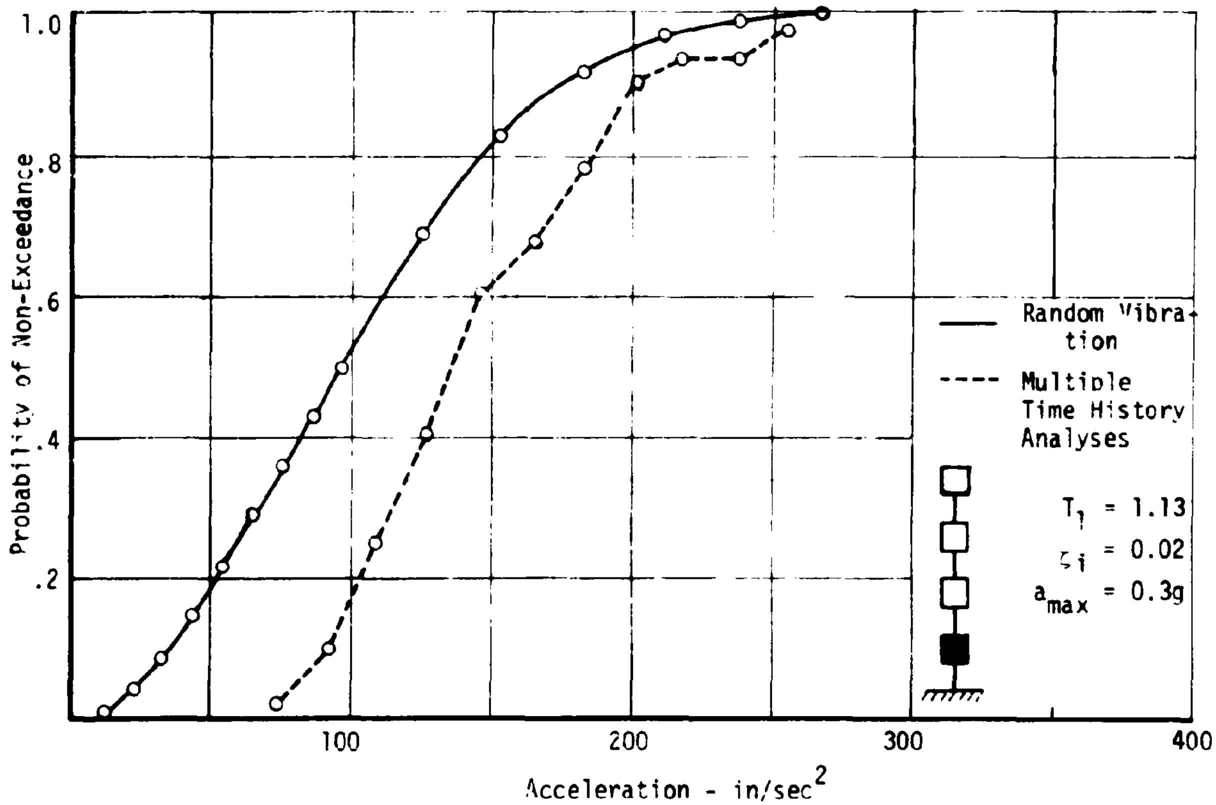

FIGURE 2.18 - CUMULATIVE DISTRIBUTION OF 1ST FLOOR ACCELERATION CONDITIONAL ON a_{max} = 0.3g

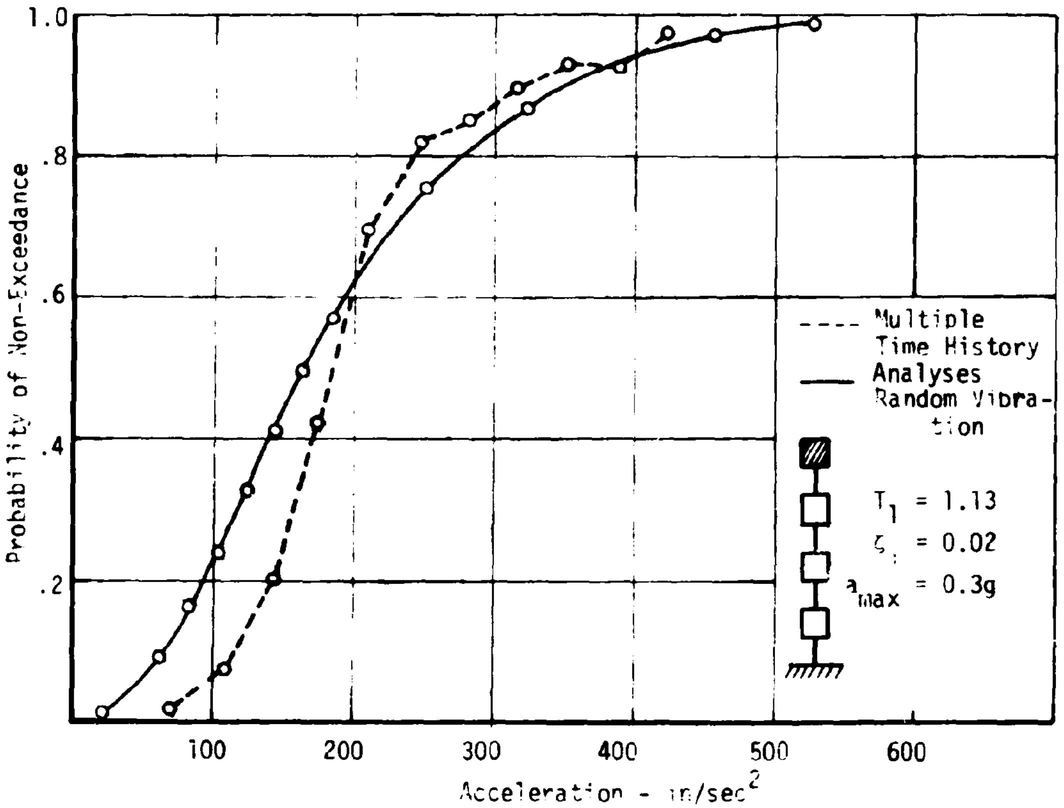

FIGURE 2.19 - CUMULATIVE DISTRIBUTION OF 4TH FLOOR ACCELERATION CONDITIONAL ON a_{max} = 0.3g

		Multiple Time History Analyses			Random Vibration Analyses (S' and ω_g Random)			Multiple Response Spectrum Analyses		
	Load Effect	m	COV	COS	m	COV	COS	m	COV	COS
$T_1 = 0.377$	1st Floor Int. Dist.	.47	.33	.11	.42	.41	.53	.46	.32	.15
	4th Floor Int. Dist.	.17	.29	.31	.16	.36	.59	.17	.29	.35
	1st Floor Acc.	180.	.21	.12	134.	.40	.51	173.	.22	.33
	4th Floor Acc.	385.	.29	.31	337.	.42	.53	385.	.29	.32
$T_1 = 1.13$	1st Floor Int. Dist.	1.46	.58	1.00	2.13	.63	1.04	1.51	.55	1.07
	4th Floor Int. Dist.	.76	.40	1.20	.92	.53	.85	.72	.37	.88
	1st Floor Acc.	143.	.31	.64	102.5	.53	.57	125.0	.24	.34
	4th Floor Acc.	194.	.40	1.20	194.	.61	1.10	170.0	.40	1.01

TABLE 2.7 - COMPARISON OF MOMENTS OF LOAD EFFECT DISTRIBUTIONS (in, in/sec^2)

tion approach stationarity (because of the larger number of cycles of response). Matches in coefficients of variation and of skewness are less accurate, although the limited statistical data base (39 responses) may itself lead to only approximate computed values for these two moments. It may further be expected that the coefficient of variation and the coefficient of skewness from the random vibration as well as the response spectrum methodology would be equal for the fourth story acceleration and interstory distortion responses. In fact, both methodologies compute spectral (or pseudo) acceleration values. That is, for the root-mean-square modal values, it is assumed in the random vibration procedure that

$$\sigma^2_{k,\mathrm{Acc.}} = \omega_k^4 * \sigma^2_{k,\ \mathrm{Rel.\ Displ.}} \qquad (2.25)$$

where k denotes a particular mode. Further, the approximate random vibration formulations to obtain distributions of peak values are different for the interstory distortion and for the acceleration responses [64]. Both of these approximations account for the observed discrepancies in the moments.

It is to be noted that all the load effect distributions are positively skewed (with positive values only), hence an assumption of a lognormal type of distribution is often made. Figures 2.20 and 2.21 are plots (on normal probability paper) of the logarithms of the 1^{st} floor acceleration and 4^{th} floor interstory distortion response values for the model having $T_1 = 0.377$ sec. A straight line would corroborate the lognormal distribution assumption. It may be observed that, at the higher

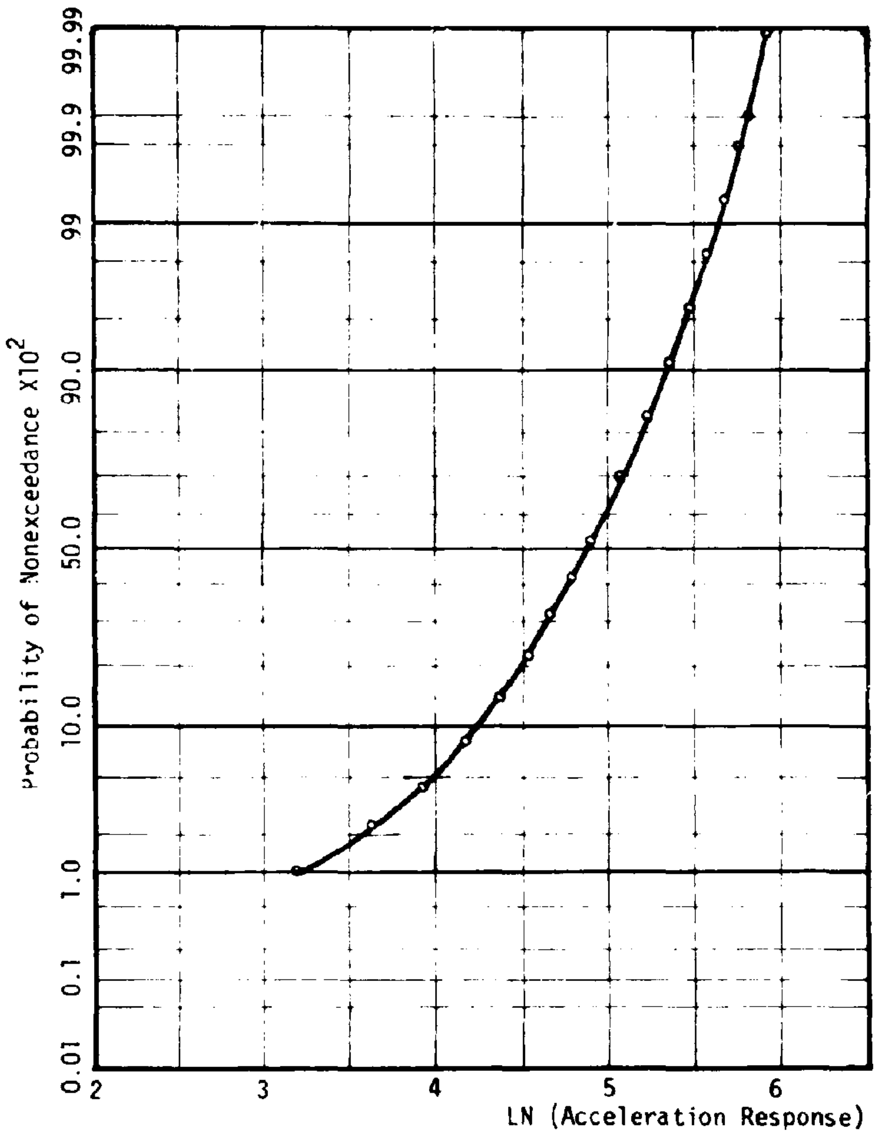

FIGURE 2.20 - LOGARITHM OF 1ST FLOOR ACCELERATION RESPONSE, T_1 = 0.377 sec. Model

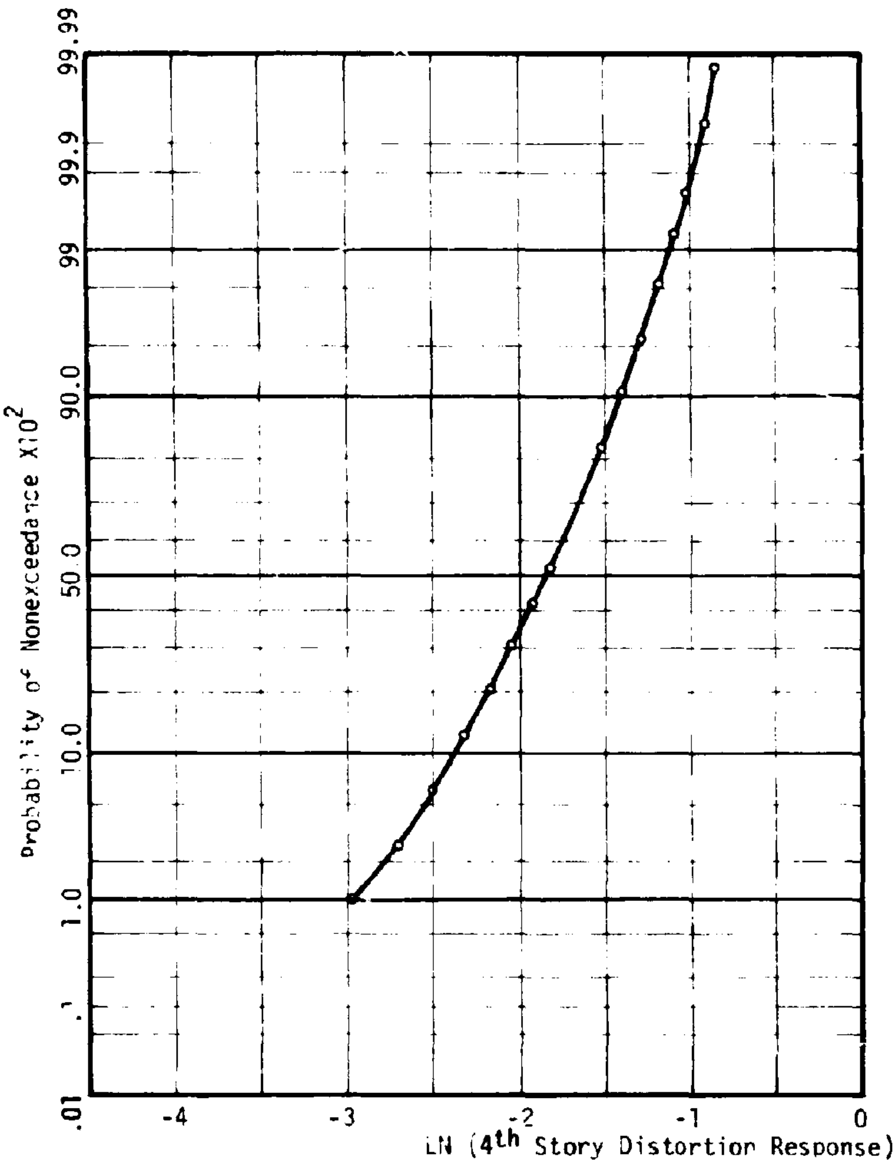

FIGURE 2.21 - LOGARITHM OF 4TH STORY DISTORTION RESPONSE

T_1 = 0.377 sec. Model

fractiles, which are of most interest in reliability calculations, deviation from linearity is small.

2.8 EFFECTS OF RANDOM PARAMETERS ON MOMENTS OF CONDITIONAL LOAD EFFECT DISTRIBUTIONS

It is pertinent to attempt to quantify the relative importance of each of the assumed random parameters (ζ, ω_g, S', T_o/T_c) in determining load effect distributions and their moments. Similarly, it is important to quantify the effects of uncertainty in the moments of the random parameter distributions on response values. Both points will be addressed in this section. It must be recognized, however, that the effects will clearly be different, depending on the type of load effect considered and the nominal value of the fundamental period of the structure. For example, given that a structure's fundamental period is in the constant acceleration range of the response spectrum, it can be anticipated that period uncertainty will have little effect on the distribution of the acceleration response. By examining variations in distribution moments for both the structural models described by Table 2.5, these points will become evident.

Consider the following studies: The coefficient of variation of each of the parameters is varied, in turn, while:

1. Assuming the other parameters as deterministic at their mean values.
2. Assuming the other parameters random with best estimates of their distributions.

The following argument is made to interpret the above procedures. From a second-moment formulation [62], the total variance of the conditional response may be expressed as (see section 2.9 for a more complete explanation).

$$\sigma^2_{Response} = \sigma^2_{\substack{Random\ Phasing\ \& \\ a_{\overline{max}}\ \sigma_a\ Randomness}} + \sum_{i=1}^{4} \left(\frac{\partial Response}{\partial x_i}\right) \sigma^2_{x_i} \tag{2.26}$$

where x_i represents any one of the four random parameters. Data from study 1 above can isolate the individual contributions in the summation. These may, in turn, be used to predict the response variance for any group of parameters considered random. Hence variances resulting from study 2 may be used to compare with (and evaluate) the second moment predictions. Actual numerical results will be given later in this section.

2.8.1 All Parameters Except One Deterministic at Their Mean Values

Figures 2.22 to 2.25 show variations in the moments (m, COV, COS) of the distributions of the following responses:

a) 1st story distortion
b) 1st story spectral (pseudo) acceleration
c) 4th story distortion
d) 4th floor spectral (pseudo) acceleration

Figures 2.22 and 2.23 are for the T_1 = .377 model; Figures 2.24 and 2.25 refer to the T_1 = 1.13 model. The variations are with respect to the basic case where the four parameters ω_g, S', ζ, T_0/T_c are considered deterministic at their mean values. In this study, each one of the parameters is, in turn, allowed to be lognormally distributed with best estimates of the moments (m, COV) as per Table 2.8 (see also Figures 2.2, 2.5, 2.9 and 2.10).

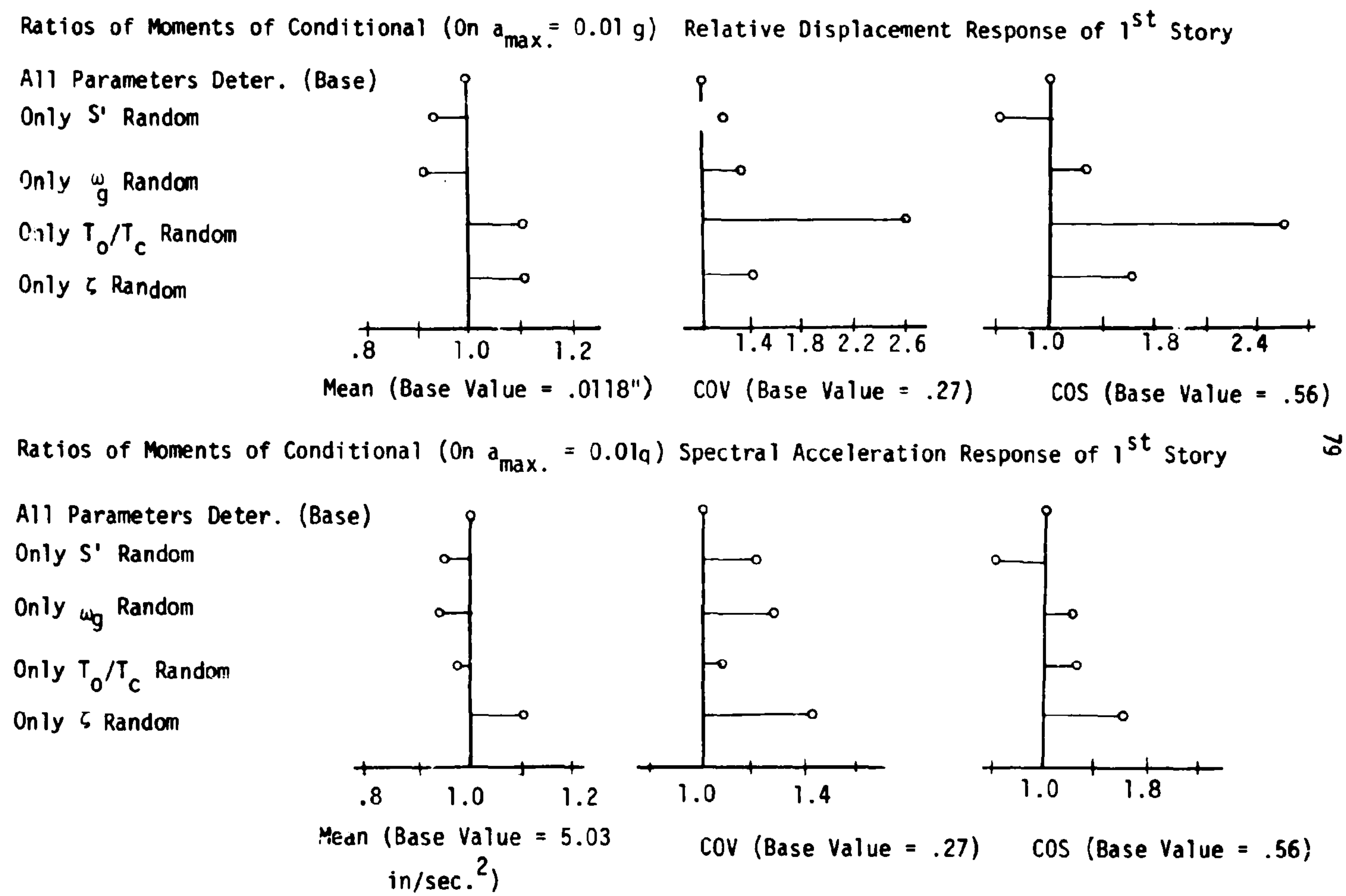

FIGURE 2.22 - VARIATION IN MOMENTS OF 1st STORY RESPONSES, T_1 = 0.377 Sec. Model

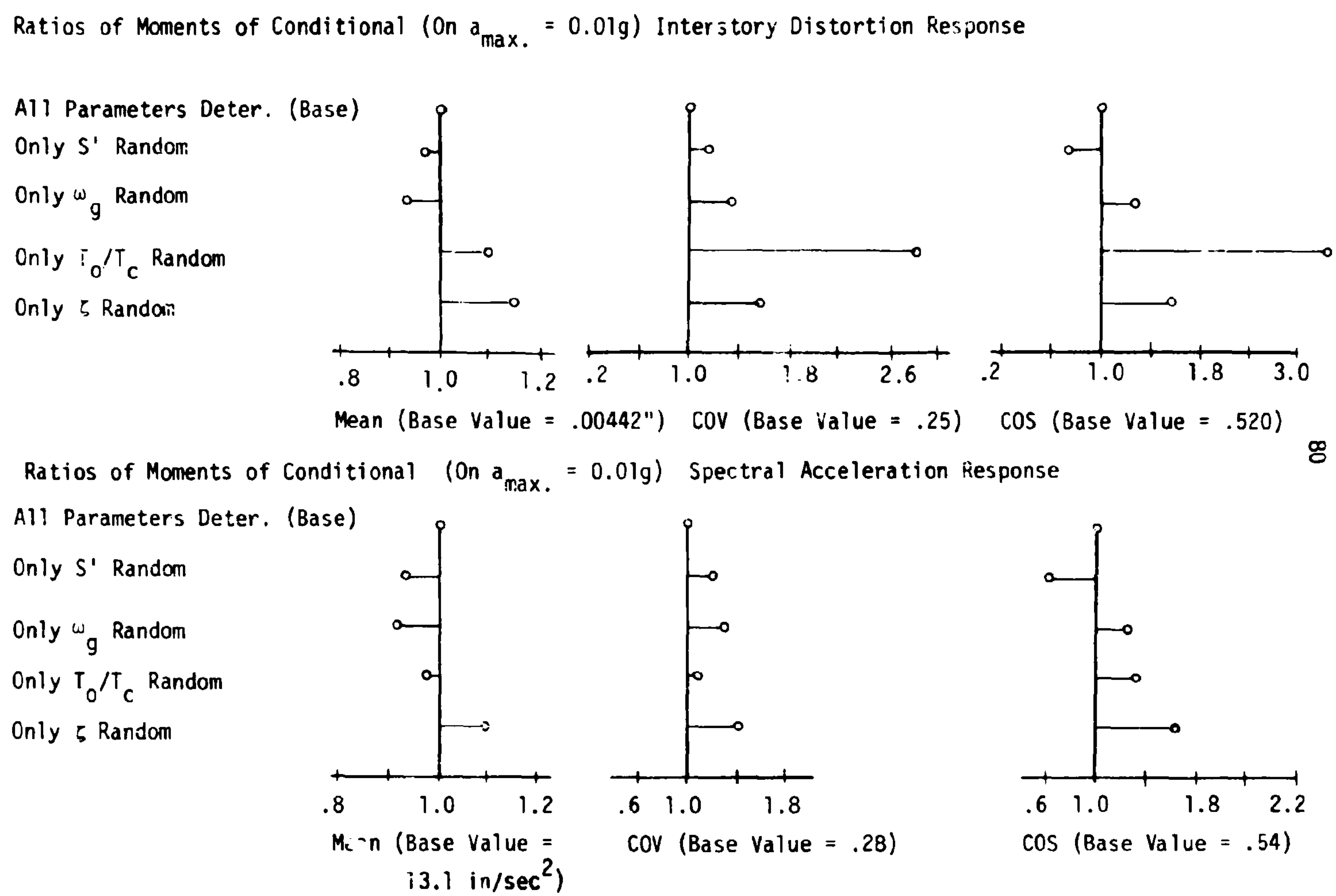

FIGURE 2.23 - VARIATION IN MOMENTS OF 4th STORY RESPONSES, T_1 = 0.377 sec.

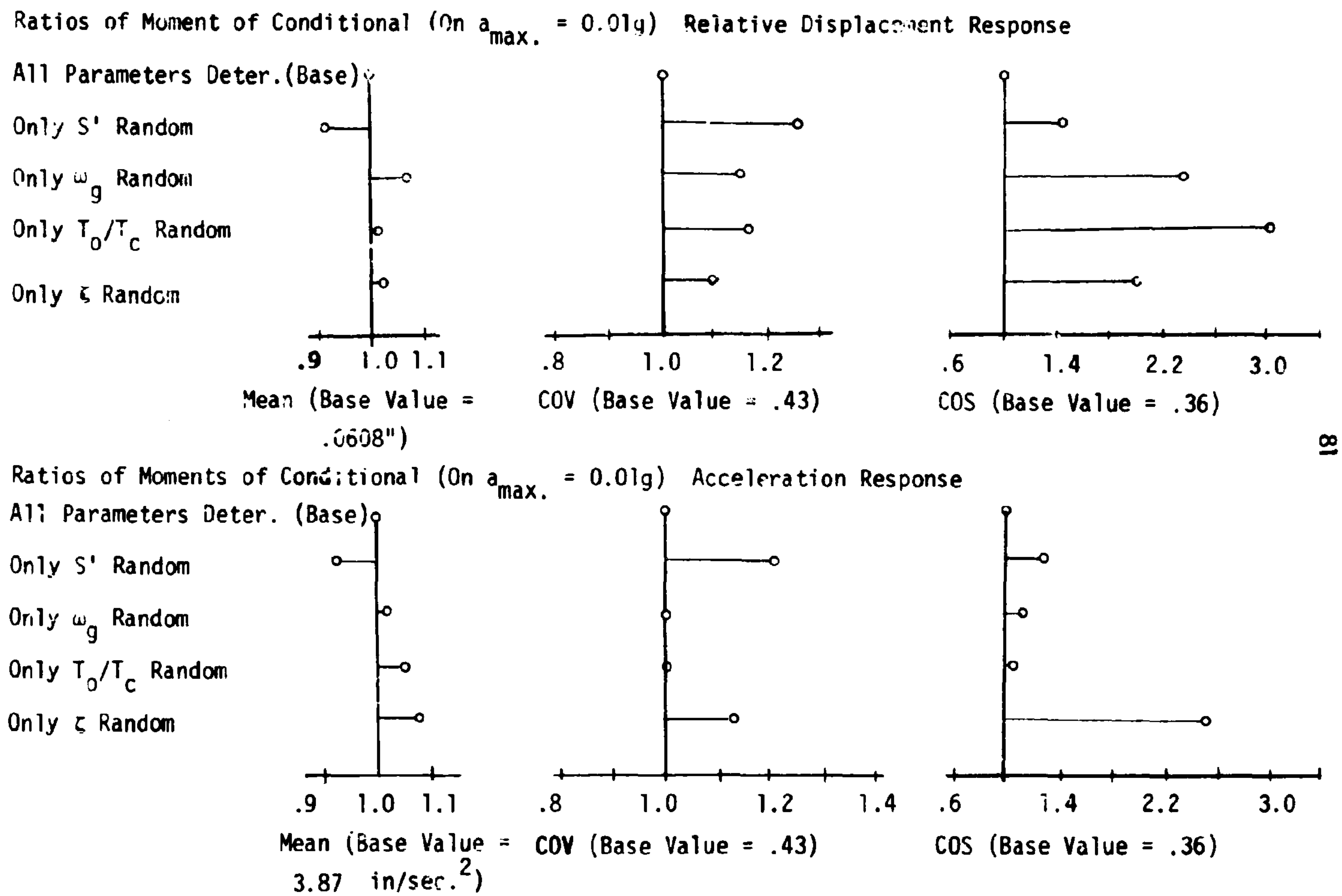

FIGURE 2.24 - VARIATION IN MOMENTS in 1^{st} STORY RESPONSE MOMENTS, T_1 = 1.13 sec.

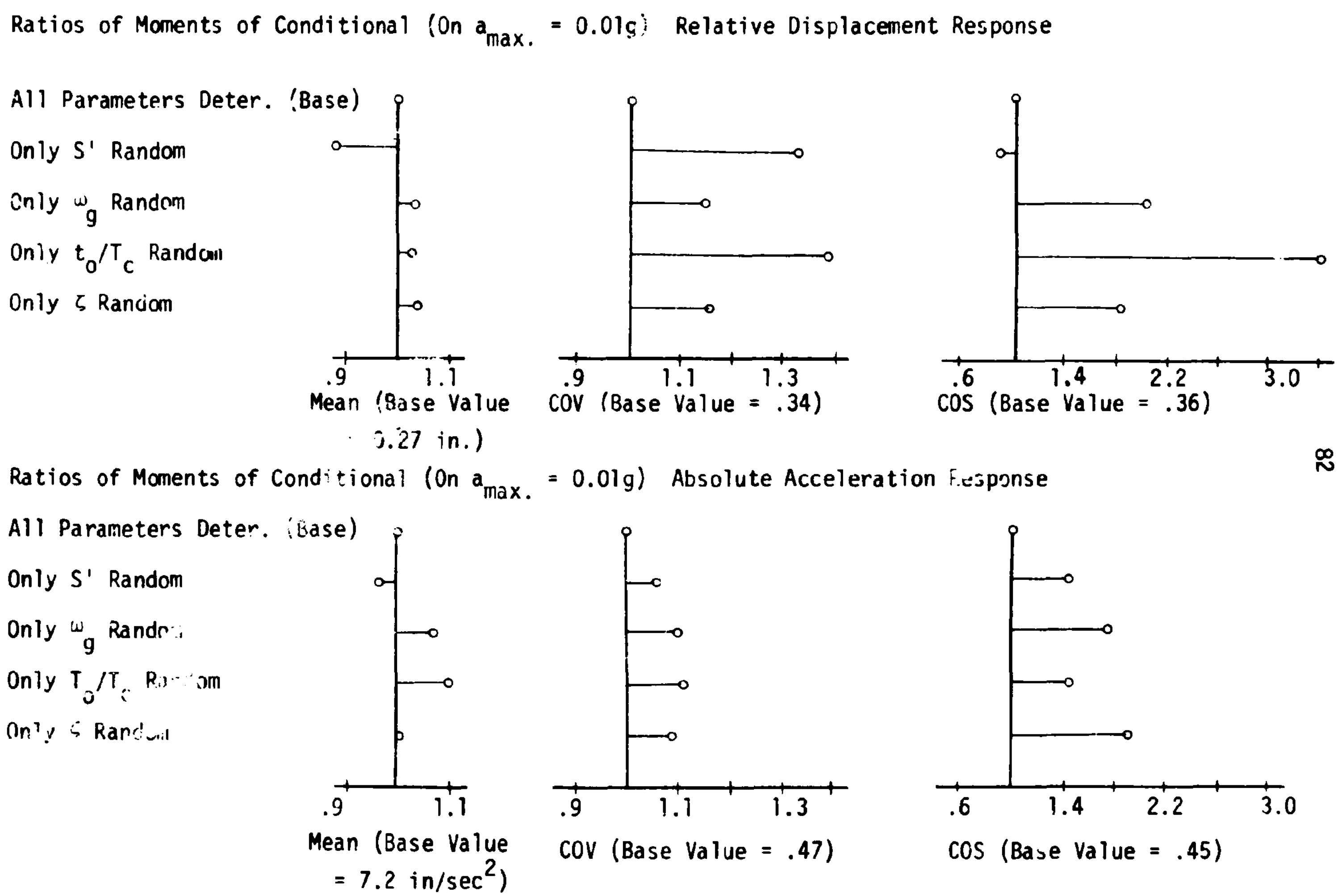

FIGURE 2.25 - VARIATION IN 4th STORY RESPONSE MOMENTS, T_1 = 1.13 sec.

	m	COV
ζ	.02	.75
T_o/T_c	.85	.33
ω_g	12 1/SEC	.5
S'	8 SEC	.75

TABLE 2.8 - MOMENTS OF LOGNORMAL DISTRIBUTIONS OF PARAMETERS ζ, T_o/T_c, ω_g and S'

Interpretation of Results - T_1 = .377 Sec. Model, First Story Distortion, Figure 2.22

Generally, it can be seen that the mean has least variability of all the moments with values generally from 90% to 110% of the base value. For each of the parameters the following additional observations are made.

S' - The mean decreases as S' is made random because at $\bar{S}'$ = 8 Sec.(A bar indicates mean value)the response may be close to stationary; therefore higher durations do not cause significantly higher responses, whereas lower S' values may imply non-stationary or lower response values. It is apparent that the relative magnitude of $\bar{S}'$ with respect to the nominal fundamental period of the structure is significant in determining whether the mean response will increase or decrease. Since for the T_1 = 0.377 Sec. model the effect of a random S' is mainly to increase the likelihood of lower responses, it is seen that, correspondingly, the coefficient of skewness also decreases.

<u>ω_g</u> - Introducing a probabilistic model for ω_g also decreases the mean load effect. Again, the relative position of the mean, $\bar{\omega}_g$, with respect to the period of the structure is likely to control such an effect. In this case $\bar{\omega}_g$ = 12 1/Sec.or $\bar{T}_g \simeq$ .52 Sec. is close to the fundamental period of the structure, T_1 = 0.377 Sec.; hence, by assigning zero probabilities to other ω_g values, we are conservatively assuming that the earthquake will have the most power in the region where it is most effective, i.e., near the natural period of the structure.

<u>T_o/T_c</u> - The coefficient of variation, as expected, increases as any parameter is made random, and notably the greatest increase is from the T_o/T_c randomness. Considering that 0.377 Sec. lies in the "constant acceleration portion of the response spectrum, it becomes clear that a change in T_1 affects the relative displacement (or interstory distortion for the first story) response the most.

<u>ζ</u> - All moments increase as this parameter is made random. Since response is a nonlinear function of ζ, lower ζ values cause extremely high responses which increase the positive skewness of the distribution.

<u>Interpretation of Results - T_1 = 0.377 Sec., First Floor Spectral Acceleration and First Story Distortion, Figure 2.22</u>

A common first-passage problem solution is used to obtain distributions for <u>both</u> spectral-acceleration and relative displacement responses once the root-mean-square values have been computed. Thus the coefficient of variation and coefficient of skewness of the <u>base</u> distributions, i.e., those obtained considering all the parameters deterministic, are common for the two responses. Similarly, if one mode dominates root-mean-square responses and T_0/T_c is deterministic, the effects (on the COV's and the COS's) of making ω_g and S' random should be similar for both acceleration and relative displacement responses. In fact, for this structure such similar variations may be observed for the two responses. The parameter T_0/T_c, which is partly a reflection of the uncertainty in stiffness and mass, causes markedly different effects on acceleration and relative displacement responses. This, again, may best be interpreted by recognizing that the fundamental period of the structure lies in the constant acceleration range of response spectra.

Interpretation of Results - T_1 = .377 Sec., Fourth Story Distortion, Floor Spectral Acceleration, Figure 2.23

Given a deterministic model with no damping, it can be expected that these two response values have the same moments. This is true since for the close-coupled, lumped-mass model being considered, force equilibrium requires that the top floor acceleration be directly proportional to the interstory distortion. Damping does exist, however, and two further points are to be remembered. One is that spectral acceleration rather than actual peak acceleration is being computed. The other is that the random vibration solution superposes modal root-mean-square response values in an SRSS fashion and subsequently uses different approximate first passage problem solutions to arrive at distributions of interstory distortion and acceleration. Given the above approximations, exact agreement is not expected. In fact, the base values of the moments and their variations are slightly different.

Given a non-deterministic model (i.e., T_0/T_C, ζ random), the moments of the two responses need not be the same since, in effect, the fourth story mass, stiffness and damping, the quantities which link the two responses, are themselves random. Hence it is not unreasonable to find that for T_0/T_C random the interstory distortion has significantly higher COV and COS in comparison with the fourth story spectral acceleration response.

Interpretation of Results - T_1 = 1.13 Sec., First Story Distortion, Figure 2.24.

As for the T_1 = 3.77 Sec. model, the mean is relatively stable at its base value. The base COV is significantly higher than that of the .377 Sec. model, an expected result given conditionality of responses on peak ground acceleration. The effects of the individual parameters may be summarized as follows.

S' - For this structure, response at $\overline{S}$ = 8 Secs. is likely to be non-stationary, hence increased durations do cause higher responses. Due to these higher responses, the COS increases rather than decreases as for the previous model.

ω_g - The increase in all three moments is due to the fact that $G(\omega)$'s with ω_g values closer to the fundamental period, say ω_g = 6 Rad/Sec, cause greater responses than the $G(\omega)$ with $\omega_g = \overline{\omega}_g$ = 12 Rad/Sec. Understandably, the effect is opposite that found for the T_1 = 0.377 Sec. structure.

T_o/T_c - In comparison with the previous model, the influence of this parameter is diminished. Both the mean and the COV are less affected, and the resultant absolute value of the COS is mucn smaller than that of the 0.377 Sec. structure.

ζ - The influences of ζ are similar, although of somewhat greater magnitude, to those found for the T_1 = 0.377 Sec. model.

Interpretation of Results - T_1 = 1.13 Sec., First Story Relative Displacement and First Floor Spectral Acceleration, Figure 2.24

The notable observation to be made is that the ω_g parameter (as it is made random) causes different effects on the moments of the relative displacement and acceleration responses, notwithstanding that a common first passage solution is used to compute load effect distributions. The implication is that the ratio of the total root-mean-square spectral acceleration response to the total root-mean-square relative displacement response varies for different values of ω_g.

Interpretation of Results - T_1 = 1.13 Sec., Fourth Story Distortion, Fourth Floor Spectral Acceleration, Figure 2.25.

As discussed for the other model, equilibrium considerations indicate that, for a deterministic structure with no damping, the moments of the top story distortion and peak floor acceleration are the same. The differences in moments of the two responses apparent in Figure 2.25 for the three pertinent cases (all parameters deterministic, only ω_g random, only S' random) are, again, due to a combination of factors. One, modal root-mean-square spectral acceleration ($\sigma_{k,a} = \omega_k^4 * \sigma_{k,y}^2$) is computed: two, modal root-mean-square responses are combined in an approximate SRSS format, and three, two different approximate first passage solutions are applied to obtain distributions of responses.

2.8.2 All Parameters Random But One

Load effect distributions were first computed assuming all the parameters to be random, lognormally distributed with estimated moments given by Table 2.8. Then, in turn, each (one) parameter was made deterministic. Figures 2.26 through 2.29 show the resultant variations of the moments of the distributions of the same four load effects considered in the previous study. The primary purpose of these runs was to calculate moments (specifically variances) which could be compared with those predicted by a second moment formulation. The data is otherwise difficult to interpret in terms of the effects of individual parameters.

Qualitatively, of course, the COV and COS generally decreased and the means remained stable. Variations in the computed moments for the basic cases, i.e., all parameters determininistic and all parameters random, are summarized in Table 2.9.

2.9 APPROXIMATE SECOND MOMENT ANALYSIS

A second-moment random variable is, by definition, described by its mean and variance. It is an incomplete description if the underlying Probability density function (PDF) is other than Gaussian. A second-moment analysis generally arrives at an expression for the mean and variance of a

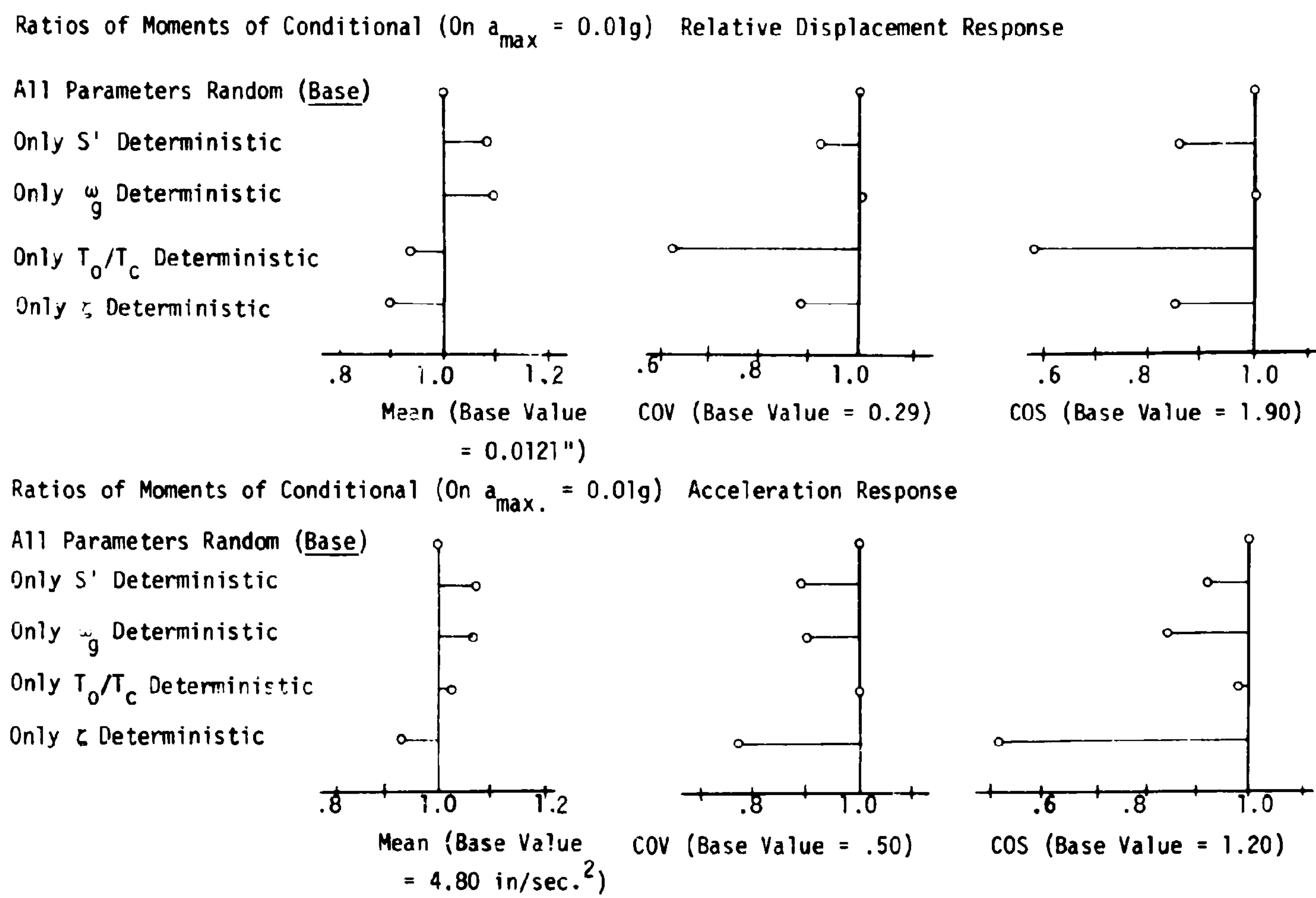

FIGURE 2.26 - VARIATION IN MOMENTS OF 1st STORY RESPONSES, T_1 = 0.377 sec.

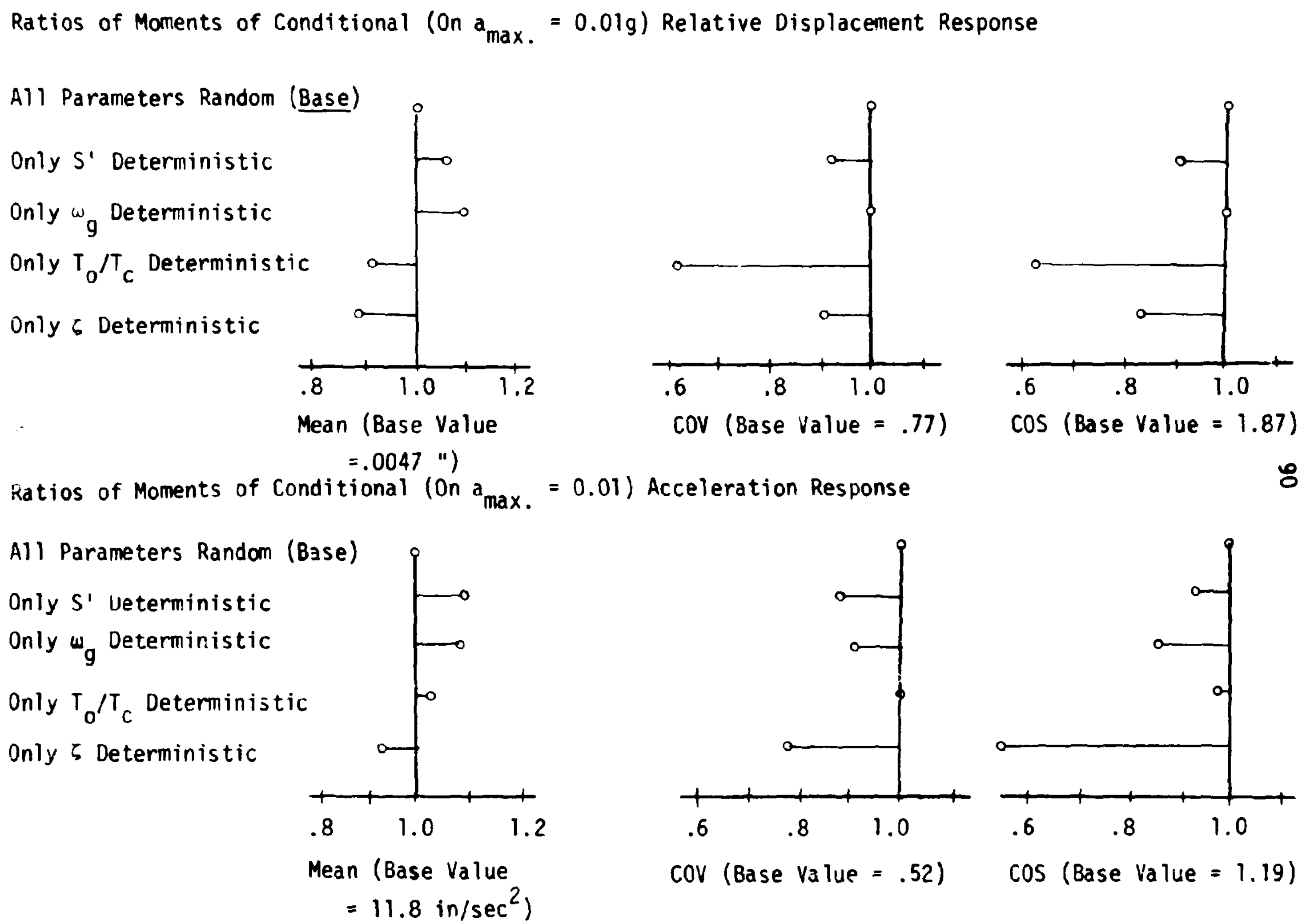

FIGURE 2.27 - VARIATION IN MOMENTS OF 4^{th} STORY RESPONSES, T_1 = 0.377

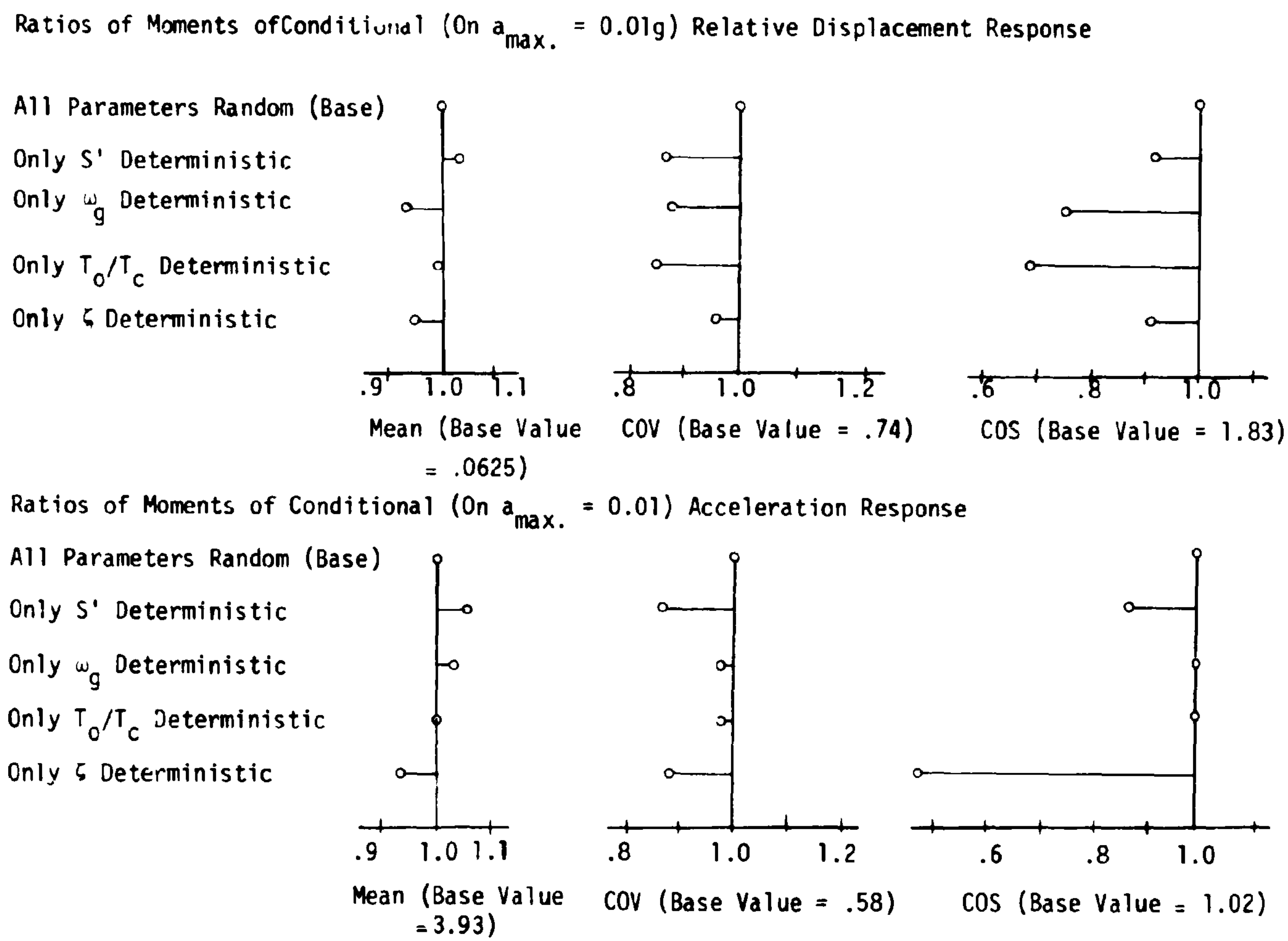

FIGURE 2.28 - VARIATION IN MOMENTS OF 1^{st} STORY RESPONSES, T_1 = 1.13 sec.

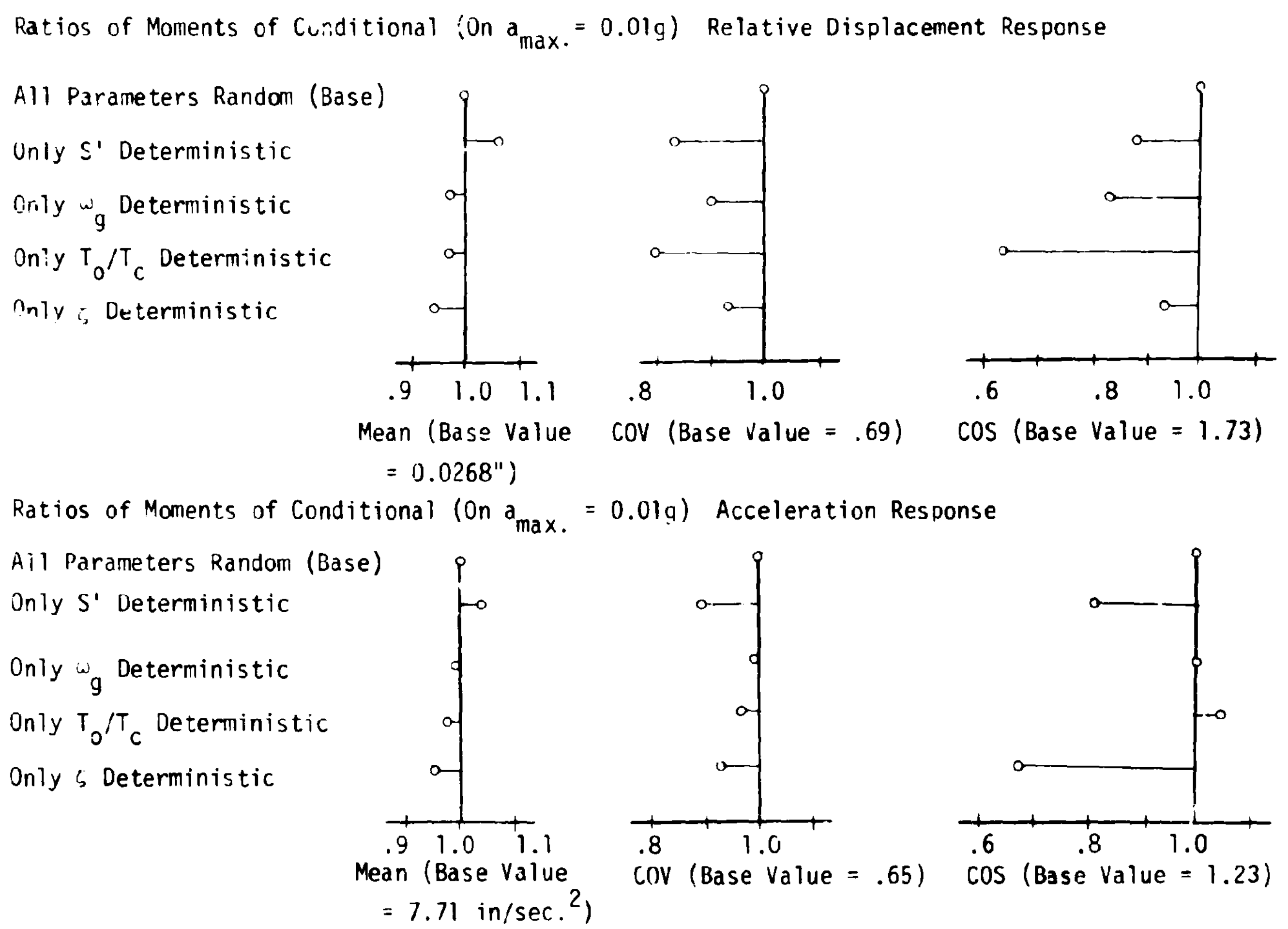

FIGURE 2.29 - VARIATION OF MOMENTS OF 4th STORY RESPONSES, T_1 = 1.13

	Response	All Parameters Deterministic Mean in-in/sec^2	COV	COS	All Parameters Random Mean in-in/sec^2	COV	COS
T_1 = .377	1st Story Dist.	0.118	.27	.56	.0121	.78	1.93
	4th Story Dist.	.0014	.25	.52	.0047	.78	1.87
	1st Floor Acc.	5.03	.27	.56	4.80	.50	1.20
	4th Floor Acc.	13.1	.28	.54	11.8	.52	1.20
T_1 = 1.13	1st Story Dist.	.0608	.43	.36	.0625	.74	1.83
	4th Story Dist.	.0265	.34	.36	.0268	.69	1.73
	1st Story Dist.	3.87	.43	.36	3.93	.58	1.02
	4th Story Dist.	7.23	.49	.45	7.71	.65	1.23

TABLE 2.9 - MOMENTS OF RESPONSE DISTRIBUTIONS

random variable of interest in terms of the means and variances of the random variables it is functionally dependent on [52]. If the functional relationship is other than linear, a linearization (by a Taylor expansion and first order truncation) must first be made. The accuracy of the linearization must clearly be checked before such an analysis may be used to estimate moments.

Briefly, then, if a response variable Y is, in general, a nonlinear function of a vector of variables:

$$Y = g(\underline{x}) \qquad (2.27)$$

a Taylor expansion and truncation give:

$$Y = g(\underline{m}) + \left[\frac{\partial g(\underline{x})}{\partial \underline{x}} \Bigg|_{\underline{x}=\underline{m}} \right] (\underline{x} - \underline{m}) \qquad (2.28)$$

and the mean and variance of Y are given by:

$$\bar{Y} = g(\underline{m}) \tag{2.29}$$

$$\sigma_Y^2 = \underline{B}\,\underline{\Sigma}_{\underline{x}}\;\underline{B}^T \tag{2-30}$$

where

$$\underline{B} = \left[\left.\frac{\partial g(\underline{x})}{\partial x_i}\right|_{\underline{x}=\underline{m}}\right] \tag{2.31}$$

is a <u>row</u> matrix

and

$$\underline{\Sigma}_{\underline{x}} = \begin{bmatrix} \sigma_1^2 & \rho_{12}\sigma_1\sigma_2 & \cdots & \\ \cdot & \sigma_2^2 & & \\ \cdot & & \ddots & \\ \text{SYM.} & \cdots & \cdot & \sigma^2 \end{bmatrix} \tag{2.32}$$

is the covariance matrix.

Further, if the random variables are considered independent, Equation (2.30) reduces to:

$$\sigma_Y^2 = \sum_i \left(\left.\frac{\partial g(\underline{x})}{\partial x_i}\right|_{\underline{x}=\underline{m}}\right)^2 \sigma_{x_i}^2 \tag{2.33}$$

In this chapter, a response Y has been expressed in terms of four random parameters ζ, T_o/T_c, ω_g, S'. It is recognized, however, that additional underlying variability comes directly from the random phasing of a motion and the inherent uncertainty in the $G(\omega)$ intensity given a peak acceleration. Hence, Equation (2.33) above may be expressed as;

$$\sigma_Y^2 = \sigma^2_{\substack{\text{Random Phasing}\\ \text{and } a_{max}/\sigma_a\\ \text{Uncertainty}}} + \sum_{i=1}^{4} \left[\left.\frac{\partial Y}{\partial x_i}\right|_{x_i = m_i}\right]^2 \sigma_{x_i}^2 \tag{2.34}$$

It is apparent then, that by considering all the parameters deterministic, the uncertainty given by the first term remains. Also, by assuming only one parameter at a time random, each term of the summation may be isolated; study 1 in fact provides such information.

As an example, data from Figures 2.22 and 2.24 is used to calculate contributions to the variance of the first story distortion for both dynamic models. Table 2.10 summarizes the results; the relative importance of any parameter clearly depends on the nominal fundamental period.

Now, data from Table 2.10 can be used to predict the variance of the same response for any combination of parameters considered random. Specifically, Table 2.11 shows computed variances (from Figures 2.26 and 2.28) and those predicted by appropriate addition of contributions given in Table 2.10. Also compared are the coefficients of variation.

2.10 SUMMARY

As a first step toward computing reliabilities in the sense described in the introduction, this chapter presented a practical method to compute conditional (on the intensity parameter a_{max}) load effect distributions. It essentially consists of weighted multiple random vibration analyses using four key random parameters, ζ, ω_g, T_o/T_c, S' to quantify the variability in elastic load effects. Some resultant distributions were compared with those obtained through multiple time history analyses; acceptable agreement was noted. Limited studies to assess the relative influence of each parameter on moments of load effect distributions were then conducted. Finally, in an attempt to predict response variances

	$T_1 = 0.377$ $in^2 \times 10^6$	$T_1 = 1.13$ $in^2 \times 10^6$
Random Phasing and a_{max}/σ_a Uncertainty.	10.0	6.9
$(\frac{\partial y}{\partial S'})^2 \quad \sigma^2_{S'}$	2.9	2.2
$(\frac{\partial y}{\partial \omega_g})^2 \sigma^2_{\omega_g}$	4.3	3.2
$(\frac{\partial y}{\partial T_o/T_c})^2 \sigma^2_{T_o/T_c}$	72.8	2.6
$(\frac{\partial y}{\partial \zeta})^2 \quad \sigma^2_{\zeta}$	14.6	1.6

TABLE 2.10 - CONTRIBUTIONS TO THE VARIANCE OF THE FIRST STORY DISTORTION

	$T_1 = 0.377$ σ^2- in^2		$T_1 = 1.13$ σ^2- in^2		$T_1 = 0.377$ COV		$T_1 = 1.13$ COV	
	Observed $\times 10^6$	Predicted $\times 10^6$	Observed $\times 10^4$	Predicted $\times 10^4$	Observed	Predicted	Observed	Predicted
All Parameters Random	90.8	104.6	21.2	16.5	.79	.86	.74	.67
All But S' Random	88.	101.7	17.4	14.3	.73	.85	.64	.62
All But ω_g Random	110.	100.3	14.5	13.3	.80	.85	.64	.60
All but T_o/T_c Random	31.8	31.8	14.9	13.9	.51	.48	.63	.61
All But ζ Random	62.1	90.0	16.0	14.9	.72	.80	.71	.64

TABLE 2.11 - COMPARISON OF COMPUTED AND PREDICTED VALUES OF VARIANCES AND COV'S OF 1^{ST} STORY (CONDITIONAL) DISTORTION RESPONSE

for an arbitrary combination of random and deterministic parameters, a second moment formulation was utilized.

It may be stated that the relative influences of the parameters ω_g and S' are very sensitive to the nominal period of the structure. Therefore, if a second moment format is to be used to predict response variances, sets of influence coefficients must be computed, each applicable in a narrow period range only.

CHAPTER 3

DISTRIBUTION OF STRENGTH MEASURE

3.1 INTRODUCTION

A methodology to arrive at load effect distributions at the member level was only briefly outlined on Figure 1.1. Chapter 2 focused on developing a method to arrive at distributions of responses at the floor or dynamic model level for a general linear system defined by eigenvalues, eigenvectors and participation factors. However, only close-coupled shear beam models were used therein to illustrate the capabilities developed and to perform parametric studies. It is within the context of such models that strength measures are discussed in this Chapter. Further, although shear beam models have been adapted to represent the behavior of braced frames, shear wall structures, and infilled frame buildings [29], they are evidently more applicable to rigid frame systems. It is only for such systems, then, that strength measures and their uncertainty will be examined.

It is noted that by considering floor level responses only, the dynamic analysis is simplified, but the strength measure becomes more difficult to quantify analytically. Further, experimental data quantifying strength at the floor level is not available. Conversely, reliable studies on strength at the member level [18,19,59] have been conducted, but the analytical procedures to arrive at distributions of dynamic load effects at that level are more difficult and costly.

It is known that strength uncertainty is a function of the material used, and the level of inspection and control exercised during manufacture.

As an example, concrete as a construction material may have to satisfy a variety of acceptance criteria or performance specifications, depending on the design philosophy; concrete for NPP reactors must meet much more extensive requirements [81] that would ordinarily not be imposed. Reference [51] notes:

> "It should be understood structural components important to nuclear safety require more stringent material, fabrication erection and inspection controls, quality assurance and control requirements than are required for conventional structures. Qualitatively such procedures should result in a more reliable structure..."

The consequences of variable control requirements on strength uncertainty will not explicitly be addressed herein.

Further, gross errors in construction (e.g., connection details) fabrication or design may significantly affect the strength and the reliability of a structure. Veneziano [65] points out that failures at very small (earthquake) intensities are primarily due to such errors rather than to the seismic load. Of course the knowledge that the system has survived previously applied loads ensures truncation of the resistance density at low intensity levels [65]. It is assumed herein that such errors are precluded, and that only "normal" strength uncertainty resulting from "normal" control is present.

In summary, this Chapter quantifies probabilistically floor level strength measures used to model the behavior of rigid frame structures with shear-beam type models. A detailed design is presented to illustrate the sources of uncertainty and the level of assumptions required.

3.2 FRAME BEHAVIOR

A typical building rigid frame is shown in Figure 3.1a . Assuming shear, buckling, and axial failure modes have been precluded, it generally exhibits static interstory shear vs. distortion behavior similar to that depicted in Figure 3.1b.

The exact form of the shear distortion behavior is a function of the relative strength and stiffness of the members and the loading conditions, i.e., presence of gravity loads, distribution of lateral loads along height, etc.. Pique [48] has quantified some of these dependencies for 4-story, 10-story and 16-story frames. His results will be referred to herein.

3.3 SHEAR BEAM MODELS AND PARAMETERS

As a first approximation, the simplest dynamic model for predicting the dynamic behavior of such a frame is generally the lumped mass, close-coupled shear beam system shown on Figure 3.2. Each spring is generally assumed to have one of the idealized shear-deformation relationships shown in Figure 3.3[48].

If strictly elastic behavior is to be modelled, only the stiffness K_1 needs to be estimated for each floor (Chapter 2 implicitly treated K_1 as random by assuming the natural periods of the structure to be random). If reliability is to be estimated and if a limit-elastic failure criteria is adopted as has been done herein, a limiting resistance (R, R', etc.) or distortion (Δ_Y,Δ_Y', etc.) measure of strength must be defined. Of course if inelastic behavior is to be predicted, the full-range of the shear

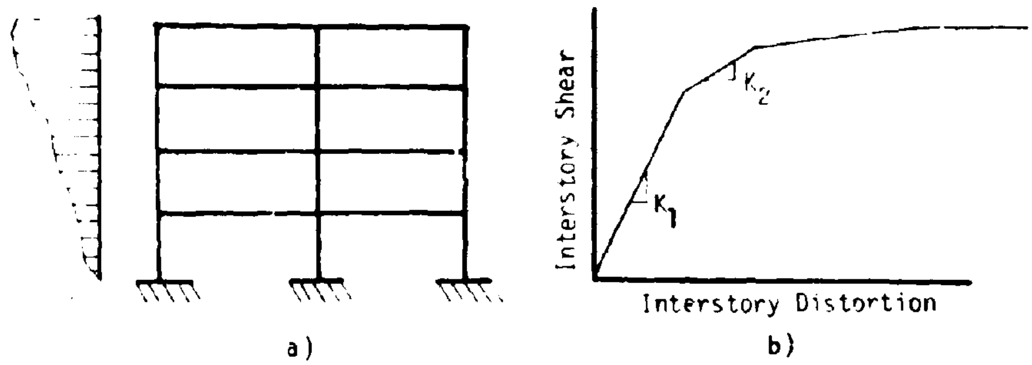

FIGURE 3.1 - TYPICAL BEHAVIOR OF A RIGID FRAME SUBJECTED TO LATERAL LOADS

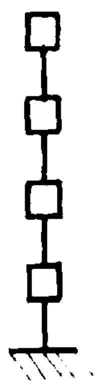

FIGURE 3.2 - SIMPLE DYNAMIC MODEL OF RIGID FRAME

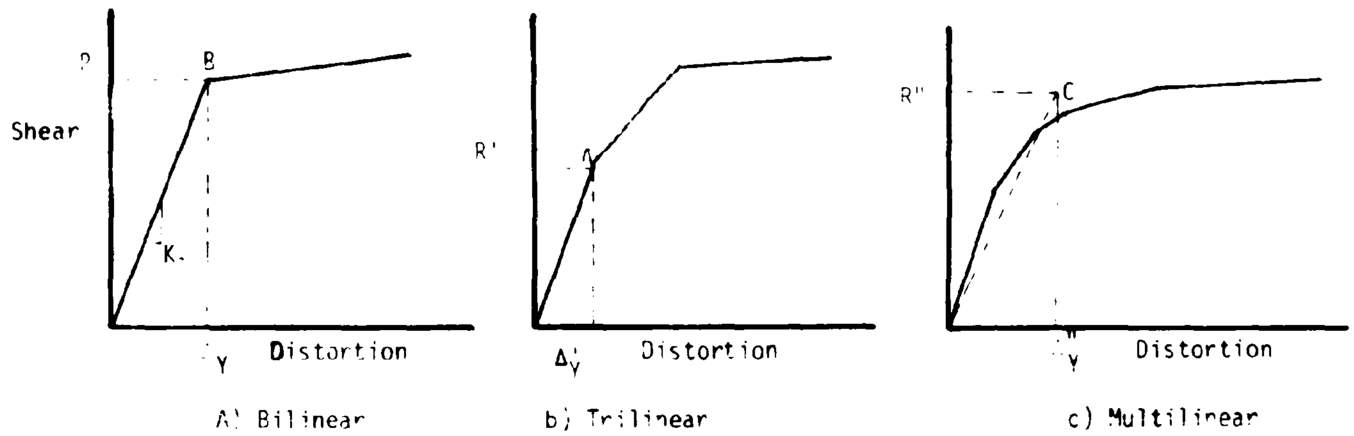

FIGURE 3.3 - IDEALIZED SHEAR-DISTORTION CHARACTERISTICS FOR A STORY IN A RIGID FRAME

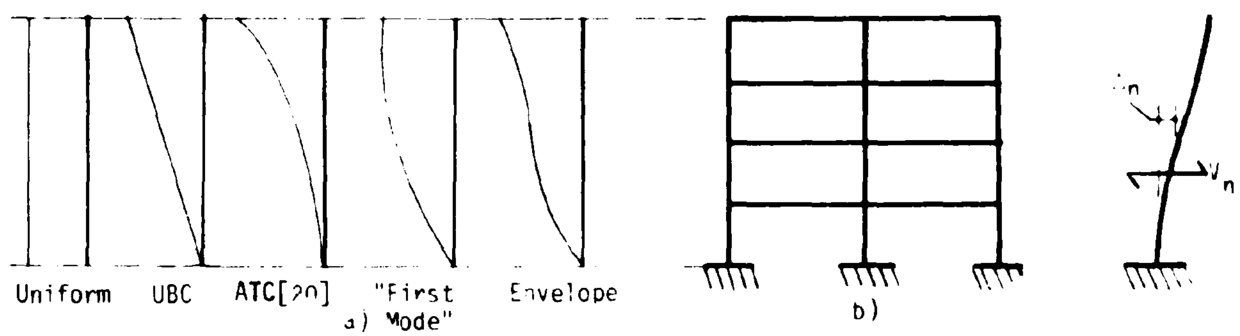

FIGURE 3.4 - METHODOLOGY FOR COMPUTING SHEAR-DISTORTION CHARACTERISTICS OF A STORY IN A RIGID FRAME

distortion properties must be defined. Roesset and Piqué [48], and Anagnostopoulos [29] have recently examined the relative merits of alternate methodologies for defining spring properties for purposes of inelastic dynamic analysis. To illustrate the types of uncertainties inherent in the shear-beam model, such methodologies are briefly discussed herein.

3.3.1 Stiffness K_1

The stiffness K_1 is fictitious in the sense that other displacements are allowed to occur at the same time as the individual interstory distortion of interest. Generally, Eq. (3.1) [29]

$$K_1 = \frac{24E}{h^2}\left\{\frac{1}{\frac{2}{\Sigma K_c} + \frac{1}{\Sigma K_{g,a}} + \frac{1}{\Sigma K_{g,b}}}\right\} \tag{3.1}$$

ΣK_c = Sum of column stiffnesses I/L in a story

$\Sigma K_{g,a}$ = Sum of girder stiffnesses in floor above

$\Sigma K_{g,b}$ = Sum of girder stiffnesses in floor below

is used to estimate K_1. The main assumptions used in deriving Equation (3.1) are that the column shears above and below a joint are equal and that the rotation of all joints in a floor are equal. Equation (3.1) reduces to the classical linear, lateral stiffness of fixed-end bending members as $\Sigma K_{g,a}$ and $\Sigma K_{g,b}$ approach ∞. Equation (3.1) does not account for the decrease in lateral stiffness because of axial deformation in the columns. Of course for concrete frames it is difficult to estimate proper values of E and I. An alternative procedure, followed by Piqué [48], is to perform incremental, nonlinear static analyses under lateral loads having assumed distributions as shown in Figure 3.4a) and to calculate the floor stiffnesses directly as:

$$K_1 = \frac{V_n}{\Delta_n} \tag{3.2}$$

The lateral stiffness obtained through such a methodology clearly includes the effects of column axial deformation. Piqué has found that the K_1 for the lower stories (for the three frames analyzed) is stable and independent (all values with $\pm$ 3%) of the type of load distribution considered. The stiffnesses of the higher stories, however, are sensitive to the type of load distribution and such sensitivity increases as the number of stories increases. Differences in stiffness ranging from 3% for the four-story structure to $\approx$ 15% for the sixteen story structure are noted [48] as the load distribution is changed.

In effect, then, even with a perfectly deterministic structure, the concept of an equivalent shear spring stiffness K_1 is a function of the type of excitation experienced.

3.3.2 Story Yield Strength

At the present only preliminary observations on the variability of shear-beam story yield strength for deterministic structures are available [48]. It is believed that such a strength measure is primarily dependent on the form of the strength interaction diagram for the individual beam column members, or, in a related way, on the type of failure mechanism which occurs. Several investigators [31,49] have formulated probabilistic descriptions of story yield strength conditional on the occurrence of a specified failure mechanism. It is apparent, in view of the paucity of data regarding mechanism uncertainty, and the difficulty of an analytical formulation, more meaningful reliability estimates may be made for structures in which such uncertainty is precluded.

3.4 DEFINITION OF STRENGTH MEASURE

Since an estimate of component safety is desired, and failure has been defined as exceeding a distortion level Δ_Y, it is necessary to arrive at a probability distribution of Δ_Y. To this end, Δ_Y must first be defined and the sources contributing to its uncertainty identified.

Several interpretations for Δ_Y may be used: Figure 3.3 illustrates three possibilities: the point A at which deviation from elastic behavior first occurs, the fictitious point B which corresponds to the intersection of the initial stiffness and the maximum resistance lines, or point C which is the intersection of a fictitious stiffness line (whose purpose is to provide an idealized curve with the same included area as the actual curve) with the maximum resistance line.

The point A is not a good measure of the strength of a story. It varies significantly with the actual magnitude of gravity loads. Additionally, considering steel structures, it will be highly dependent on the residual stress distribution of the members. The point C can only be defined a posteriori of an inelastic analysis. Hence the Δ_Y corresponding to point B is assumed herein to be the story yield level strength measure.

It is apparent that uncertainties in <u>both</u> R and K_1 affect the probability distribution of Δ_Y. Uncertainty in the level R is, in turn, a result of uncertain failure mechanisms (as noted previously) and strengths of individual members. Similarly, the fictitious K_1 may be dependent on the loading condition as well as uncertain individual member stiffnesses, uncertain joint conditions and the presence/stiffness contribution of nonstructural elements.

Only <u>one</u> of the above sources of uncertainty is explicitly considered herein, i.e.. the one arising from uncertain member strengths. Uncertainty in failure mechanism is precluded by the type of building discussed (see section 3.5). For purposes of defining Δ_Y from estimates of R, the stiffness <u>K_1 is assumed deterministic</u> at the value predicted by Equation (3.1). This approximation may be realistic for the 4-story building considered herein; Piquè has noted least variation in K_1 for the shortest rigid frames [48]. It must further be noted that no methodology is proposed herein to arrive at the entire probability distribution of Δ_Y, rather, a second moment description is attempted. Clearly an analytical probability distribution must subsequently be assumed to arrive at an estimate of safety.

It seems desirable, for purposes of comparison of design methods (Chapter 5), to arrive at the second moments of Δ_Y directly from a design load effect such as interstory shear. That is, it is desirable to avoid actual member design and simply state:

$$(\bar{\Delta}_Y, \sigma^2_{\Delta_Y}) = (k\Delta_{DES}, \sigma^2_{\Delta_Y}) = (k \frac{V_{DES}}{K_1}, \sigma^2_{\Delta_Y}) \tag{3.3}$$

The type of distribution is assumed as well as its variance, with the Δ_Y mean value a multiple of the design interstory distortion. Such an approach will be followed in Chapter 5. To arrive at acceptable values for k and $\sigma^2_{\Delta_Y}$, however, a more detailed approach is followed herein; i.e., actual members of a specific building are designed by a desired method and performance criteria and then the mean and variance of Δ_Y are predicted through a second moment approach.

3.5 EXAMPLE PROBLEM

The simplest example problem, a 2-D shear beam model, is first postulated as follows. A hospital structure with interstitial space (i.e., trusses between columns), unbraced, may behave in a manner which can be rightly represented by a simple shear beam model. Assuming symmetry, a 2-D model may be used for analysis. Figure 3.5 depicts the actual 4-story 2-bay structure which will be considered. For illustration (and since the methodology presented in Chapter 2 was for obtaining elastic load effects), it is assumed that the structure is to be as "seismically safe" as a nuclear power plant; therefore NRC-like seismic force levels, design philosophy and performance criteria are to be used. As an introduction, then, both the ACI-AISC and the NRC (like) criteria are briefly reviewed.

3.5.1 Design Criteria

ACI-AISC Criteria. The normal ACI-AISC design criteria, listed in Table 3.1, assume UBC-like seismic design load levels and performance criteria to arrive at load factors or allowable stress levels when seismic forces

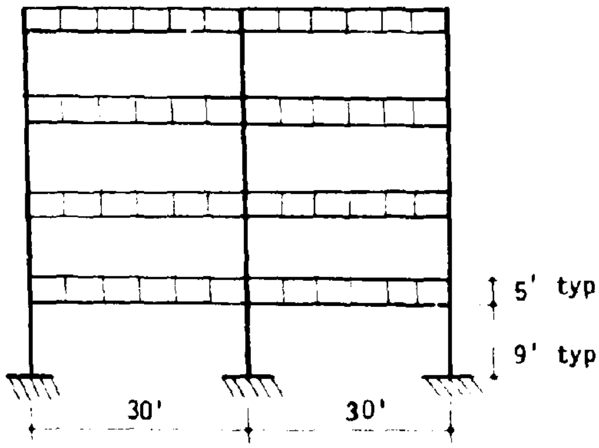

FIGURE 3.5 - SIMPLE FRAME TO BE DESIGNED FOR SEISMIC LOADS

ACI		Acceptance Criteria
Strength Design	$1.4D + 1.7L$ $.75(1.4D + 1.7L + 1.7W)$ $.75(1.4D + 1.7L + 1.1(1.7E))$ $.9D + 1.3W$ $.9D + 1.1\ (1.3E)$	ϕ *Strength $\geq$ Design Ultimate Load Effect
Alternate Design Method	All Load Combinations above with L.F. = 1.0	$f_c \leq .45\ f'_c$ $f_s \leq .4\ f_Y$ 1/3 Increase with W or E.
AISC		Acceptance Criteria
Plastic Design	$1.7(D + L)$ $1.3(D + L) + 1.3(E)$ $1.3(D + L) + 1.3(W)$	$\frac{P}{P_Y} + \frac{M}{1.18\ M_p} \leq 1.0$ $M \leq M_p$
Elastic Design	All Load Combinations above with L.F. = 1.0	AISC Allowable Stresses. 1/3 Increase with W or E.

TABLE 3.1 - ACI-AISC SEISMIC DESIGN CRITERIA

are included. Implicit in the design criteria is the fact that properly designed structures will have considerable capacity for ductile behavior during a real earthquake.

NRC Design Criteria - Stevenson et al. [51] have most recently summarized the design philosophy generally followed for nuclear power plants. Some key statements from that reference will be quoted herein.

To emphasize differences in performance criteria, he first states:

> "...the consequences of risk associated with postulated accidents or extreme environment effects require protection and evaluation of events in a range of 10^{-7} probability of occurrence per year during the life of the (NPP) structure. This compares to conventional structural design where probabilities of occurrences of phenomena explicitly considered in design are not less than 10^{-3} probability per year."

Further,

> "Central to extreme load design philosophy... is the reduction of structural safety factors as the probability of extreme load occurrence is also reduced. This in general requires that the actual response of structures to extreme loads must be predicted with a higher degree of confidence than is typically the case with conventional structures. As a result, quality control and quality assurance requirements... are considerably more stringent than would be the case for conventional structures."

And, more specifically regarding loads,

> "Conventional structures are usually designed for two levels of load which include the normal or service loads expected during the life of the facility and severe environmental loads which typically include the 25 or 50 year mean maximum wind and a design basis earthquake as defined by the UBC.... Nuclear facilities in addition to the two levels considered in conventional design are typically designed for a third load level termed the extreme load which includes such natural phenomena as the maximum earthquake potential for the site which considers the regional and local geology and seismology and local foundation conditions. It also includes tornado wind and associated airborne missiles as well as postulated design basis accident loads consisting of high energy ruptures which result in pipe break reactions and impingement loads, pipe whip and associated accident generated missiles and pressurization of building components, flooding and high thermal gradients."

Associated with the various load levels mentioned above are different behavior requirements. For NPP, Stevenson states:

> "... It has become common practice in compliance with Regulatory Agency requirements to use the same conventional structure service load behavior limits for both the service and severe load conditions ... extreme load behavior stress limits are typically increased approximately 2/3 above the service load WSD limits and for FLD (Factored Load Design) load factors are reduced to approximately 1.0..."

Neglecting consideration of extreme loads due to tornadoes (generally tornadoes are treated in the same way as SSE seismic loads), thermal gradients, accidents, hurricanes, swells and surges, tsunamis, missiles, etc., the following load combinations and acceptance criteria remain applicable. Distinction is made between concrete and steel as design materials and between WSD and FLD design methods.

I) CONCRETE STRUCTURES

A) Service load (or severe environmental) conditions

1) WSD

Load Combinations	Acceptance Criteria
D + L D + L + E D + L + W	ACI "alternate method" allowable stresses without a 33% increase

2) FLD

Load Combinations	Acceptance Criteria
1.4D + 1.7L 1.4D + 1.7L + 1.9E 1.4D + 1.7L + 1.7W 1.2D + 1.9E 1.2D + 1.7W	Member strength *$\phi \geq$ design load effect

B) Extreme load conditions

1) FLD

Load Combinations	Acceptance Criteria
D + L + E'	Member strength *$\phi \geq$ design load effect.

In the above, E indicates OBE seismic levels, E' indicates SSE seismic load levels, and W indicates approximately a "100-year" wind. It is to be noted that, under load condition A) the ACI normally includes a 0.75 load factor or a 33% allowable stress increase for load combinations which include W or E. The NPP criteria allow similar modifications only if thermal loads or transient pipe reactions are included in the load combinations. Also, for load condition B) only the FLD method is recommended, with load factors equal to 1.0.

II) STEEL STRUCTURES

A) Service load (or severe environmental) conditions

1) WSD

Load Combinations	Acceptance Criteria
D + L D + L + E D + L + W	AISC allowable stresses without 33% increase

2) FLD

Load Combinations	Acceptance Criteria
1.7D + 1.7L 1.7D + 1.7L + 1.7E 1.7D + 1.7L + 1.7W	Member plastic strength $\geq$ design load effect

B) Extreme load conditions

1) WSD

Load Combinations	Acceptance Criteria
D + L + E'	1.6*AISC allowable stresses

2) FLD

Load Combinations	Acceptance Criteria
D + L + E'	Member strength * 0.9 $\geq$ design load effect.

It is noted that for steel both WSD and FLD are acceptable design methods under extreme load conditions.

3.5.2 Design.

Beyond the initial choice of a structural material and preliminary static and dynamic analyses to estimate member sizes, member design consists of an iterative sequence of the following steps:

i) Eigenvalue solution to obtain T_i, Γ_i, ϕ_i

ii) Static and dynamic analyses

iii) Design for appropriate load effect combinations.

For simplicity, steel is chosen as the structural material. Uncertainty in individual member strength is, then, generally a function of only one variable, F_y [18,19] and WSD design methods may be applied for both service/severe load conditions and extreme load conditions. Three load conditions are considered:

Load Combination	Acceptance Criteria
1) D + L + E (or D + L + E'/2) 2) D + L + W	AISC allowable stresses
3) D + L + E'	AISC allowable stresses*1.6

Given Design Parameters

FRAME AS SHOWN IN FIGURE 3.5
FRAMES AT 20 ft O.C. (columns braced in weak direction)
DL = 80 psf
LL = 100 psf for floors, 30 psf for roof (no live load reduction)
WIND = 20 psf
SEISMIC SSE a_{max} = 0.2g NBK response spectrum
OBE a_{max} = 0.1g NBK response spectrum
DAMPING = 0.02

Design DL, LL, and W load effects

Table 3.2 contains (final iteration) design load effects for the column members as computed with a static frame analysis program.

Eigenvalue Problem Results

Shown in Table 3.3 are the (final) periods, mode shapes and participation factors as obtained by using APPLE PIE [53].

Member	P_{DL}	P_{LL}	P_W	P_{OBE}	P_{SSE}	M_{DL}	M_{LL}	M_W	M_{OBE}	M_{SSE}
1	83.6	86.1	8.2	61.0	121.8	23.2	41.5	24.6	180.6	371.2
2	62.4	60.0	4.2	38.2	76.5	31.1	54.5	15.9	176.8	345.5
3	41.2	33.5	1.6	19.0	37.8	31.1	53.0	9.4	139.1	278.1
4	20.1	7.5	.2	5.2	10.4	42.1	23.7	3.1	89.8	179.6
5	216.8	223.8	0	0	0	0	46.3	47.2	348.7	697.2
6	163.2	156.0	0	0	0	0	59.7	30.3	308.6	617.1
7	109.7	89.0	0	0	0	0	61.5	17.8	240.0	429.8
8	55.8	21.0	0	0	0	0	33.3	5.5	133.3	266.6

TABLE 3.2 - DESIGN LOAD EFFECTS (K, K-Ft)

		MODE 1	MODE 2	MODE 3	MODE 4
	T_i	.3166	.1307	.0819	.0585
	Γ_i	3.470	1.385	-.8186	.5598
FLOORS	$\phi_{4,i}$	.3886	-.3180	-.1248	-.0189
	$\phi_{3,i}$	.2803	.1894	.3708	.1272
	$\phi_{2,i}$	.1774	.3053	-.1748	-.3360
	$\phi_{1,i}$	.0840	.1946	-.2906	.3724

TABLE 3.3 - DYNAMIC MODEL PROPERTIES

Dynamic Analysis Load Effects

The program APPLE PIE was further used to obtain member design load effects utilizing the 2% damped NBK design spectrum normalized to 0.2g as seismic input. The entire set of spectra is shown in Figure 3.6 The conservatism of this design procedure is discussed in subsequent chapters. It is noted in Table 3.2 that the OBE load effects are one-half those of the SSE.

Final Design

Figure 3.7 indicates the final member sizes which satisfy the stated acceptance criteria for all the load combinations considered.

3.6 PROBABILISTIC DESCRIPTION OF Δ_Y

To reiterate, for the example at hand, failure mechanism uncertainty has been precluded as well as any other failure (shear, buckling, etc.) mode. The stiffness K_1 is assumed deterministic and the variable strength of the members is the only source which defines uncertainty in the yield level.

The following steps are then used to arrive at a second moment description of Δ_y.

1) Assume nominal P/P_Y
2) Choose nominal member M_p (AISC interaction formula)
3) Compute real mean values of plastic moment capacity

$$\overline{M}_p = Z * \overline{F}_Y$$

4) Using second moment formulation, arrive at $\overline{\mathbf{R}}$.
5) Assume correlations and compute σ_R'.
6) Assume deterministic stiffness and compute corresponding $\overline{\Delta}_Y$ and $\sigma^2_{\Delta_Y}$.

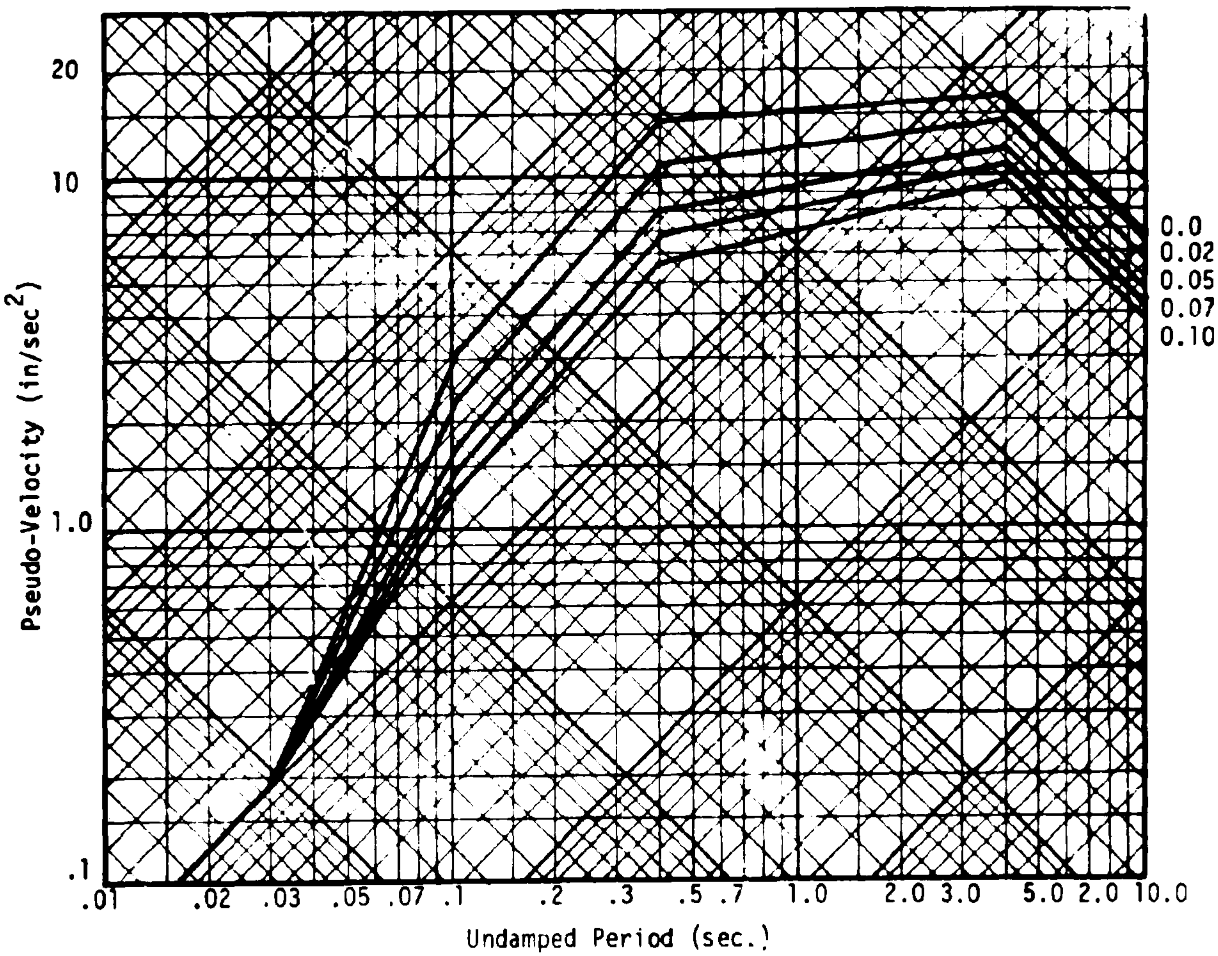

FIGURE 3.6 - NEWMARK, BLUME, KAPUR [45] DESIGN RESPONSE SPECTRA NORMALIZED TO a=0.1g

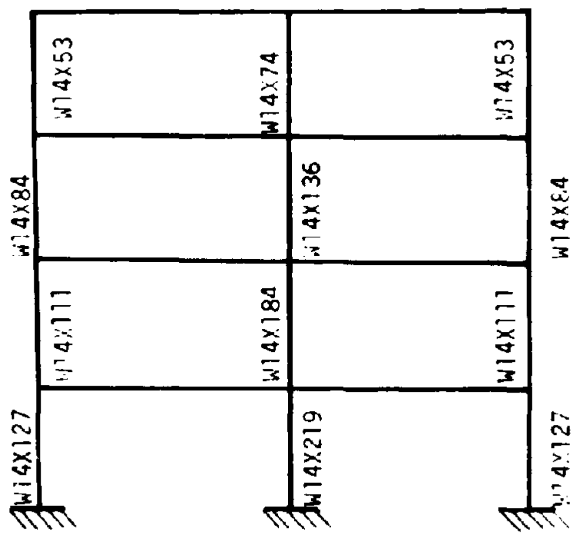

FIGURE 3.7 - FINAL DESIGN MEMBER SIZES

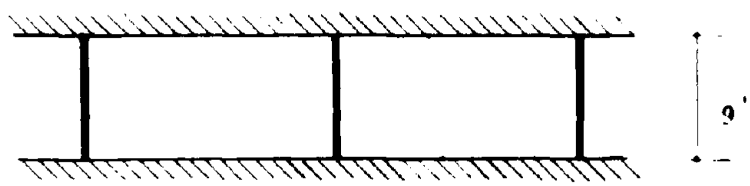

FIGURE 3.8 - IDEALIZED SYSTEM FOR DETERMINING SECOND MOMENTS OF STORY STRENGTH MEASURE

In 1) and 2) above, P is assumed to be the axial load due to $D + \frac{1}{4} L$. Table 3.4 gives the corresponding P/P_Y. It is seen that $P/P_Y < 0.15$ in all cases; therefore, according to the AISC, the full plastic moment capacity may be used for all the beam-column members.

3.6.1 Individual Member Plastic Moment Capacity

In connection with step three, given nominal section and steel properties, three alternatives are available to estimate actual mean beam plastic moment capacities. First, statistical information on the ratio $M_p/M_{p,nom.}$, if available, may be used directly. Second, since

$$M_p = Z * F_Y \tag{3.4}$$

observed statistics of the random variable F_Y may be assumed applicable to M_p if Z is considered deterministic. Third, a distribution (or second moments) for M_p may be derived from appropriate distributions (or second moments) of both Z and F_Y.

It is apparent that direct statistical data on the ratio $M_p/M_{p,nom.}$ is limited. Baker [19], in England, performed and reported some tests on two British wide flange sections of mild steel (approximately a W12x31 and a W18x64). A summary of the results is given in Table 3.5. Alpsten [18] reports similar data for Swedish steel shapes. Figure 3.9 [18] shows the cumulative density function of the ratio $M_p/M_{p,\ nom.}$ for sections of three different flange thicknesses. It may be observed that the mean of the ratio generally decreases as the size of the members (or the thickness of the component plates) increases. This is mainly due to the observed

Member	P	P/P_y	Z
1	100	.074	226
2	77	.065	196
3	50	.056	145
4	22	.039	87.1
5	273	.118	408
6	202	.104	338
7	1[illegible]2	.092	243
8	61	.078	126

TABLE 3.4 - P/P_y RATIOS FOR COLUMNS OF RIGID FRAME

Beam	Mill	No. of Samples	$\overline{M}_p/M_{P,nom.}$	COV
W12	All	13	1.21	.0488
	A	4	1.25	.0420
	B	5	1.22	.0138
	C	4	1.16	.0637
W18	All	10	1.09	.0645
	A	3	1.15	.0298
	B	2	1.04	—
	C	3	1.03	.020
	D	1	1.[illegible]4	—
	E	1	1.18	—

TABLE 3.5 - $\overline{M}_p/M_{P,nom.}$ STATISTICS FOR BRITISH W12 and W18 SECTIONS [19]

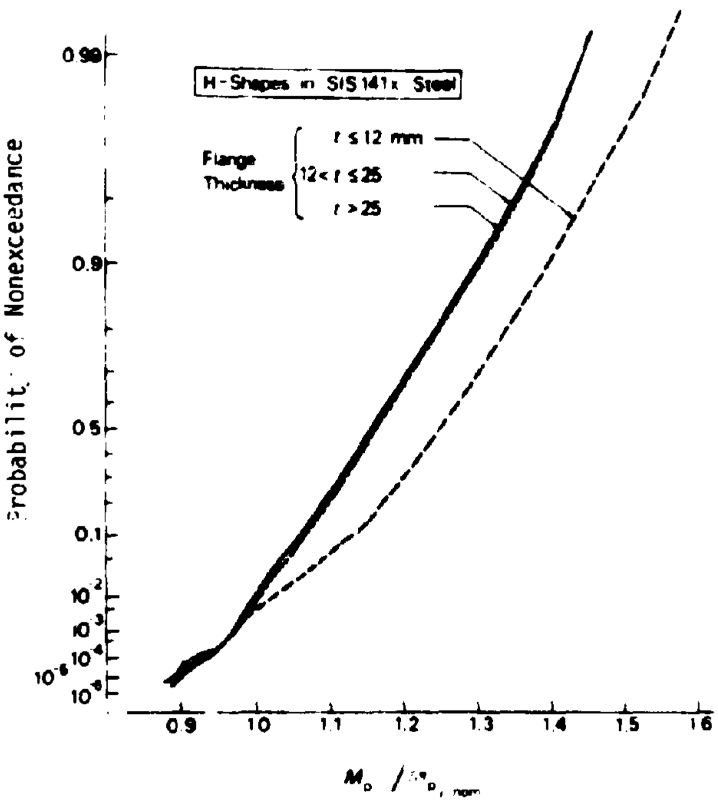

FIGURE 3.9 - CUMULATIVE DISTRIBUTION OF $M_p/M_{p,nom}$. FOR SWEDISH STEEL SHAPES [18]

fact that the mean yield stress of a steel decreases with sample sets of increasing thicknesses [19].

In relation to the second alternative stated above, Alpsten [18] and Baker [19] both conclude that variations in the cross-sectional properties of plates and sections from the nominal size are less important than variations in yield strength in governing the strength of structural members. Table 3.6, a summary version of data presented by Baker, indicates typical statistics for the thickness of mild steel plates (British). Data was lumped from four different mills.

$t_{nom.}$	$\bar{t}$	cov_z
.25	.254	.036
.50	.447	.018
.75	.744	.013
1.00	1.000	.010
1.25	1.248	.010
1.50	1.496	.009
2.00	1.992	.007

TABLE 3.6 - SECOND MOMENTS OF THICKNESSES OF BRITISH STEEL PLATES [19]

Also, Table 3.7 summarizes statistics for the plastic section modulus for two (British) W sections derived from a set which included samples from three mills.

Beam	$Z_{nom.}$ in^3	No. of	$\bar{Z}$	cov_z
W12	43.1	13	43.3	0.013
W18	136.2	10	135.0	0.02

TABLE 3.7 - SECOND MOMENTS OF THE PLASTIC MODULUS OF BRITISH W12 and W18 SECTIONS [19]

Making the assumption, then, that Z is deterministic, available statistical data for F_Y may, in theory, be utilized to evaluate the variability in M_p. In reality several precautions must be observed before yield point data may be interpreted. For one, Alpsten [18] notes that at least six alternate definitions of the yield point exist and are in use. Also, both Alpsten and Baker indicate that considerable variation can occur in the level of yield strength actually recorded because of the method of specimen preparation, the rate of loading, and the dynamic behavior of the testing machine.

Even assuming a common definition and testing procedure, the bulk of the data, which is in the form of mill test results, must still be carefully categorized. Assuming constant the factors which cause systematic variations in F_Y;i.e., nominal grade of steel or chemical composition, type of section rolled, thickness of finished material, and characteristics of the rolling and cooling processes, the yield strength remains a random variable which varies from mill to mill, within a cast or an ingot, along the length of the member, and within the member cross-section. Baker systematically identifies the relative importance of these sources of uncertainty [19].

Of primary interest is the fact that mill tests may or may not be highly correlated with member flexural strength depending on the location from which the specimen is taken. Table 3.8, a summary version of a table given by Baker, indicates various mean mill test yield values: $\bar{\sigma}_{YC}$ denotes the mean of the "mill certificate yield strengths," $\bar{\sigma}_{YSF}$ denotes the mean of the mill yield strengths using flange specimens and tested by the author, $\bar{\sigma}_{YSW}$ denotes the mean of the mill yield strengths obtained using web specimens and tested by the author.

Beam	Mill	No. of Samples	$\sigma_{Y,nom.}$	$\bar{\sigma}_{YC}$	$\bar{\sigma}_{YSF}$	$\bar{\sigma}_{YSW}$
W12	ALL	10	247 $\frac{N}{m^2}$	320.	263.4	284.6
W18	All	9	247 $\frac{N}{m^2}$	313.4	244.5	277.6

TABLE 3.8 - VARIOUS MEAN YIELD STRENGTHS FOR BRITISH W12 AND W18 SECTIONS [19]

It is to be noted that the "certificate mill strength": i.e., that supplied by the mill as proof of compliance with specifications, is significantly higher than the other values. This is generally true because a web sample is specified by British (as well as ASTM) standards and usually the upper yield strength [19] is recorded by a manufacturer. Table 3.9, also presented by Baker, shows that, in fact, the average mill certificate strength is poorly correlated with actual member flexural strength. The highest correlation is between the laboratory measured mean flange yield strength, $\bar{\sigma}_{YSF}$, and observed plastic capacity M_{PC}. $\bar{\sigma}_{YSF}$ is, in turn, from Table 3.8, very close to the specified minimum value.

	M_{PC}	$\bar{\sigma}_{YC}$	$\bar{\sigma}_{YSF}$	$\bar{\sigma}_{YSW}$
M_{PC}	1.0	.348	.916	.769
$\bar{\sigma}_{YC}$		1.0	.364	.485
$\bar{\sigma}_{YSF}$	SYM		1.0	.815
$\bar{\sigma}_{YSW}$				1.0

TABLE 3.9 - CORRELATIONS BETWEEN VARIOUS REPORTED YIELD STRENGTHS AND SECTION PLASTIC CAPACITY [19]

In view of the biases apparent in mill strength results, the few actual test results which measured $M_p/M_{P,nom.}$ are herein considered to form the most reliable basis for making an assumption regarding $M_{P,act.}$ Specifically, the following assumptions are made

$$\frac{\overline{M}_{P,\,act.}}{M_{P,nom.}} = 1.08 \qquad (3.5)$$

$$\mathrm{COV} = 0.08$$

The implication is that the nominal F_Y is approximately one standard deviation below the actual average $\overline{F}_Y$ of a member. To obtain actual average member plastic capacities, then, the values of the plastic section modulus listed in column three of Table 3.4 are multiplied by 1.08 (36) = 39 ksi.

3.6.2 Second Moment Formulation

In essence the second moments of the strength of the ductile, parallel system shown in Figure 3.8 are to be estimated. The appropriate equations are:

$$\overline{R} = \frac{1}{h} \sum_{i=1}^{n} \overline{M}_{P,i}$$

$$\sigma_R^2 = \frac{1}{h^2} \sum_{i=1}^{n} \sigma^2_{M_{P,i}} + \frac{1}{h^2} \sum_{i \neq j}^{n} \sum^{n} \sigma_{M_{P,i}} \sigma_{M_{P,j}} \rho_{ij}$$

where ρ_{ij} = correlation coefficient between the i and j cross section capacities

n = number of sections attaining their full capacities at system failure.

The assumptions are made that cross-sections at the ends of a member are perfectly correlated (i.e., $\rho = 1$) and that separate members are uncorrelated. The above assumptions are consistent with the trends found by Baker [19]. He concluded that the variation in yield strength in the direction of rolling is small in comparison with variation across the section for any particular bar rolled from a single ingot. Separate members, implying different sizes or plate thicknesses, different "heats" of steel and cooling rates are essentially random selections from a population. (Of course, in a concrete building the strength of adjacent columns, which are likely poured from the same batch of concrete, may be highly correlated). For the specific example being considered, the above equations reduce to:

$$\bar{R} = \frac{\bar{F}_Y}{h} (4Z_1 + 2Z_2)$$

$$COV_R = COV_{F_Y} \cdot \frac{\sqrt{3}}{2} \quad \frac{\sqrt{2 + (Z_2/Z_1)^2}}{2 + Z_2/Z_1} \tag{3.7}$$

where the subscript 1 indicates exterior column properties and 2 indicates interior column properties. Table 3.10 lists the computed values for the four floors. Also shown in Table 3.10 is the ratio of the R value to the interstory shear, V, from the SSE dynamic analysis. The increase in the ratio from the top story to the bottom is indicative of the greater influence of gravity loads in determining column sizes.

Floor	$\bar{R}$ - K	COV_R	V-K	$\bar{R}$/V
4	217.	.0405	139	1.56
3	386.	.0407	231	1.67
2	528.	.0410	291	1.81
1	621.	.0412	323	1.93

TABLE 3.10 - RATIOS OF MEAN STORY LATERAL STRENGTHS TO COMPUTED SEISMIC INTERSTORY SHEARS

3.6.3 Deterministic Stiffness

An assumption must now be introduced regarding the deterministic stiffness in order to arrive at second moments of Δ_Y from the data of Table 3.5. It is useful to note that, for this model, the column axial stiffnesses significantly affect the lateral stiffness of the frame. Figure 3.10 shows two lateral stiffness matrices: a) is obtained using actual column areas, b) is obtained using arbitrarily large column areas. b) is essentially the expected lateral stiffness matrix which represents true shear beam behavior and which is predicted by Equation 3.1 as $\Sigma K_{g,A}$ and $\Sigma K_{g,B}$ approach ∞.

$$
\begin{matrix}
30.42 & -13.93 & 0.10 & 0.00 \\
 & 23.78 & -10.03 & 0.06 \\
 & & 15.43 & 5.57 \\
\text{SYM.} & & & 5.41
\end{matrix}
\qquad\qquad
\begin{matrix}
34.98 & -15.93 & 0.01 & 0.00 \\
 & 27.32 & -11.41 & 0.01 \\
 & & 17.62 & -6.22 \\
\text{SYM.} & & & 6.22
\end{matrix}
$$

a) b)

FIGURE 3.10 - LATERAL STIFFNESS MATRICES. K/FT * 10^{-3}

By using actual column areas, then, the lateral stiffnesses are approximately 85% of those predicted by shear beam behavior. The other dynamic properties, i.e., participation factors, and mode shapes are essentially the same for the two models, although the fundamental period decreased from 0.317 sec. to 0.291 sec. as the column areas were made arbitrarily large.

For the example herein, the lateral stiffnesses given by Figure 3.10b were used to compute corresponding average yield levels $\bar{\Delta}_Y$; the results are given in Table 3.11. Although Table 3.10 shows slight differences in COV's of resistances of the floors, a common COV = 0.04 is assumed for all the floor yield levels.

Floor	$\bar{R}$-Kips	K- K/FT * 10^{-3}	$\bar{\Delta}_Y$ - FT
4	217	6.22	0.0348
3	386	11.4	0.0338
2	527	15.9	0.0330
1	620	19.0	0.0326

TABLE 3.11 - COMPUTED MEAN VALUES OF STORY STRENGTH MEASURE Δ_Y

3.6.4 Distribution Assumption

The additional assumption of a normal probability distribution for Δ_Y is finally made. The appropriateness of this assumption may be supported by observed statistical distributions of steel yield strength. Baker, having defined a single population as:

> "All the plates or sections of a single nominal size and grade of steel rolled by a single mill during a period of time when the production process is statistically in control."

concludes that sets of yield strengths are effectively normally distributed [19]. He does further state, however, that lumping yield strength data from a set of mills tends to result in distributions which are significantly positively skewed. Even for such data, Baker concludes that, at low strengths, the cumulative frequency of the sample data follows the normal distributions more closely than the lognormal. Of course it is the low strengths that are more significant in controlling reliability.

3.6.5 Discussion

The main limitation of the example given herein is that it does not quantify uncertainty in Δ_Y due to an unknown failure mechanism and stiffness. It appears that mechanism uncertainty must first be studied empirically: i.e., structures must be designed and an appropriate program (FRIEDA [12]) used to observe and quantify uncertainty in "yield levels." Only then may probability of failure estimates be made reliably for general plane frames.

It is likely that concrete frames exhibit more nonlinear behavior and have more uncertainty in both stiffness and strength than do steel frames. Hence quantifying a single yield level for concrete is much more difficult.

3.7 SUMMARY

This Chapter examined the type of uncertainties involved in defining a strength measure to be used in conjunction with a shear beam model. A structure was designed and second moments of the yield interstory displacements were calculated. A normal strength distribution was assumed. With the capability to obtain load effect distributions as developed in Chapter 2, the data developed herein casts the prediction of failure probabilities into a standard form: i.e., a numerical solution of Equation (3.8) may be performed.

$$P_F = 1 - \int_0^{\infty} f_R(r) F_L(r)\, dr \qquad (3.8)$$

where $F_L(r)$ = Cumulative density function of a load effect.

$f_R(r)$ = Probability density function of the resistance measure.

The following Chapter presents results of such calculations as well as a procedure for the use of seismic risk information to arrive at an overall assessment of safety.

CHAPTER 4

ESTIMATION OF FAILURE PROBABILITIES

4.1 INTRODUCTION

Utilizing the work described in the previous chapters, reliability estimates are derived herein for the structure designed in detail in Chapter 3 and the shear beam models introduced in Chapter 2. Story reliabilities, conditional on occurrence of an intensity a_{max}, are first evaluated. Seismic risk analyses are then briefly reviewed and overall story reliabilities are estimated. Comparisons and evaluations of the results in view of estimates developed by other investigators are then made. Finally, the assumptions required for an assessment of system reliability are briefly explored.

4.2 CONDITIONAL STORY RELIABILITY

4.2.1 Structure Designed in Chapter 3, T_1 = 0.317 sec.

Chapter 3 derived moments of the distributions of Δ_Y (Tables 3.10,3.11) a limiting distortion which defined the story strengths of the four-story structure. The assumption was then made that Δ_Y was normally distributed. A distribution of load effects for that structure, conditional on a peak intensity, must then be computed (using the method described in Chapter 2) to arrive at reliability estimates.

The results of the eigenvalue problem, Table 3.3 , define the structure. The parameters ω_g, S', ζ and T_o/T_c are assumed to be lognormally distributed with parameters given by Table 2.8, repeated here.

	m	V
ζ	.02	.75
T_o/T_c	.85	.33
ω_g	12 1/sec.	.50
S'	8 secs.	.75

TABLE 2.8 - MOMENTS OF LOGNORMAL DISTRIBUTIONS OF PARAMETERS ζ, T_o/T_c, ω_g, S'

The justifications for such parameters are given in Chapter 2. It is important to note again that the ω_g and S' moments were derived from the 39 earthquakes listed in Table 2.2 . Attempts to further categorize a site by using statistics derived from a chosen subset of all the earthquakes were not made. As an example, Figure 4.1 shows the resultant conditional (on $a = a_{des.} = 0.2g$) distribution of the first floor interstory distortion.

As noted in Chapter 3, the problem of calculating conditional failure probabilities has been cast in a standard form. Therefore, assuming independence of load effects and capacities, Equation (3.8) can be evaluated numerically for several conditional load effect distributions. Figure 4.2 shows resultant probabilities of exceeding yield levels Δ_Y in a story, conditional upon a seismic occurrence of intensity $a/a_{des.}$ The sensitivity of these curves to the actual design spectrum used will be partially quantified in Chapter 5.

4.2.2 Models Defined in Chapter 2

Deterministic interstory distortions were computed for the $T_1 = 0.377$ sec. and $T_1 = 1.13$ secs. models defined in Table 2.5 , using the

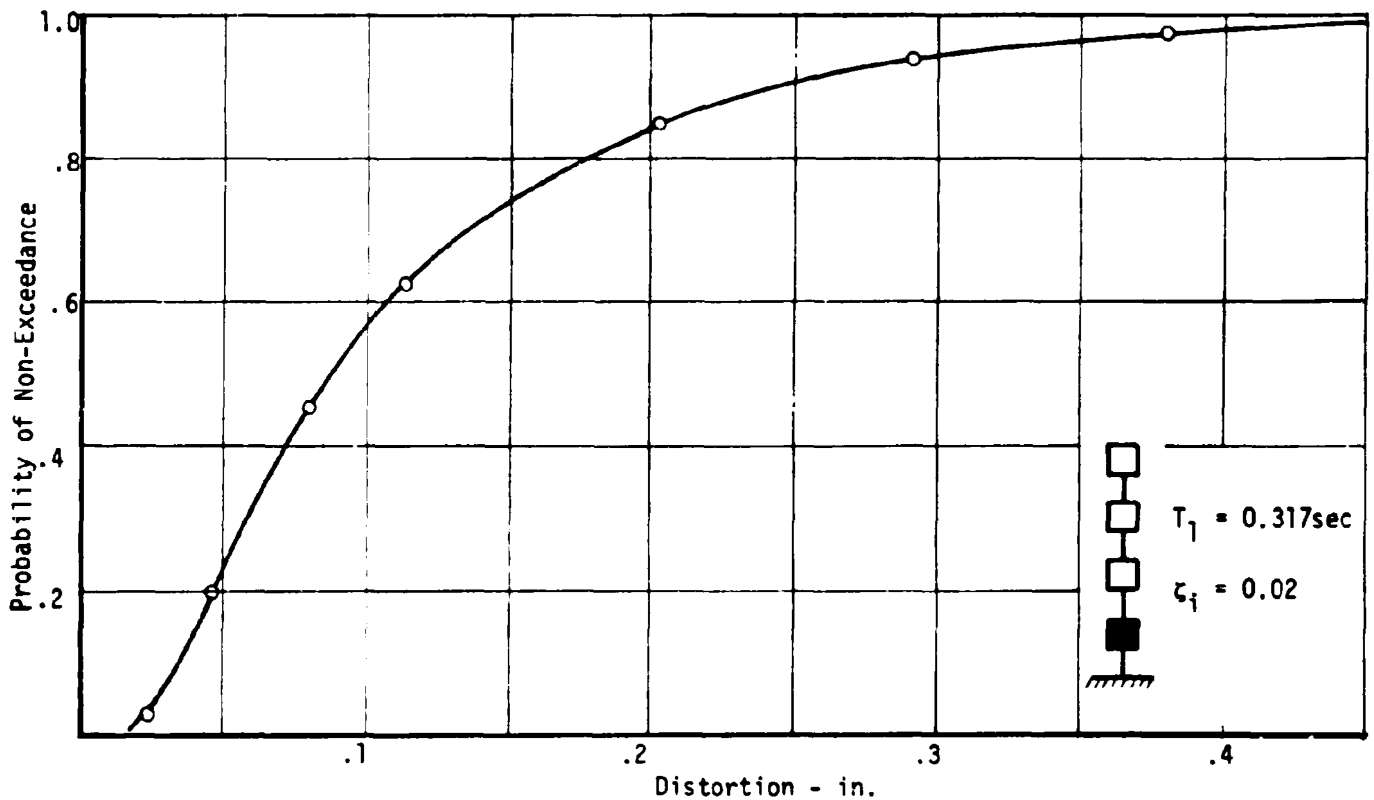

FIGURE 4.1 - CUMULATIVE DISTRIBUTION OF 1^{ST} FLOOR INTERSTORY DISTORTION CONDITIONAL ON a = 0.2g

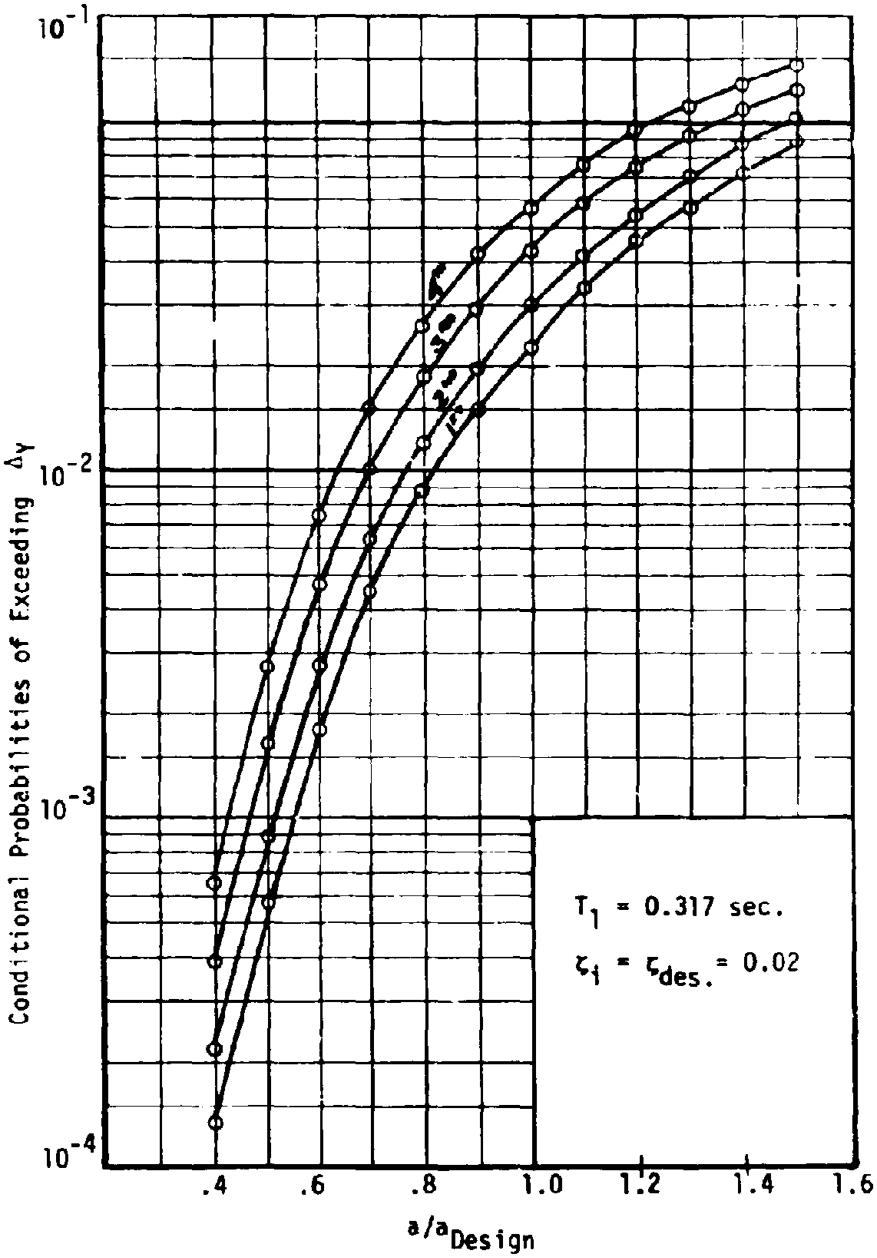

FIGURE 4.2 - CONDITIONAL PROBABILITIES OF EXCEEDING STRENGTH MEASURE Δ_Y FOR EACH STORY

same seismic design procedure (NBK, $\zeta_{des.} = .02$, $a_{des.} = 0.2g$) as in Chapter 3. Table 4.1 shows the computed results.

Story	$T_1 = 0.377$ DD	$T_1 = 1.13$ DD
1	.51	2.17
2	.45	1.92
3	.33	1.42
4	.18	.76

TABLE 4.1 - DESIGN INTERSTORY DISTORTIONS (in)
NBK 2% SPECTRUM $a_{des.} = 0.2g$

In lieu of a complete design, then, the strength measure, Δ_Y, is assumed to be normally distributed with moments

$$\bar{\Delta}_Y = \bar{c} = 1.5 * (\text{Design Interstory Distortion}) = k * DD$$

$$V_{\Delta_Y} = V_c = 0.10 \tag{4.1}$$

Using the conditional load effect distributions derived in Chapter 2, conditional probabilities of failure were computed; Figure 4.3 shows the results. It is to be noted that for the same design spectrum the conditional failure probabilities are greater for the longer period structure. This may be attributed to the larger dispersion in the load effect distributions of the $T_1 = 1.13$ sec. structure; a consequence of normalizing load effect distributions to peak ground acceleration.

Sensitivity of Conditional Failure Probabilities

It is pertinent to check the sensitivity of the resultant conditional probabilities to the assumptions made regarding V_c, k and $\zeta_{des.}$

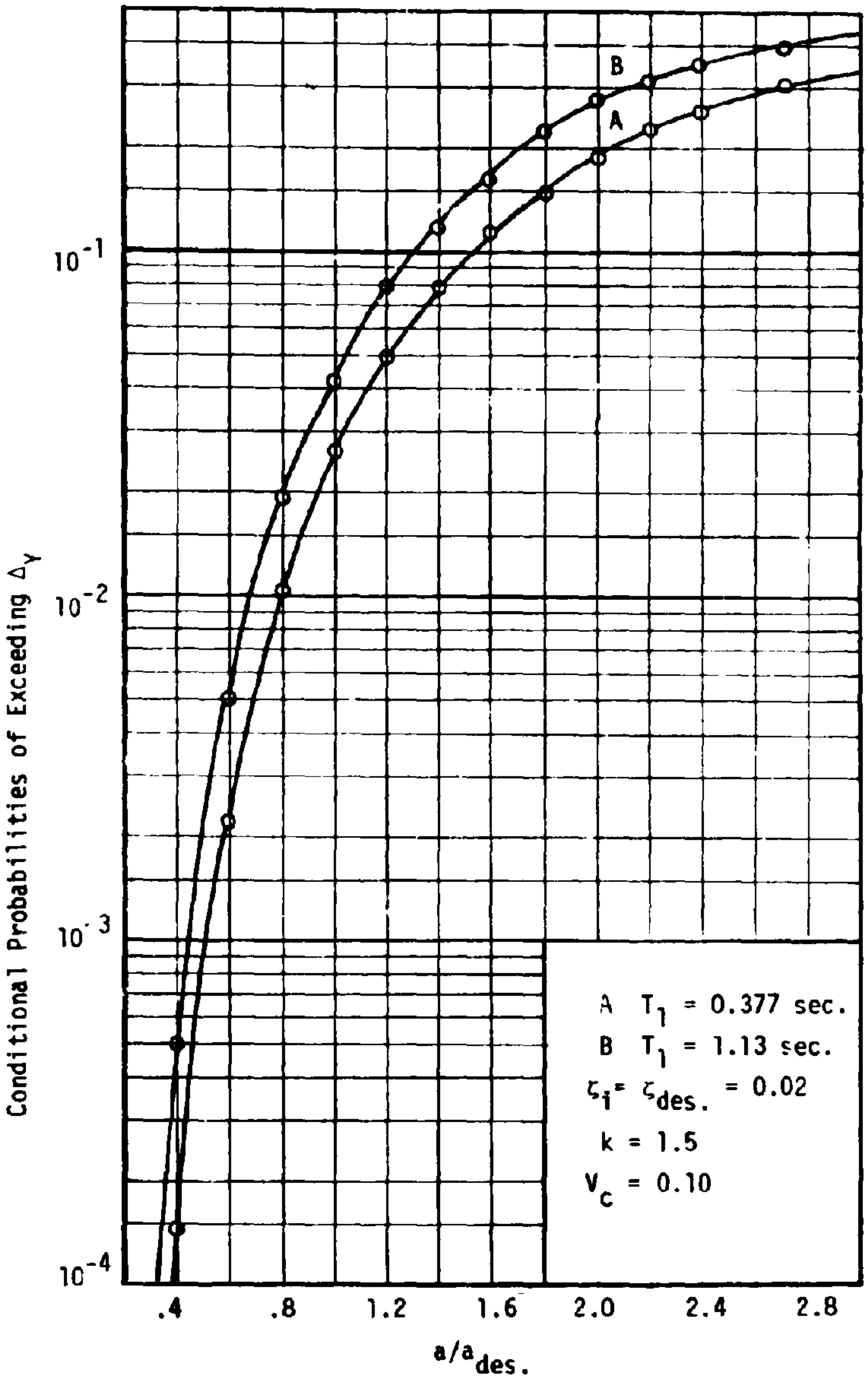

FIGURE 4.3 - CONDITIONAL PROBABILITIES OF EXCEEDING STRENGTH MEASURE Δ_Y IN FIRST STORY

Figures 4.4 and 4.5 indicate the resultant effects on first-story conditional failure probabilities as V_c is varied, keeping $\zeta_{des.}$ and k constant. It may be noted that the effects are similar for both structures. Increasing V_c affects conditional failure probabilities ($P[F|a/a_{des.}]$) due to small a/a_{des} ratios the most. This is understandable since $P[F|a/a_{des.}]$ for low a/a_{des} ratios are most dependent on the probability of having very low strengths which increases as V_c increases. As V_c grows large (i.e., $V_c \simeq 0.4$) the strength distribution becomes very broad, hence even for small a/a_{des} ratios significant conditional failure contributions arise, which, when combined with the higher probability of achieving such low intensities, may even become the dominant contributions to the overall story failure probability. Veneziano [65] similarly noted that for models having large statistical uncertainty in the resistance parameter, overall risk contributions may even increase with decreasing intensity and that such cases are characterized by "the presence of an intensity range below the mean resistance which contributes rather uniformly to the seismic risk." In any case, it is likely that, given survival of a system under normal loads, a truncated strength distribution is more appropriate. In lieu of using such a truncation, a lognormal strength probability distribution was assumed for $V_c = 0.4$, resulting in conditional failure probabilities which are believed to be more representative for such broad strength distributions.

Figures 4.6 and 4.7 also show the effects on the first floor conditional failure probabilities as k is varied, keeping $V_c = 0.10$ and $\zeta_{des.} = 0.02$. It is observed that, unlike the intensity dependent effects of

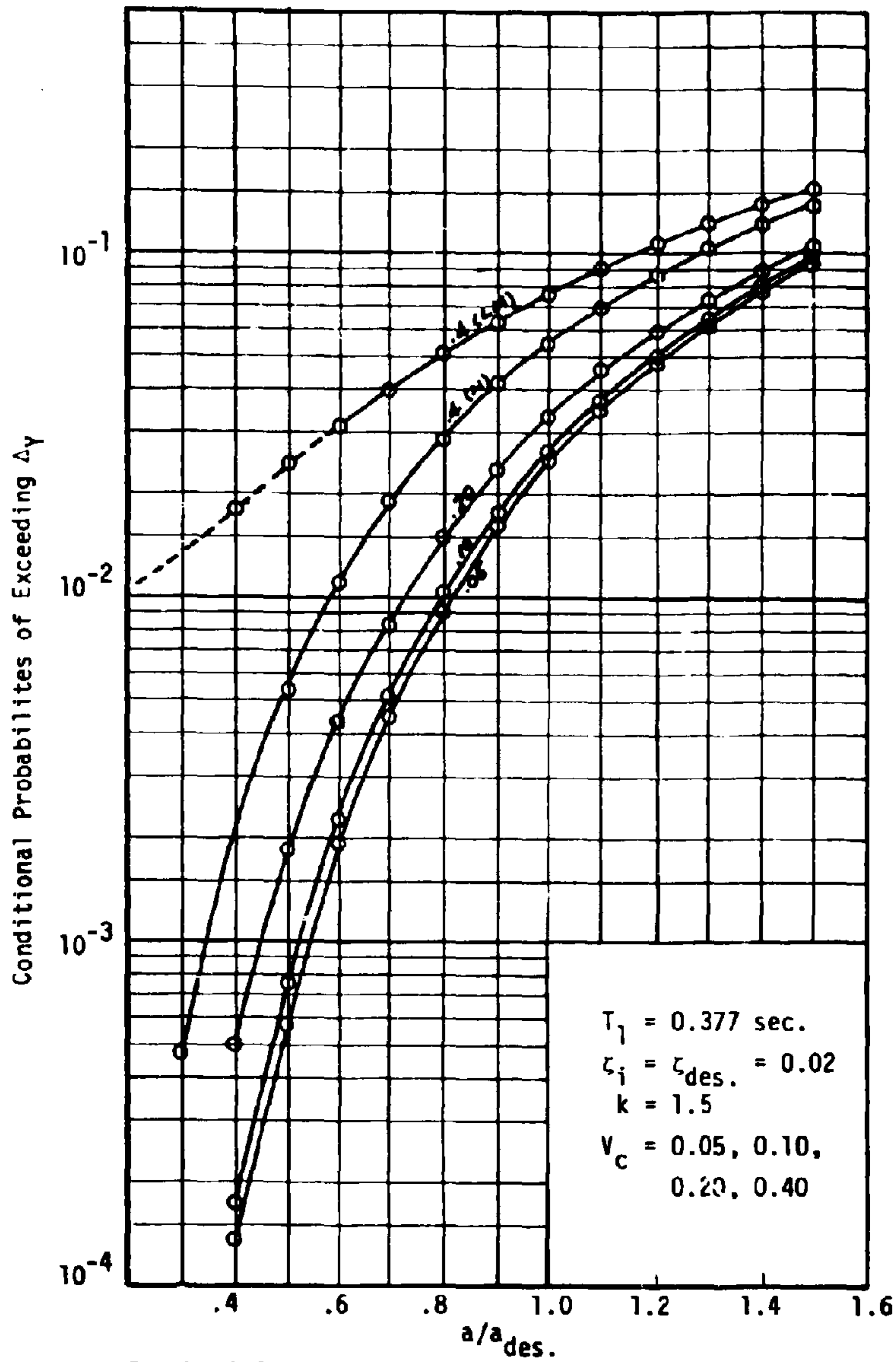

FIGURE 4.4 - CONDITIONAL PROBABILITIES OF EXCEEDING STRENGTH MEASURE Δ_Y IN FIRST STORY

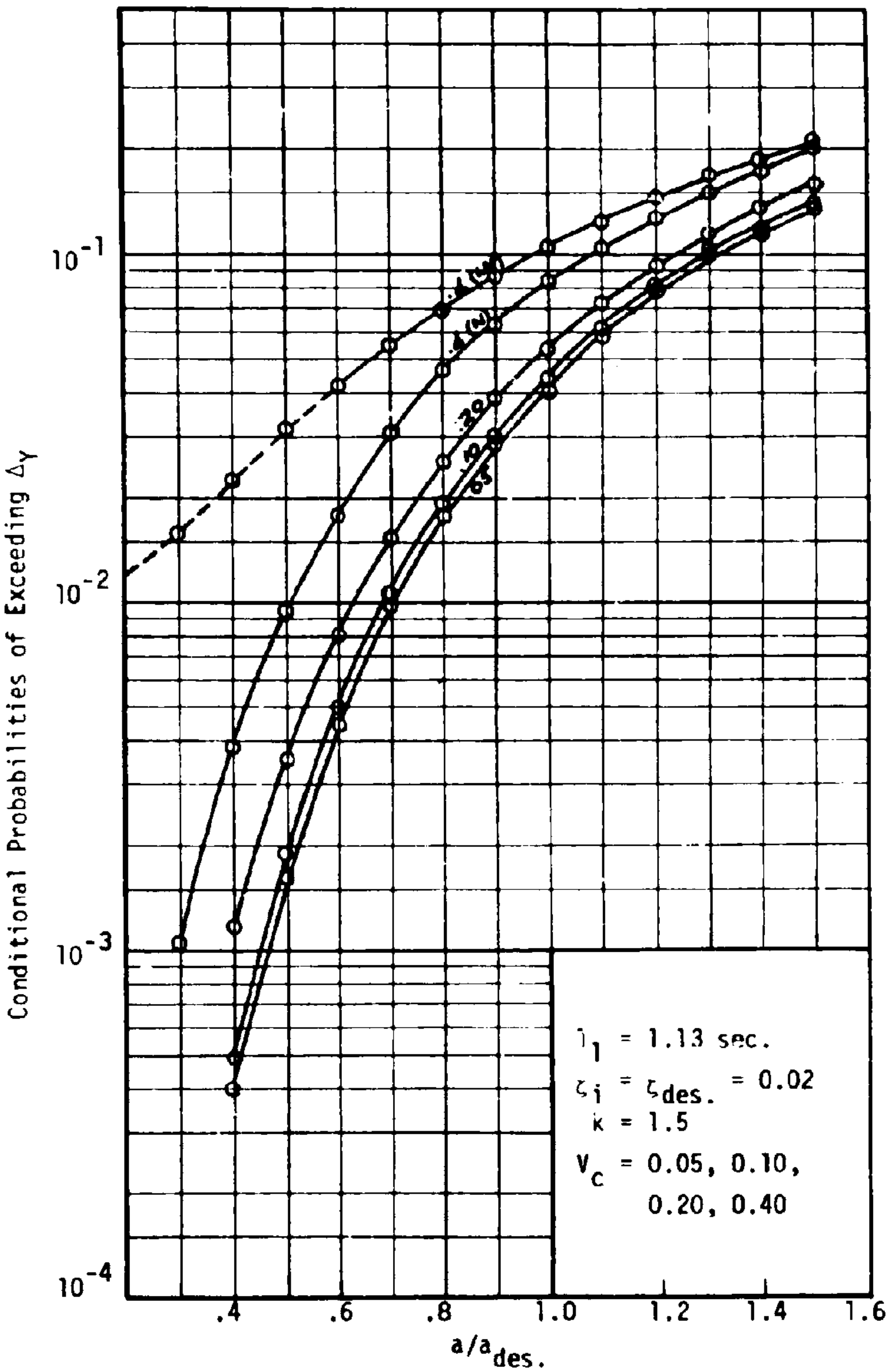

FIGURE 4.5 - CONDITIONAL PROBABILITIES OF EXCEEDING STRENGTH MEASURE Δ_Y IN FIRST STORY

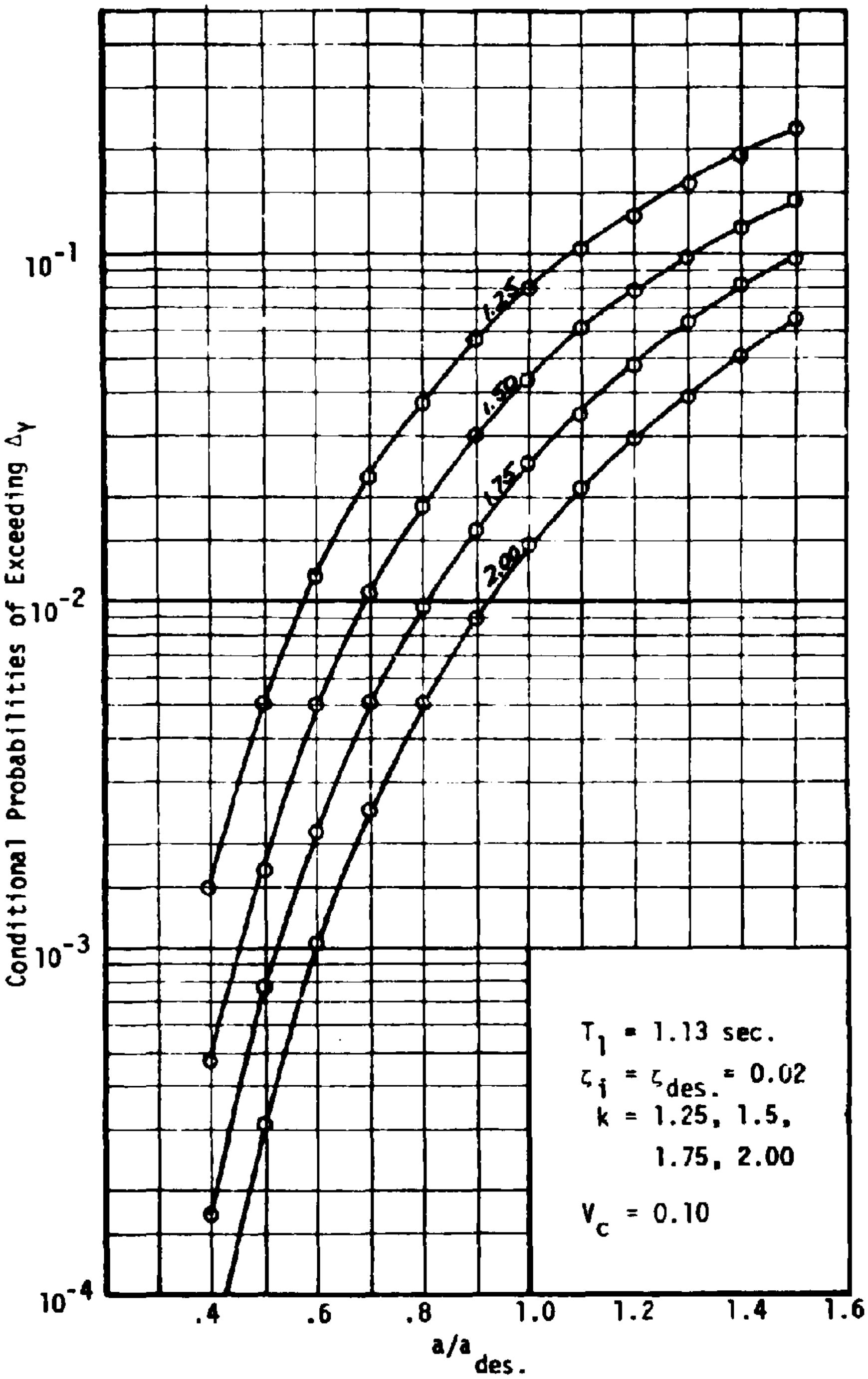

FIGURE 4.6 - CONDITIONAL PROBABILITIES OF EXCEEDING STRENGTH MEASURE Δ_Y IN FIRST STORY

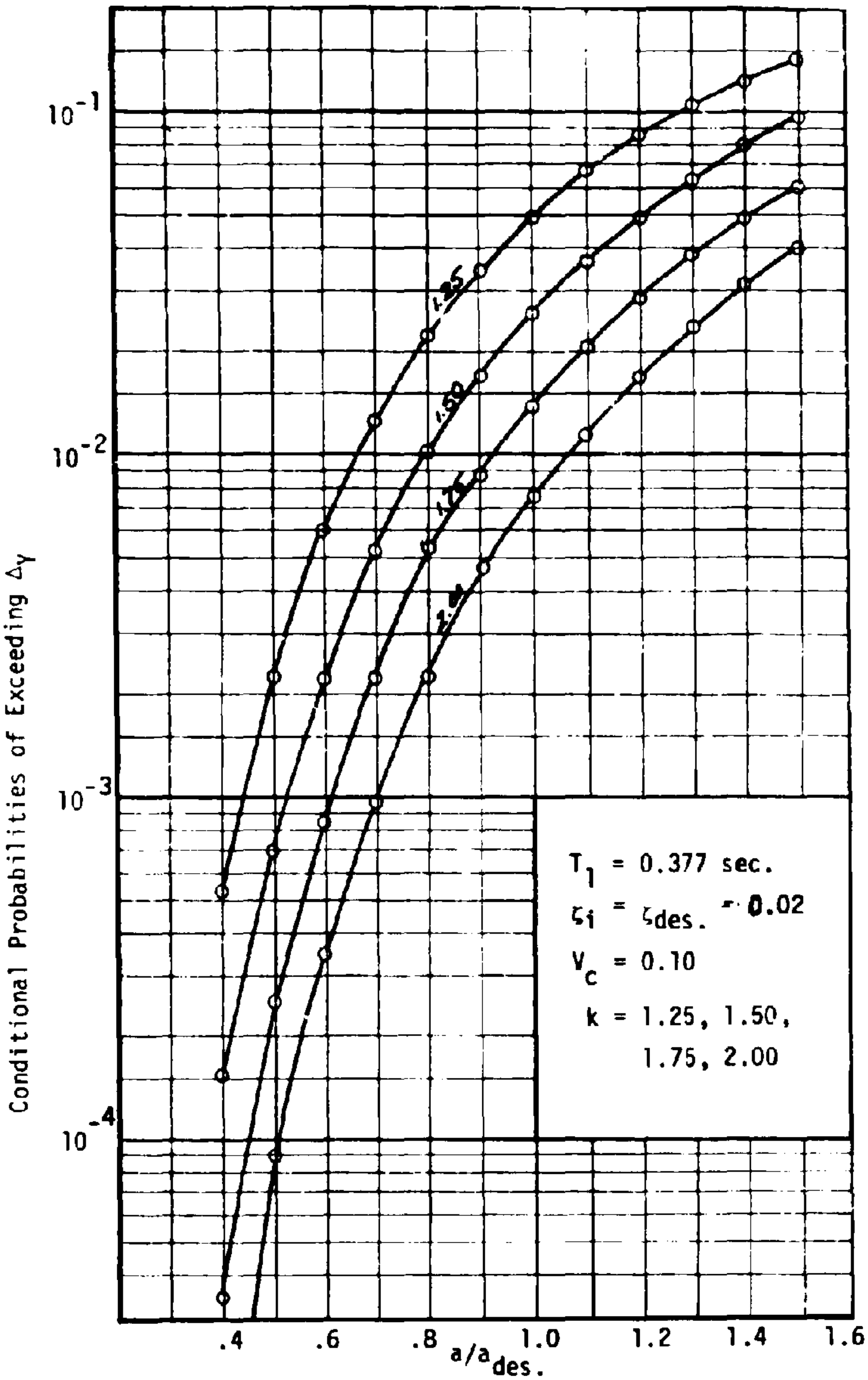

FIGURE 4.7 - CONDITIONAL PROBABILITIES OF EXCEEDING STRENGTH MEASURE Δ_Y IN FIRST STORY

V_c variation, the curves are essentially shifted with different k assumptions. Hence uncertainty in the mean strength is of greater importance in computing conditional failure probabilities at high (design) intensities.

Lastly, design interstory distortions were computed with the NBK spectrum ($a_{des.}$ = 0.2g) using alternate assumptions for $\zeta_{des.}$. The results are shown in Table 4.2

	T_1 = 0.377 sec.			T_1 = 1.13 sec.		
Floor	$\zeta_{des.}$=.005	$\zeta_{des.}$=.02	$\zeta_{des.}$=.05	$\zeta_{des.}$=.005	$\zeta_{des.}$=0.02	$\zeta_{des.}$=.05
1	.75	.51	.39	2.53	2.17	1.47
2	.66	.45	.34	2.23	1.92	1.30
3	.49	.33	.25	1.65	1.42	.96
4	.26	.18	.14	.89	0.76	.52

TABLE 4.2 - INTERSTORY DISTORTIONS (in.) COMPUTED USING ALTERNATE NBK SPECTRA ($a_{des.}$ = 0.2g)

It is to be noted that the mean of ζ and its distribution for purposes of arriving at load effect distributions remained the same (i.e., $\bar{\zeta}$ = 0.02) Hence the effect of alternate $\zeta_{des.}$ assumptions is a shift in the strength distribution; i.e., alternate k values are implied. Figures 4.8 and 4.9 indicate variability in $P[F|a/a_{des.}]$ for the two structures designed using alternate ζ's$_{des.}$ with k = 1.5 and V_c = 0.1 constant. For the T_1 = 1.13 sec. model, the $P[F|a/a_{des.}]$ curve for $\zeta_{des.}$ = 0.005 is essentially the same as the case $\zeta_{des.}$ = 0.02, k = 1.75, V_c = 0.10 in Figure 4.7 . This is true since, in effect, the mean resistance is essentially equal for the two (i.e., m_c = 2.53 (1.50) ≈ 2.17 (1.75)).

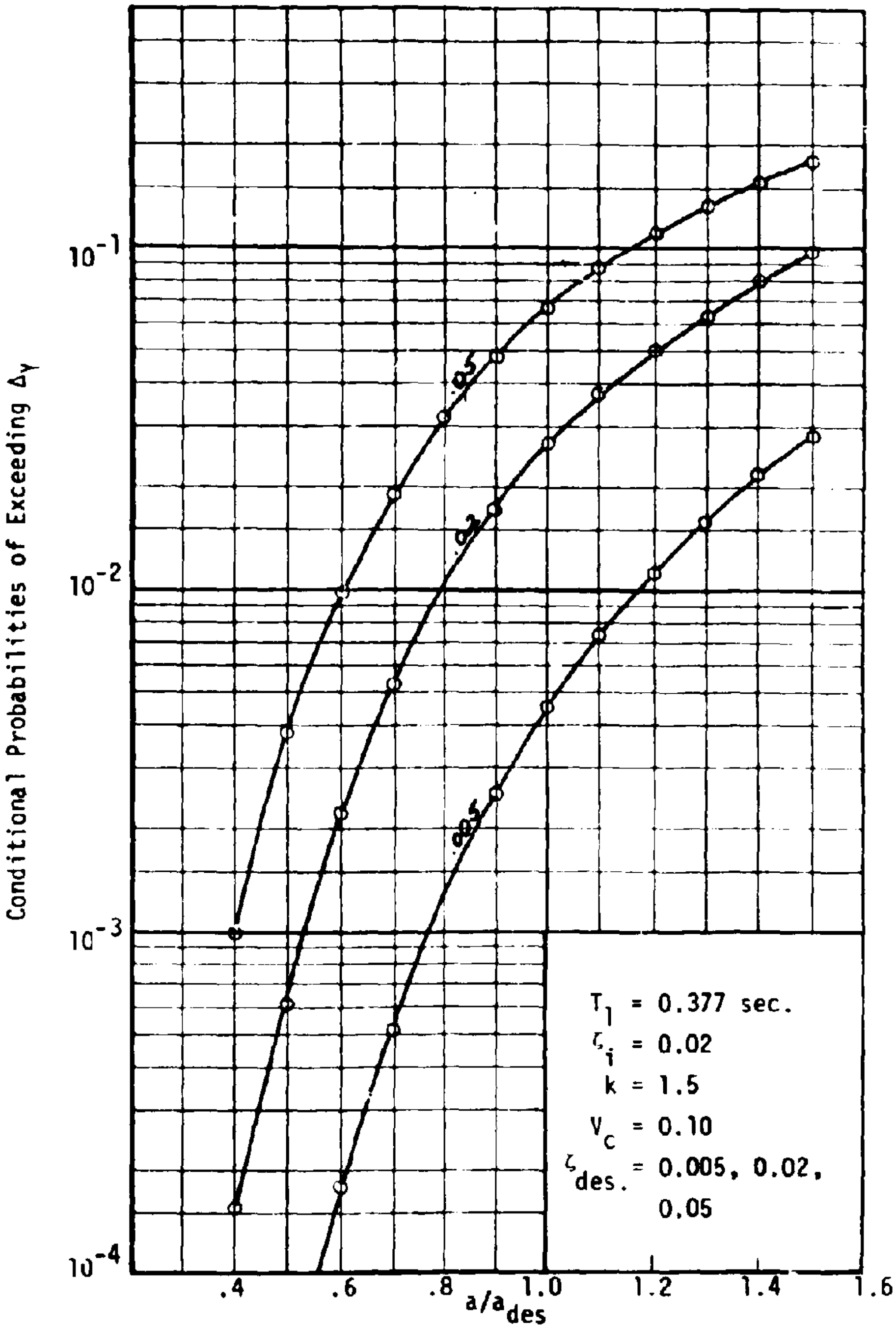

FIGURE 4.8 - CONDITIONAL PROBABILITIES OF EXCEEDING STRENGTH MEASURE Δ_Y IN FIRST STORY

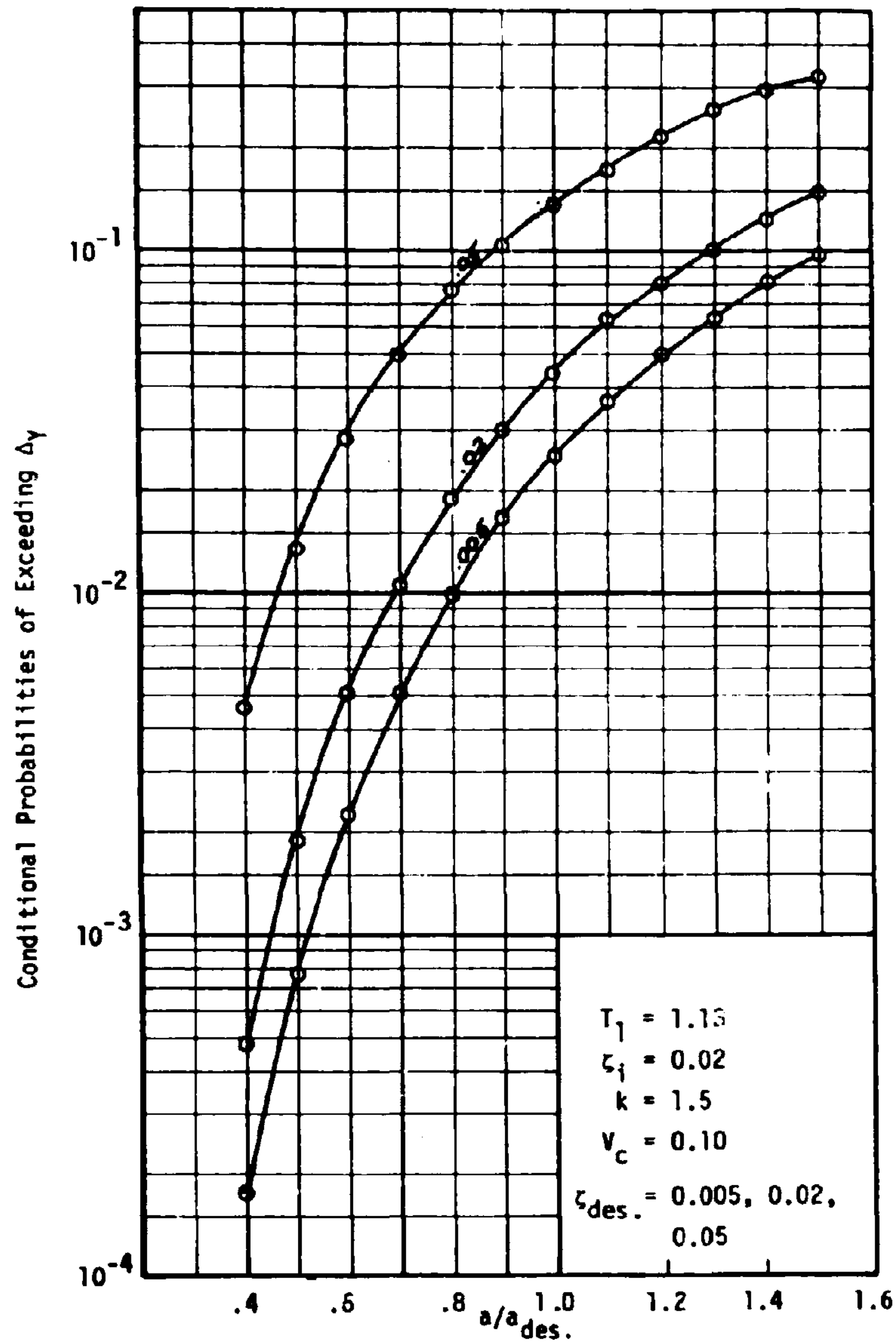

FIGURE 4.9 - CONDITIONAL PROBABILITIES OF EXCEEDING STRENGTH MEASURE Δ_Y IN FIRST STORY

4.3 SEISMIC RISK

The intent herein is simply to use available seismic risk information derived from established methodologies to arrive at overall estimates of reliability. It is important, however, to review the major assumptions made and the inherent uncertainty in a seismic risk estimate.

The final result of a seismic risk analysis is a statement regarding the probability of occurrence of a site intensity measure in time. Most commonly the site intensity measures are peak ground acceleration or MMI when the seismic history includes only a few, if any, instrumental magnitude or site acceleration recordings. Other site intensity measures, i.e., v_{max}, d_{max}, S_V, σ_a, $|f(\omega)|$ may also be used to quantify the seismic risk.

The mathematical methods to arrive at risk statements, as developed by Cornell [24], involve assumptions of models concerning:

1) The rate of occurrences of earthquakes of varying magnitude
2) The relation between magnitude, peak ground intensity and the distance R from the site to the epicenter.

It is known that uncertainty in the assumed models and/or their parameters, called statistical or "inductive" uncertainty, exists. Seismic risk analyses may or may not include it in arriving at a final statement of intensity vs. probability [6,65]. Veneziano [65] has recently quantified the effects of statistical uncertainty through penalty factors on "probabilistic" failure rates; i.e., those obtained without considering statistical uncertainties. His estimates of failure probabilities will be further discussed in Section 4.4.3.

Figures 4.10 and 4.11 illustrate two seismic risk curves. Figure 4.10 was derived by Donovan [17], using methods developed by Cornell, for the San Francisco Bay area. Figure 4.11 was derived by Cornell and Merz for a Boston site. Roughly, if intensity at a certain probability is lognormally distributed, the "most likely" risk curve may correspond to the mode of the distribution and the "Bayesian" risk curve may correspond to the mean of the distribution. It must be noted that such risk information is meant to apply to firm ground or rock sites only, and must be modified for soft ground sites.

Since the Cornell-Merz curve is used herein to arrive at "overall" failure probability assessments, assumptions made in its development are briefly stated. First, since there is no history of recorded strong motion near Boston, the analysis was made in terms of Modified Mercalli Intensity (MMI). Statistical uncertainty in the models and other assumptions was included; Figure 4.12 shows the reported range as a result of different assumptions regarding the attenuation laws, upper bounds on intensities, and geometric configuration of earthquake source areas. These different assumptions were subsequently combined in a Bayesian fashion by assigning the various alternatives relative weights reflecting the subjective degree of belief in each exclusive alternative. Curve BWE is the resultant Bayesian Weighted Estimate seismic risk curve. To arrive at Figure 4.11, i.e., site seismic risk in terms of peak group acceleration, nominal values of peak ground acceleration were assigned to various intensity levels and assigned a weight of 0.50. It was further assumed that, given a particular predicted intensity, an " acceleration

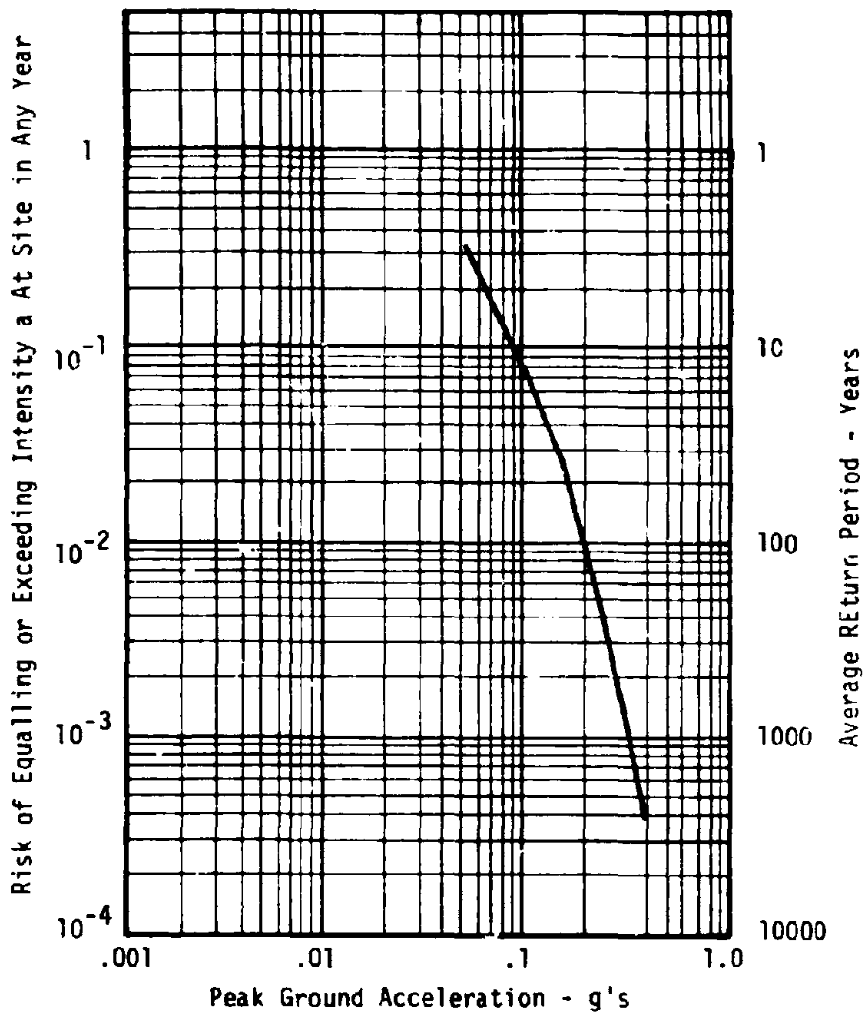

FIGURE 4.10 - SEISMIC RISK CURVE FOR CALIFORNIA SITE (Donovan [17])

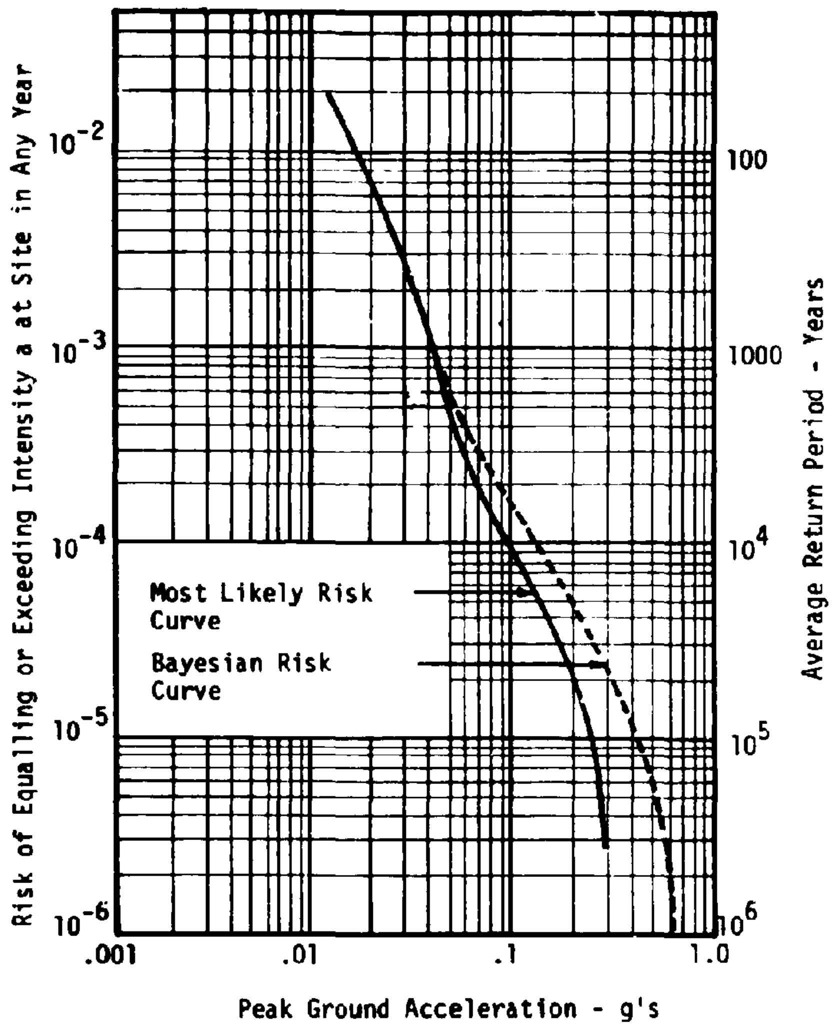

FIGURE 4.11 - SEISMIC RISK CURVES FOR BOSTON SITE (Cornell [6])

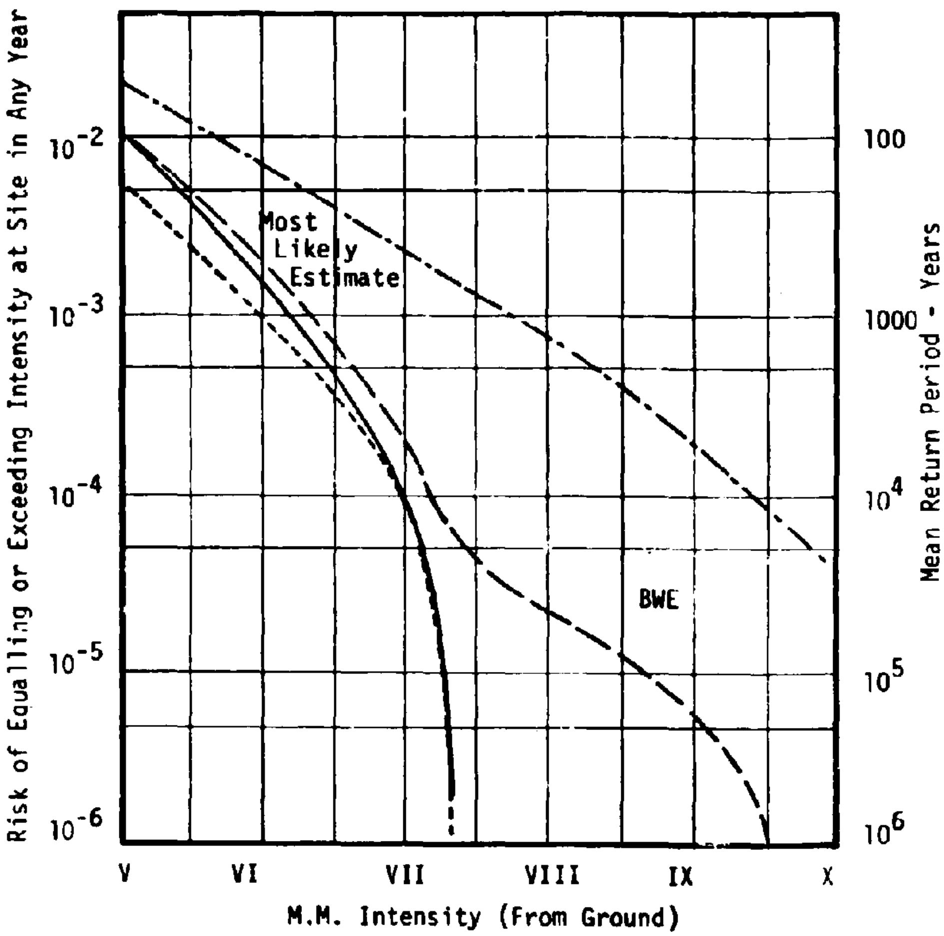

FIGURE 4.12 - RANGE OF POSSIBLE SEISMIC RISK PREDICTIONS FOR BOSTON (Cornell [6])

value one level below (about one half) or one level above (about twice) the nominal value might be experienced." These upper and lower values were each assigned probabilities of 0.25.

4.4 OVERALL STORY RELIABILITY

The conditional story reliability results as derived in Section 4.2 may then be combined with the seismic data given by Figures 4.10 and 4.11 by the approximate numerical expression:

$$P_F = \sum_{\text{All } a_o} P[F|a_o]\ (P[a \geq a_o - \Delta a] - P[a \geq a_o + \Delta a]) \quad (4.2)$$

to obtain mean annual floor probability of failure estimates. Specifically such computations were performed on the three structures considered in Section 4.2 using the Cornell-Merz "most likely" risk curve.

4.4.1 Examples

Structure Designed in Chapter 3, T_1 = 0.317 sec.

Figure 4.13 shows contributions to the overall probability of failure for each floor, i.e., contributions to the summation in Equation (4.2), arising from various $a/a_{des.}$ ratios. It can be seen that significant contributions arise from the entire range of likely intensities, with maximum contributions from acceleration intensities ≈ $1.2a_{des.}$. Individual contributions are very sensitive to seismic risk ordinates and deviations from the smooth curve are due to errors in reading of the seismic risk curve. Table 4.3 contains the sum of all contributions or

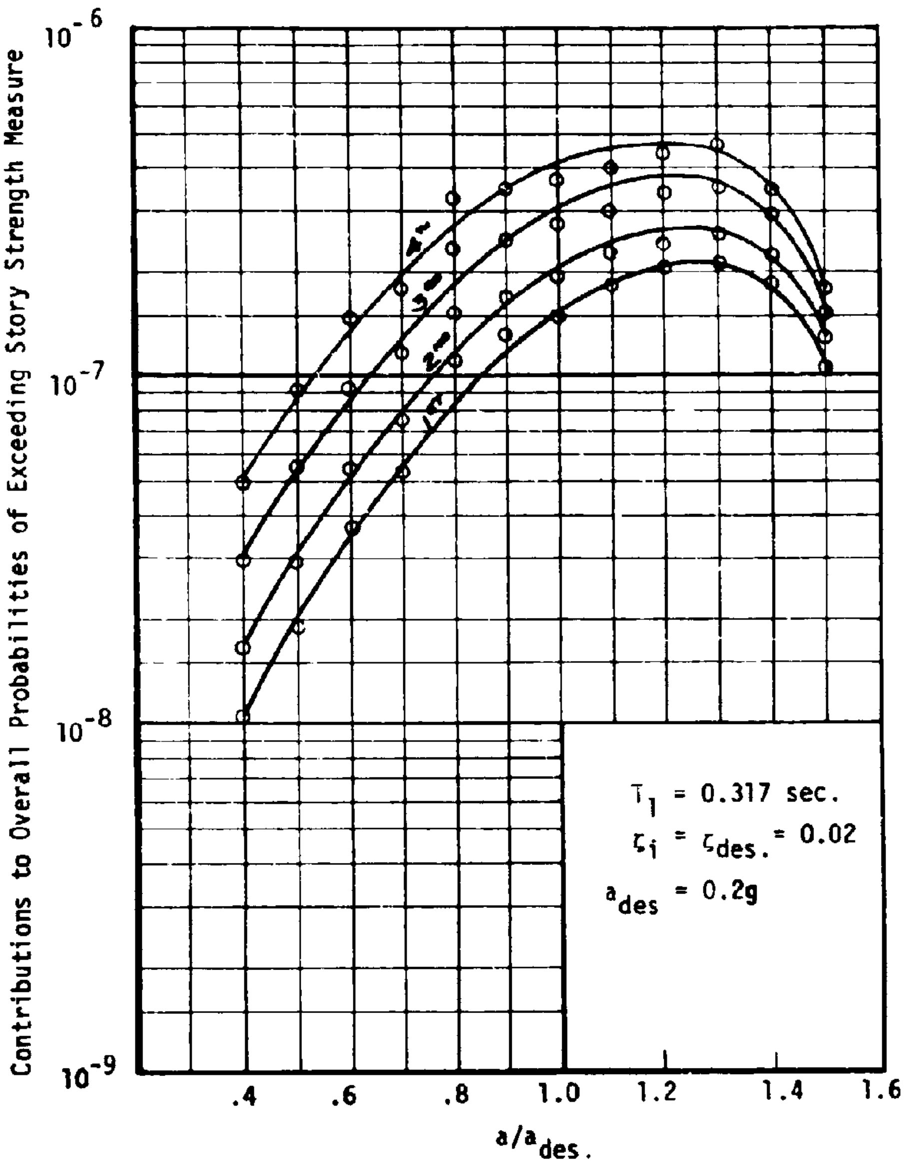

FIGURE 4.13 - CONTRIBUTIONS TO OVERALL PROBABILITIES OF EXCEEDING STORY STRENGTH MEASURES - CORNELL-MERZ SEISMIC RISK CURVE

the overall probabilities of exceeding the yield level interstory distortions.

Story	$P[\Delta \geq \Delta_Y]$
1	1.40
2	1.76
3	2.48
4	3.29

TABLE 4.3 - OVERALL PROBABILITIES OF EXCEEDING FLOOR YIELD LEVELS * 10^6

Comparison of such estimates with those of other investigators is made in Section 4.4.3. Sensitivity of such results with k, V_c, and the seismic risk assumptions is quantified for the subsequent models only.

<u>Models Defined in Chapter 2 by Table 2.5</u>

Analogous failure probabilities for the T_1 = 0.377 sec. and T_1 = 1.13 sec. models are given in Table 4.4. To reiterate, the design assumptions were: $\zeta_{des.}$ = 0.02, NBK design spectrum with $a_{des.}$ = 0.2g, k = 1.50, V_c = 0.10 and normally distributed strength (unless indicated).

Story	T_1 = 0.377	T_1 = 1.13
1	1.55	2.59
2	1.41	2.24
3	1.73	3.03
4	2.12	4.47

TABLE 4.4 - OVERALL PROBABILITIES OF EXCEEDING FLOOR YIELD LEVELS * 10^6

4.4.2 Sensitivity

The parameters k, V_c, $\zeta_{des.}$ and the seismic risk curve may be varied about their best estimates to observe the sensitivity of the probability of failure estimates. Tables 4.5 through 4.7 indicate the results of such studies for the T_1 = 0.377 sec. and T_1 = 1.13 sec. models. Tables 4.5b and 4.6b show that failure probabilities remain essentially constant for $0.05 \leq V_c \leq 0.2$. For the T_1 = 0.377 sec. model, an order of magnitude change in failure probabilities results as $\zeta_{des.}$ is varied from 0.005 to 0.05 (remembering that to obtain load effect distributions $\bar{\zeta} = 0.02$).

Table 4.7 indicates variation in overall failure probabilities as the seismic risk curve is shifted from the "most likely" position. Roughly, at the probability ordinate corresponding to $a = a_{des.} = 0.02g$ on the "most likely" risk curve, the Bayesian curve predicts a = 0.3g (see Figure 4.11). Therefore as an indication of possible risk variations, the entire curve was shifted to predict intensity levels 50% above and below those of the most likely curve. It may be seen that resultant probabilities vary by factors ranging from 50 to 100 for the seismic risk range considered. For the T_1 = 1.13 sec. structure, however, variation in $\zeta_{des.}$ from 0 to 0.05 causes as great effects on overall reliabilities as a shift from "most likely" seismic intensities to values 50% greater.

4.4.3 Significance of Failure Estimates

Failure has been defined herein as exceeding a story level limit-elastic response in a structure designed by NRC-like seismic design criteria. Clearly then, given the different seismic design and failure criteria inherent in the UBC and similar codes, the failure estimates

Story	V_c = 0.05	V_c = 0.10	V_c = 0.20	V_c^* = 0.40
1	1.5	1.6	2.0	3.8
2	1.3	1.4	1.8	3.5
3	1.6	1.7	2.2	4.1
4	2.0	2.1	2.7	4.9

a) $\zeta_{des.}$ = 0.02, k = 1.5 , V_c Variable, CSR
* Lognormally distributed strength

Story	k = 1.25	k = 1.50	k = 1.75	k = 2.00
1	2.9	1.6	.86	.49
2	2.7	1.4	.77	.43
3	3.2	1.7	.96	.55
4	3.8	2.1	1.20	.70

b) $\zeta_{des.}$ = 0.02, k variable, V_c = 0.10, CSR

Story	$\zeta_{des.}$ = 0.005	$\zeta_{des.}$ = 0.02	$\zeta_{des.}$ = 0.05
1	.31	1.6	3.9
2	.28	1.4	3.6
3	.36	1.7	4.3
4	.46	2.1	5.1

c) $\zeta_{des.}$ variable, k = 1.5, V_c = 0.10, CSR

Table 4.5 - T_1 = 0.377 FAILURE PROBABILITIES * 10^6 NBK
Design Spectrum, $a_{des.}$ = 0.2g

Story	V_c = 0.05	V_c = 0.10	V_c = 0.20	V_c^* = 0.40
1	2.5	2.6	3.3	6.0
2	2.1	2.2	2.8	5.3
3	2.9	3.0	3.8	6.9
4	4.3	4.5	5.4	9.5

a) $\zeta_{des.}$ = 0.02, k = 1.5, V_c variable, CSR

* Lognormally Distributed Strength

Story	k = 1.25	k = 1.50	k = 1.25	k = 2.00
1	4.7	2.6	1.5	.89
2	4.1	2.2	1.3	.76
3	5.4	3.0	1.8	1.07
4	7.8	4.5	2.7	1.65

b) $\zeta_{des.}$ = 0.02, $k_{variable}$, V_c = 0.10, CSR

Story	$\zeta_{des.}$ = 0.005	$\zeta_{des.}$ = 0.02	$\zeta_{des.}$ = 0.05
1	1.5	2.6	8.6
2	1.3	2.2	2.6
3	1.8	3.0	9.8
4	2.7	4.5	13.3

c) $\zeta_{des.}$: Variable, k = 1.5, V_c = 0.10, CSR

TABLE 4.6 - T_1 = 1.13 FAILURE PROBABILITIES * 10^6
$a_{des.}$ = 0.2g, NBK Design Spectrum

Story	.5 * CSR	.8 * CSR	1.0 * CSR	1.2 * CSR	1.5 * CSR
1	.06	.64	1.6	2.9	5.9
2	.05	.57	1.4	2.7	5.5
3	.07	.72	1.7	3.0	6.5
4	.09	.90	2.1	3.8	7.7

a) $T_1 = 0.377$

Story	.5 * CSR	.8 * CSR	1.0 * CSR	1.2 * CSR	1.5 * CSR
1	.13	1.1	2.6	4.7	9.5
2	.11	.97	2.2	4.1	8.4
3	.16	1.36	3.0	5.5	10.9
4	.27	2.07	4.5	7.8	15.0

b) $T_1 = 1.13$

TABLE 4.7 - OVERALL FAILURE PROBABILITIES * 10^6 WITH ALTERNATIVE SEISMIC RISK ASSUMPTIONS

$\zeta_{des} = 0.02$, NBK Design Spectrum, $a_{des.} = 0.2g$

$k = 1.5$, $V_c = 0.10$

obtained herein are not meaningful for conventional buildings. Further, for nuclear power plants where failure is generally defined to be the occurrence of an initiating accident or of an accident sequence or of core melt or of a large release of radioactivity [47], the overstress event defined herein does not necessarily imply a system failure. An analytical formulation to assess system failure is indeed complicated because of "the complexity of NPP systems, the sequentiality of accident events leading to failure, the built-in redundancy and the different levels of resistance of various subsystems and components [65]." Nonetheless, the implication of elastic design criteria is that nuclear systems or subsystems performance when the <u>structure</u> is performing in the inelastic range is uncertain. Therefore inelastic structural behavior may lead to (or be correlated with) the occurrence of an event which initiates system failure. As Veneziano has remarked for his failure estimates, then, the probabilities derived herein are related to the mean annual rate of accident initiation in a specific mode.

Comparison of the methodology and estimates of Newmark [46] and Veneziano [65] with those described herein follows.

<u>Failure Estimates of Newmark</u>

To quantify the seismic safety of nuclear power plants, Newmark [44] uses the following approach. The assumption is first made that probability distributions (conditional on design earthquake occurrence) are lognormal for both the "resistance," R, and the "earthquake hazard," H. He then defines

$$FS_H = \frac{\text{Design Hazard}}{\text{Median Hazard}} = \frac{\text{Design Hazard}}{\breve{m}_H}$$

$$FS_R = \frac{\text{Median Resistance}}{\text{Design Resistance}} = \frac{\breve{m}_R}{\text{Design Resistance}}$$

and from Figure 4.14, then $\breve{m}_R/\breve{m}_H = FS_H * FS_R$. If both R and H are lognormally distributed, the conditional failure (defined by Newmark [44] as "exceeding the design limit") probability is given by (see Chapter 5 or Reference [3]) the analytical expression:

$$P_f = \Phi \frac{\ell n(\breve{m}_H/\breve{m}_R)}{\sqrt{\sigma^2_{\ell n_R} + \sigma^2_{\ell n_H}}} \tag{4.3}$$

or

$$P_f = \Phi \frac{\ell n\left(\frac{1}{FS_H * FS_R}\right)}{\sqrt{\sigma^2_{\ell n_R} + \sigma^2_{\ell n_H}}} \tag{4.4}$$

where Φ is the CDF of the standardized normal variate U. FS_R, FS_H, $\sigma^2_{\ell nR}$, $\sigma^2_{\ell nH}$ (Newmark assigns the symbols β_R = $\text{Beta}_R = \sigma_{\ell nR}$ and β_H = $\text{Beta}_H = \sigma_{\ell nH}$) must then be estimated to arrive at reliability values. Newmark computes $\sigma_{\ell nR}$ and $\sigma_{\ell nH}$, in turn, from the SRSS of the standard deviations of the natural logarithms of the components of R and H which are also assumed to be lognormally distributed. FS_H and FS_R are estimated to be the products of the individual factors of safety associated with the components of R and H. Table 4.8, taken from Reference [44] lists such components and indicates estimated values for FS_H, FS_R, $\sigma^2_{\ell n_H}$, $\sigma^2_{\ell n_R}$ for <u>ordinary civil structures</u>.

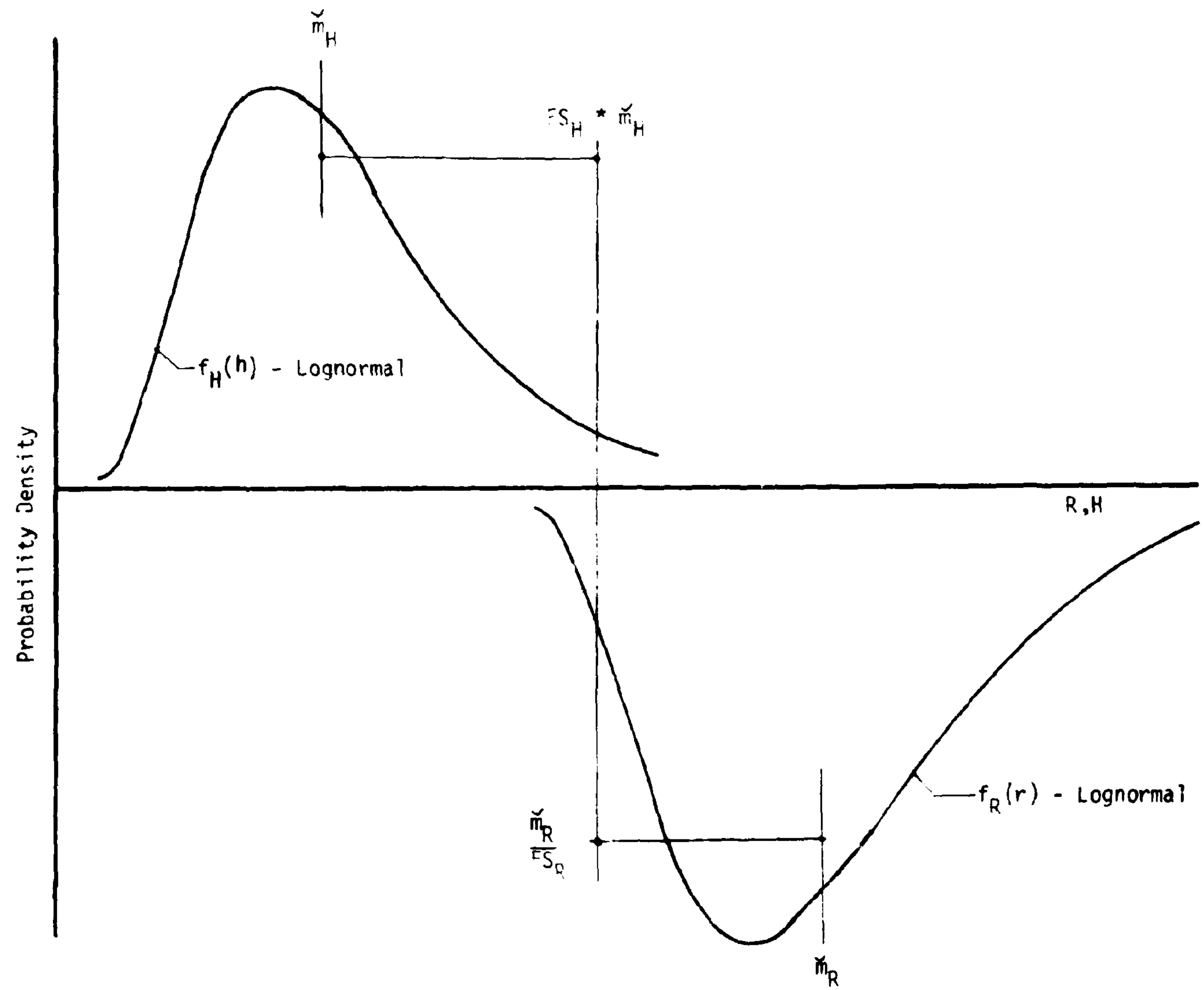

FIGURE 4.14 - NEWMARK'S METHODOLOGY FOR OBTAINING RELIABILITY ESTIMATES

Hazard Component	$Beta_H$	FS
Magnitude	.3	1
Distance	.3	1
Site Acceleration	.7	1.35
Site Modification	.3	1.0
Hazard Total	0.87	1.35

Resistance Component	$Beta_R$	FS
Soil-Structure Interaction	.3	1
Response Spectrum	.3	1
Damping, Ductility, etc.	.3	5
Resistance Total	.52	5

TABLE 4.8 - NEWMARK'S ESTIMATE OF PARAMETERS FOR COMPUTING CONDITIONAL FAILURE PROBABILITIES [44]

With such estimates, then,

$$P_{f|a_{des.}} = \Phi \frac{\ell n\left(\frac{1}{1.35 * 5.}\right)}{\sqrt{(0.87)^2 + (0.52)^2}} = \Phi\left(-\frac{1.91}{1.01}\right)$$

$$P_{f|a_{des.}} = \Phi\ (-1.89) = 0.03$$

The above is a conditional probability of failure given the occurrence of the design earthquake. For nuclear power plants Newmark uses $\sqrt{\sigma^2_{\ell nR} + \sigma^2_{\ell nH}} = 1.01$, and he estimates [46] $FS_R * FS_H \approx 20$, implying a conditional probability of failure

$$P_{f|a_{des.}} = \Phi\ \frac{\ell n(1/20)}{1.01} = \Phi(-3.00) = 0.0015$$

The assumption is then made that the total yearly failure probability is

$$P_F = P_{F|a_{des.}} * P[a_{des.}] \tag{4.5}$$

Such an assumption is clearly unconservative since it does not consider contributions to failure probabilities from intensities above and below the design earthquake. This has been recognized by Vanmarcke and Veneziano [65] and others, and is evident from Figure 4.13. In any case, Newmark estimates that yearly probabilities of occurrence of a nuclear power plant design earthquake are of the order of 10^{-4} and 10^{-5} and hence concludes that "the net probability of failure per year under seismic conditions will be ... of the order of 1 part in 10^8 or less for nuclear power plants."

Setting aside considerations of the unconservatism of Equation (4.5) and the $P[a_{des.}]$ estimate, the assumptions of FS_R and FS_H are crucial to the Newmark methodology. Detailed documentation of such assumptions is not presently available.

Failure Estimates by Veneziano

Veneziano has recently estimated mean annual failure probabilities for a NPP sighted in Massachusetts. His methodology and results are as follows. The measure of intensity used to characterize both seismic risk and resistance was Modified Mercalli Intensity. Under the assumption that the actual risk function decays exponentially and that the actual resistance distribution is normal, he postulated two models: a probabilistic or "deductive" model with deterministic parameters, and a statistical or "inductive" model which explicitly considered uncertainty in the key seismic risk and resistance parameters. The probabilistic model formally is developed as follows. If

$$\lambda(i) \propto \begin{cases} e^{-\beta_I i} & \text{for } i \leq i_1 \\ 0 & \text{for } i > i_1 \end{cases}$$

where $\quad i$ = MMI at site

$\lambda(i)$ = Mean rate of events exceeding <u>site</u> intensity i

β_I = Decay parameter

and $\quad R \sim N\ (\mu_R;\ \sigma_R^2)$

$$R_N = (R - \mu_R)/\sigma_R \sim N(0,1) \tag{4.6}$$

then $\lambda(r_n)$, the mean rate of events exceeding a normalized resistance value r_n, is [65]:

$$\lambda(r_n) = \lambda_o\ e^{-\beta_I \sigma_R r_n} = \lambda_o\ e^{-\beta_N r_n} \tag{4.7}$$

where λ_o is the mean rate of seismic events with site intensity $> \mu_R$. Also the <u>mean failure rate</u> λ_f <u>is given by</u> [65]:

$$\lambda_f = \lambda_o\ e^{\beta_N^2/2} \tag{4.8}$$

The statistical model considers uncertainty in the parameters λ_o, β_N, μ_R, and σ_R. For each combination of known/unknown parameters, the inductive (Bayesian) mean failure rate is calculated; the effect of statistical uncertainty is also quantified through a multiplicative penalty factor on the deductive result using best parameter estimates [65]. The statistical model, then, requires estimates of the following parameters:

$\hat{\mu}_R$ = estimate of the mean value of resistance μ_R

S_R = estimate of standard deviation of resistance σ_R

$i_{N_0} = (i_0 - \mu_R)/\sigma_R$ = estimate of lower truncation point of the normalized resistance measure

i_{N_1} = estimate of maximum possible reduced site intensity

$\mu_{\ell n\lambda_0}$ = mean of $\ell n\lambda_0$ (the natural logarithm of the mean rate of occurrences of site intensities larger than $\hat{\mu}_R$)

$\sigma_{\ell n\lambda_0}$ = standard deviation of $\ell n\lambda_0$

μ_{β_N} = mean of β_N (decay parameter in equation (4.8)

σ_{β_N} = standard deviation of β_N

ρ = correlation coefficient between β_N and $\ell n\lambda_0$

ν = a "confidence parameter" on the estimates $\hat{\mu}_R$ and S_R.

(For μ_R and σ_R known, the normalized resistance

$$R' = \left(\frac{n}{n+1}\right)^{1/2}\left(\frac{R-\hat{\mu}_R}{S_R}\right)$$

has a predictive t-distribution with $\nu = n-1$ degrees of freedom. n is generally associated with the number of observations in a statistical sample of a random variable which is used to estimate moments of a distribution. The smaller n (or $\nu = n-1$) is, the more uncertainty in the μ_R and σ_R estimates $\hat{\mu}_R$ and S_R.)

To arrive at a reliability estimate for a Massachusetts site, Veneziano assumed the following values of the above parameters:

$\hat{\mu}_R = 9.5$ $\quad S_R = 0.75$ $\quad \nu = 10(5)$ $\quad i_{N_0} = -5$

$\mathrm{Exp}(\mu_{\ell n\lambda_0}) = .45\times10^{-5}(.292\times10^{-8})$ $\quad \sigma_{n\lambda_0} = 1.6\ (3.49)$ $\quad \rho = 0.75(.51)$

$i_{N_1} = -1(4)$ $\quad \mu_{\beta_N} = 1.4$ $\quad \sigma_{\beta_N} = 0.2\ (.3)$

The resultant mean annual failure rate is 1.23×10^{-5}. If a pessimistic set of the parameters (given in parentheses) is used, the corresponding failure rate is 5.92×10^{-5}. It is important to note that $\hat{\mu}_R$ was estimated as follows. For Massachusetts $MMI_{SSE} = 8$ was postulated, then, accepting the WASH 1400 conclusion that the probability of failure of a reactor system or component subjected to the SSE is in the range 10^{-1} - 10^{-2}, a corresponding $\hat{\mu}_R$ was chosen. Similar values for $P_{F/SSE}$ were estimated herein (see Figure 4.3), but Newmark has suggested failure probabilities for nuclear reactor equipment under the design earthquake, of the order of 10^{-2} - 10^{-4} or smaller. Also, since S_R statistics are available only for ordinary buildings, Veneziano used S_R estimates inferred from Newmark [46].

It is to be noted that Veneziano believes that his failure estimates, "refer to the mean annual rate of accident initiation in a specific mode," and are not assessments of the overall system reliability.

SUMMARY

The two approaches summarized and the one developed herein are basically heuristic in the sense that each primarily illustrates the uncertainties involved in a methodology for systematically arriving at reliability estimates. An argument will not be made regarding the relative merit of each overall reliability estimate, although a significant difference exists in estimates of the failure probabilities conditional on the design earthquakes. Newmark generally states values which are two or more orders of magnitude smaller than those stated by WASH 1400 [47], Veneziano [65] and herein.

It is important rather to summarize the limitations of each of the methodologies. Newmark's failure estimates are clearly very dependent on the "total factor of safety" or on the ratio m_R/m_H. Quantitative analyses to substantiate the individual contributions to this overall factor of safety have not, to the present, been published. Assessment of the total failure probability with Equation (4.5) is unconservative. Effects of uncertainty in structural modeling have not been quantified.

Veneziano does not explicitly consider individual sources of uncertainty within either risk or resistance and, as such, indicates no direction for minimizing uncertainty or risk. The parameter estimate $\hat{\mu}_R$ implicitly acknowledges the validity of the WASH 1400 estimate of the probability of system failure given the design earthquake.

The method developed herein treats only elastic systems. Uncertainty in the strength measure has not been totally quantified even for a plane frame. Local site modification and soil-structure interaction effects have not been considered, although variation of the frequency content may indirectly account for such effects. The methodology becomes increasingly expensive as the number of degrees of freedom (or the number of load effect distributions to be computed) increases. Additional conservatism due to the treatment of the NBK spectra as component spectra has not been considered. Statistical uncertainty may only be quantified by simulation, i.e., by performing repeated analyses for alternate parameter values.

4.5 SYSTEM RELIABILITY

Within the context of the three idealized 4-DOF systems considered herein, the following question may be asked: "What is the probability that yielding will not occur in any of the stories?" Choosing to define the model as a series or weakest link system in which failure of any one of (only) four modes (yielding of a story) is considered a system failure, bounds on the "system reliability" may be established [10]. Such bounds are given by Equation (4.9):

$$\underset{i=1}{\overset{M}{\mathrm{MAX}}}\ P_i \leq P_{\substack{\text{System}\\ \text{Failure}}} \leq \sum_{i=1}^{M} P_i \qquad (4.9)$$

where M = Number of failure modes (4)
P_i = Marginal probability of failure of story (or mode) i.

The lower bound of the inequality is based on the assumption of perfect stochastic dependence among failure modes, whereas the upper bound implies complete independence of the failure modes. For the three models considered (designed using the NBK spectrum with $a_{des.} = 0.2g$ and $\zeta_{des.} = 0.02$ and with an assumed normal strength distribution with $k = 1.5$ and $V_c = 0.10$). Table 4.9, derived from Tables 4.5 and 4.6, summarizes the bounds of system reliability under the assumption of the Cornell-Merz seismic risk curve (Figure 4.11).

	$\underset{i=1}{\overset{4}{\mathrm{MAX}}}\ P_i$	$\sum_{i=1}^{4} P_i$
$T_1 = 0.317$	3.3	8.9
$T_1 = 0.377$	2.1	6.8
$T_1 = 1.13$	4.5	12.3

TABLE 4.9 - BOUNDS TO SYSTEM FAILURE PROBABILITIES * 10^6

It may be noted that Vanmarcke [63] proposed an approximation which incorporates the effect of dependence between any two pairs of modes through the coefficient of correlation between their modal safety margins, defined by Equation (4.10) as the modal resistance C_i minus the modal load effect D_i.

$$M_i = C_i - D_i \tag{4.10}$$

However, given the sensitivity of the marginal modal failure estimates apparent in Figures 4.4 through 4.9 and the simplicity of the model (i.e. the small number of failure modes) the bounds in Table 4.9 are believed sufficiently close. Further, assuming much greater coefficients of variation of load effects than those of resistance, modal safety margins can be expected to be highly correlated, implying that the system failure probability is closer to that of the lower bound. In effect, if one mode or story survives an earthquake, the implication is that a high load is not present and that the remaining modes or stories will also survive.

4.6 CONCLUSIONS

Probabilities of exceeding limit-elastic interstory distortions for three models were computed herein. An NRC-like seismic design methodology was used to obtain strength estimates, i.e., the NBK spectra normalized to $a_{des.} = 0.2g$ were used to compute seismic design load effects.

The sensitivity of the probability estimates to the parameters which define the strength distribution, i.e., V_c and m_c (or k) as well as to $\zeta_{des.}$ and the seismic risk curve was examined. The sensitivity of the probability estimates to the parameters which control the load effect distribution, i.e., T_o/T_c, ζ, S', ω_g, was not quantified.

It is observed that, given the same design assumptions, the implied reliability of the T_1 = 0.377 sec. and T_1 = 1.13 sec. models is not equal but rather is somewhat smaller for the longer period structure.

Contributions to overall story probabilities of failure arise from the entire range of possible site intensities. Small intensities may even make dominant contributions if the variation in the strength measure is high and the strength probability distribution is not truncated. The magnitude of the coefficient of variation of strength, V_c, then, affects probability of failure contributions from small intensities the most, whereas contributions from design level intensities are relatively insensitive to V_c. Conversely, uncertainty in the location of the mean strength m_c (or k) has similar effects throughout the intensity range, implying that in comparison with V_c it is of greater importance in controlling contributions at design level intensities.

The seismic risk uncertainty, as conventionally believed, does cause the greatest variations in reliability estimates, although for the T_1 = 1.13 sec. model, changing $\zeta_{des.}$ from 0.02 to 0.05 caused approximately the same increase in overall story failure probability estimates as that caused by increasing the seismic risk to 1.5 times that given by the Cornell-Merz curve.

A direct interpretation of the failure estimates derived herein in terms of nuclear power plant seismic safety cannot be made. It is noted, however, that significant differences exist among alternate estimates of an equivalent central safety factor for nuclear power plants, given the occurrence of the design earthquake. Newmark assumed that the ratio of median resistance to median hazard is significantly higher than that estimated by Veneziano or that computed herein for the simple T_1 = 0.317 sec. model.

CHAPTER 5

COMPARISON OF METHODS

5.1 LIMITATIONS

5.1.1 Alternate Structural Systems and Optimization

The design process initially involves a choice of an overall structural system to resist applied loads. It is assumed that, at least initially, the objective is not to compare the effectiveness of alternate structural systems nor to consider optimizing the overall cost of seismic protection or any other "utility function." Rather, it is assumed that a structural system has been chosen and that the focus is on the subsequent phase; i.e., the iterative process of proportioning member stiffness and strengths, performing analyses to compute load effects and reproportioning members to resist the chosen critical design load effects. In the latter phase, performance criteria must first be chosen, an analytical model formulated, appropriate loadings specified, and design load effects chosen.

5.1.2 Alternate Performance Criteria

A structure may be designed to resist extreme loads such as earthquakes by performing in the elastic or inelastic ranges (see also Chapter 3). For purposes of definition, the following performance criteria are stated:

> NUCLEAR REGULATORY COMMISSION: Define two seismic load levels; the structure must perform within "working stress" ranges when subjected to the lesser load; the structure may perform up to "yield stress" levels when subject to the higher load.

UNIFORM BUILDING CODE-ATC [69]: Allow inelastic action but prevent significant structural damage in a moderate earthquake; prevent collapse in a severe earthquake. (It should be noted that dual-level seismic loads and design criteria have also been proposed (Donovan [17]) for "ordinary" building structures and that, in general, revision of the above criteria is continual, see ATC-3 [20]).

The choice of criteria constrains choices of structural models, methods of specifying loadings, methods of analysis and choices of design load effects. Work performed by Biggs [11], Roesset and Pique [48], et al. [29,12,79] has focused primarily on developing design procedures consistent with UBC-ATC performance criteria. The assumption is made herein that alternate methodologies within NRC-like criteria will be examined.

5.1.3 Dynamic Models

Two- or three-dimensional lumped mass models having varying degrees of freedom (and which may or may not include the local soil) are used. The simplest elastic dynamic model is a close-coupled two-dimensional MDOF system classically representing the shear beam type of behavior. It, exclusively, will be considered herein. It must be noted, however, that use of such a model together with the NRC-like performance criteria poses difficulties in interpretation of results. This is true because in general much more complex 3-D (since NBK design spectra are defined as component spectra) models are used for nuclear power plants.

5.2 BASIC METHODS USED FOR OBTAINING LOAD EFFECTS

The focus here is on defining methods of obtaining dynamic load effects which are can be used; i.e., response spectrum analyses, time history analyses, or random vibration techniques.

5.2.1 Response Spectrum Methods (RS)

An outline of alternatives associated with the use of response spectra may be as follows:

I) Definition of Spectrum
   A) Type
      1) NBK [45]
      2) Smoothed m, m+σ, or fractile of an arbitrary set of recorded response spectra
      3) McGuire "constant risk" response spectra [43]
   B) Intensity
      1) Normalization to peak ground acceleration a_{max}
      2) Other intensity measures (v_{max}, d_{max}, etc.)

II) Point of application of spectrum
   A) Ground level
   B) Foundation level
   C) Bedrock (use of augmented model)

III) Treatment of spectrum as a component or resultant

IV) Method of modal superposition and number of modes considered.

5.2.2 Time History Methods (TH)

Alternatives available within time history techniques are:

I) Real time histories (RTH)
   A) Number and type of real earthquakes
   B) Choice of intensity (a_{max})
   C) Choice of dominant frequency
   D) Choice of response level for design (m, m+σ)

II) Artificial time histories (ATH)
   A) Number of earthquakes
   B) Types
      1) Random impulses and other methods

2) Superposition of sinusoids
   a) Frequency content (stationary or non-stationary)
      i) Band limited white noise
      ii) Kanai-Tajimi (filtered white noise)[39]
      iii) $G(\omega)$ derived from a smooth target response spectrum [73,36]
      iv) Geophysical prediction of $|f(\omega)|$ or $G(\omega)$ [8]
   b) Time variation - duration of motion
   c) Intensity of $|f(\omega)|$ or $g(\omega)$
      i) Obtained directly from S_v to $G(\omega)$ conversion
      ii) M, D (or seismic risk) to a_{max} to σ_a to K-T $G(\omega)$ [30]
      iii) Geophysical prediction from M, D, depth, and length of rupture
   d) Other acceptance criteria
      i) Matches or envelopes a target S_v (with or without specified smoothness)
      ii) Matches peak acceleration

C) Choice of response level for design $(m, m+\sigma)$

5.2.3 Random Vibration Methods (RV)

Random vibration techniques may be broadly classified as follows:

I) Formulation to obtain RMS response
   A) Time domain
   B) State space approach
   C) Frequency domain
      1) Frequency content of input (stationary or nonstationary
         a)
         b)
         c)
         d) Same as for artificial earthquakes
      2) Intensity
         a)
         b)
         c) Same as for artificial earthquakes
      3) Duration of strong motion

II) Formulation for approximate first passage problem solution[26,61]

III) Choice of design load effect.

5.3 COMPARISON OF METHODS

5.3.1 Previous Work

Figure 5.1 summarizes the methodology used in reference [72] for comparing load effects obtained through alternate methods. Statistics of load effects were computed for three plane, 4-DOF shear beam models (two are the same as those defined in Table 2.5) with deterministic periods (T_1 = 0.377, T_1 = 1.13, T_1 = 2.26) and damping (ζ = 0.02). The main conclusions regarding the moments of the calculated load effects were as follows.

Means

Methods 1, 3, 5, 7 equally well predict mean load effects for all three structures. Method 4 also yielded comparable mean values. It must be noted that the methodology to arrive at $G(\omega)$ from S_v was that developed by Vanmarcke and described in [36]. Also, the artificial time histories were those generated using the program SIMQKE, which is documented in Reference [36]; the program is essentially based on the work of Hou [30]. The random vibration formulation was the same as the one described in Chapter 2.

Coefficients of Variation (COV)

Methods 1 and 7 yielded essentially equal COV's for all responses. The COV's generally decreased with decreasing fundamental period, primarily because of the normalization of the responses to peak ground acceleration [72]. Methods 3 and 4 also yielded essentially equal COV's, but for the three models considered, their values were significantly smaller than

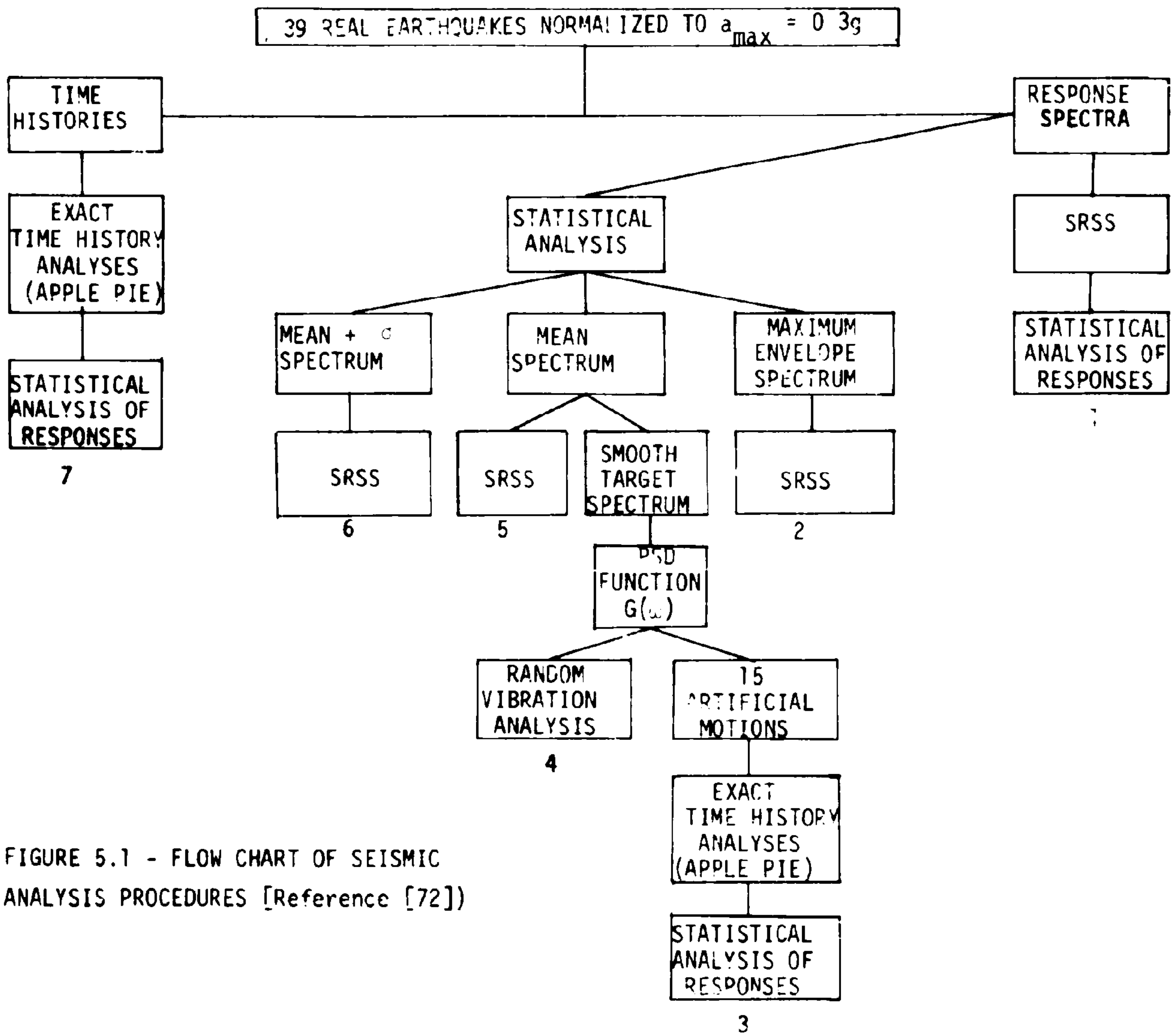

FIGURE 5.1 - FLOW CHART OF SEISMIC
ANALYSIS PROCEDURES [Reference [72])

those obtained through methods 1 and 7. The salient reason for the difference is clearly that all the artificial motions and the random vibration analysis used a single frequency content and duration, whereas the 39 real time histories and their corresponding response spectra reflect a range of frequency contents and durations. Chapter 2 presented a method to essentially reconcile the observed load effect distributions using method 4 with those achieved through methods 1 and 7. As $T \rightarrow 0$, a problem of interpretation does arise; the COV's derived through methods 1 and 7 approach zero (because all ground motion representations were normalized to peak ground acceleration). Conversely, random vibration or, equivalently, multiple artificial time histories derived from a common spectral density function, imply a random peak acceleration and hence distributions of responses as $T \rightarrow 0$. For artificial motions the generated peak ground accelerations (for the 15 motions generated [72], 74.1 in/sec^2 $\leq a_{max} \leq$ 118.1 in/sec^2; $\bar{a}_{max}$ = 94.3 in/sec^2; a_{target} = 116 in/sec^2) are artificially raised or lowered to provide a perfect match [72]. The random vibration methodology has not been similarly modified to account for non-random a_{max} as $T \rightarrow 0$.

The coefficients of variation obtained through methods 3 and 4 are, however, significant in that they indicated the possible variation in response due simply to the random phasing of the motion.

5.3.2 Additional Work

Design load effects (and their variability) from alternate analytical methods and, if possible, failure probabilities for resultant designs are to be compared. The assumptions of a common dynamic model and conditionality on peak ground acceleration are made. It is apparent that analogous methodologies must exist in RS and TH analyses; for example, if El Centro is chosen as input to a TH analysis, the analogous procedure would be to use the El Centro RS in an RS analysis. The only difference between the two methods is the uncertainty in modal combination (which is not to be examined) and the practical limitations of RS analysis output (e.g., it does not give a time history of floor acceleration). In the limit this is also true for a response spectrum analysis using the NBK spectrum and an artificial time history which matches (assume perfectly, after smoothing [36]) the NBK target spectrum. Accepting the same information regarding excitation, then, RS and TH methods are equally variable (this is evident in the response statistics summarized in Reference [72]). If comparing a RS analysis using (for example) the NBK spectrum and a time history analysis using a randomly chosen record, it is important to recognize that the two methodologies represent different information levels regarding the seismic threat.

5.4 COMPARISON OF METHODS - RESPONSE SPECTRUM ANALYSES

Three possible deterministic design procedures may be as follows:

1) Use the NBK spectra normalized to an a_{max} applied as resultants (for a 2-D model) at the foundation level.
2) (As proposed for the West Coast [13,37]) choose a set of RS corresponding to a chosen set of normalized likely earthquakes (as determined from expected magnitude, depth of shock, distance and type of and length of rupture, etc.). Use the smoothed m, m+σ, or m+2σ spectra for computing design load effects.
3) Use "constant risk" spectra as proposed by McGuire [43].

McGuire developed [43] an approach to predict site response spectra from regression equations based on computed response spectra of observed records. The independent variables used for prediction are the magnitude and hypocentral distance. (Separate regression analyses, with magnitude fixed, were performed on records from the 1971 San Fernando earthquake). The means of the distributions of responses are obtained from the regression equations; the variances are obtained from the variances of residuals and the variances of the logarithmic regression lines. The means and variances are used to fit lognormal distributions; proper fractile response spectra may then be chosen for design.

The approach is appealing, but regression analyses must be performed for a set of frequencies and damping values (although McGuire suggested performing regression analyses on 2% damped responses only and scaling the resultant mean spectrum to obtain spectra for other damping values). In lieu of such extensive work, McGuire further suggested that such consistent risk spectra may be derived through regression analyses on only two parameters: a_{max} (the one parameter conventionally used) and the maximum pseudo-velocity response of a 1-DOF oscillator with f = 1 Hz and ζ = 0.02. The latter parameter (or any other S_v value) has not been related to MMI data, and hence the approach remains to be developed for the Eastern United States.

Alternatives 1 and 2 are, in reality, similar: NBK have simply chosen their own particular set of earthquakes and the corresponding $m+\sigma$ spectrum for design purposes. Absolute judgement regarding the applicability of the NBK design spectra, versus, say, spectra derived through method 2, or the m+σ spectra for the 39 earthquakes of Reference [72], or the Cornell seismic design spectra for Boston [6], cannot be made for most sites. Each set of spectra reflects a different assumption regarding the seismic threat. Only for a few sites, Mexico City may be one, is the geophysical understanding of earthquake occurrences sufficient to define clearly better site design response spectra than those given by, say, NBK. By visual comparison the relative conservatism of alternate design spectra is evident and corresponding probabilities of failure can be computed for a specific structure, but the basis (e.g., an earthquake set) used to define the seismic threat (i.e. to arrive at distributions of ω_g and S' as in Chapter 2) in order to compute probabilities of failure, is arbitrary.

Herein, the relative importance (in terms of the resulting story probability of failure) of using the mean or m+σ or the m+2σ RS of a given set of earthquakes (which is arbitrarily assumed to define the site seismic threat) is quantified.

For the two dynamic models described in Table 2.5, (T_1 = 0.377 sec. and T_1 = 1.13 sec.), design interstory distortions were, therefore, computed using four different spectra. The first three were the m, m+σ, and the m+2σ spectra (for ζ = 0.02) corresponding to the 39 earthquakes of Table 2.2 . Figure 5.2 from Reference [72], shows the m and the m+σ spectra normalized to 0.3g peak ground acceleration. The fourth spectrum was the 2% damped NBK design spectrum as shown in Figure 3.6.

Computed design interstory distortions (DD) are summarized in Table 5.1 for $a_{des.}$ = 0.1g. It is to be noted that for the T = 1.13 sec. model, the m+2σ spectrum load effects are smaller than those of the NBK spectrum.

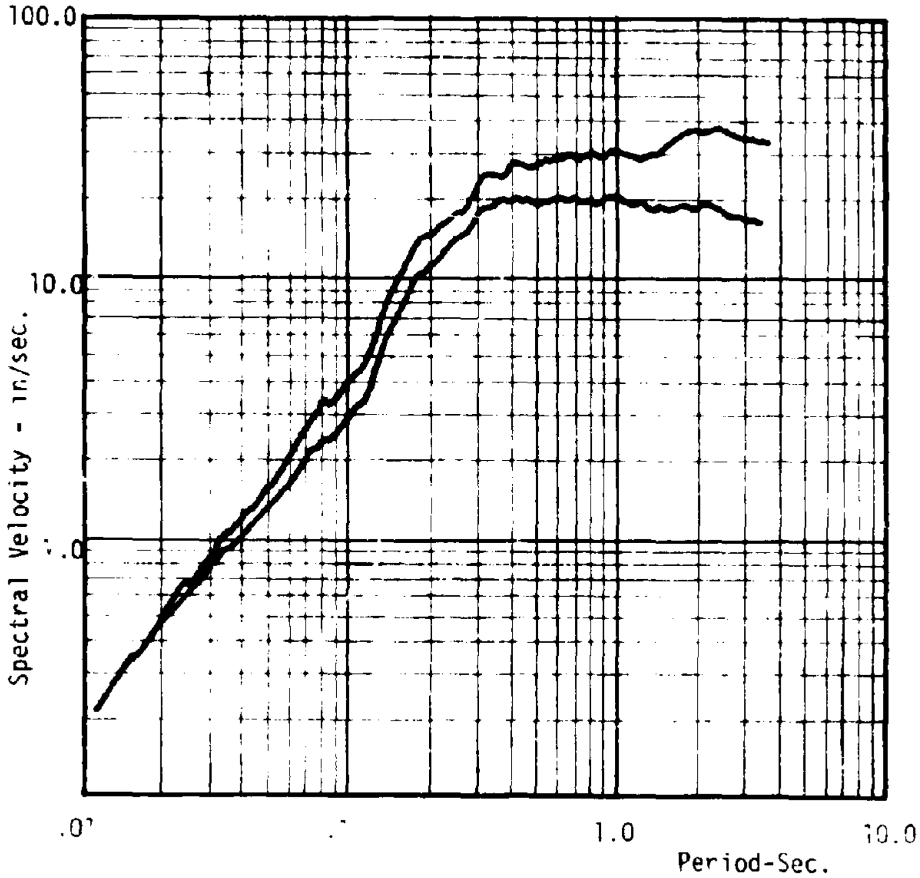

FIGURE 5.2 - MEAN AND MEAN + σ SPECTRA FOR 39 REAL EARTHQUAKES OF TABLE 2.2 [72], ζ = 0.02

Story	NBK	m of 39	m+σ of 39	m+2σ of 39
1	.255	.164	.2156	.2674
2	.225	.1445	.190	.236
3	.1665	.107	.1406	.174
4	.0896	.0575	.0757	.0938

a) T_1 = 0.377 sec.

Story	NBK	m of 39	m+σ of 39	m+2σ of 39
1	1.0873	.491	.749	.982
2	.959	.433	.661	.866
3	.709	.320	.488	.640
4	.3816	.172	.263	.3445

b) T_1 = 1.13 sec.

TABLE 5.1 - DESIGN INTERSTORY DISTORTIONS (in)

$\zeta = 0.02$, $a_{des.} = 0.1g$

Load effect distributions were calculated as described in Chapter 2 with the parameters ω_g, ζ, T_o/T_c, S' lognormally distributed with moments given by Table 2.8. The strength measure, yield interstory distortion, C, was assumed to be normally distributed with moments:

$$\begin{aligned} m_c &= k * DD = 1.5 * DD \\ V_c &= 0.10 \end{aligned} \tag{5.1}$$

The above estimates are equal to those used in Chapter 4 and are based primarily on the calculated moments of the structure designed in Chapter 3. The sensitivity of the resultant failure probabilities to the above parameters was partially quantified in Chapter 4. The seismic risk curve for Boston as developed by Cornell and Merz (see Figure 4.11) was again used to compute overall failure probabilities.

5.4.1 Conditional Failure Probabilities

Figures 5.3 and 5.4 depict conditional failure probabilities for the first floor in each of the models, given the occurrence of an excitation with intensity $a/a_{des.}$. It is to be noted that the conditional risks for the NBK spectrum are closest to those of the m+2σ spectrum of the 39 earthquakes. Further, for all of the spectra, the implied conditional risks vary with fundamental period T_1; i.e., they increase as T_1 increases. This is primarily a result of normalizing the spectra with respect to a_{max}; COV's of responses increase as T_1 increases. Conversely, in the limit, as $T \to 0$, all spectra should have a common conditional risk curve.

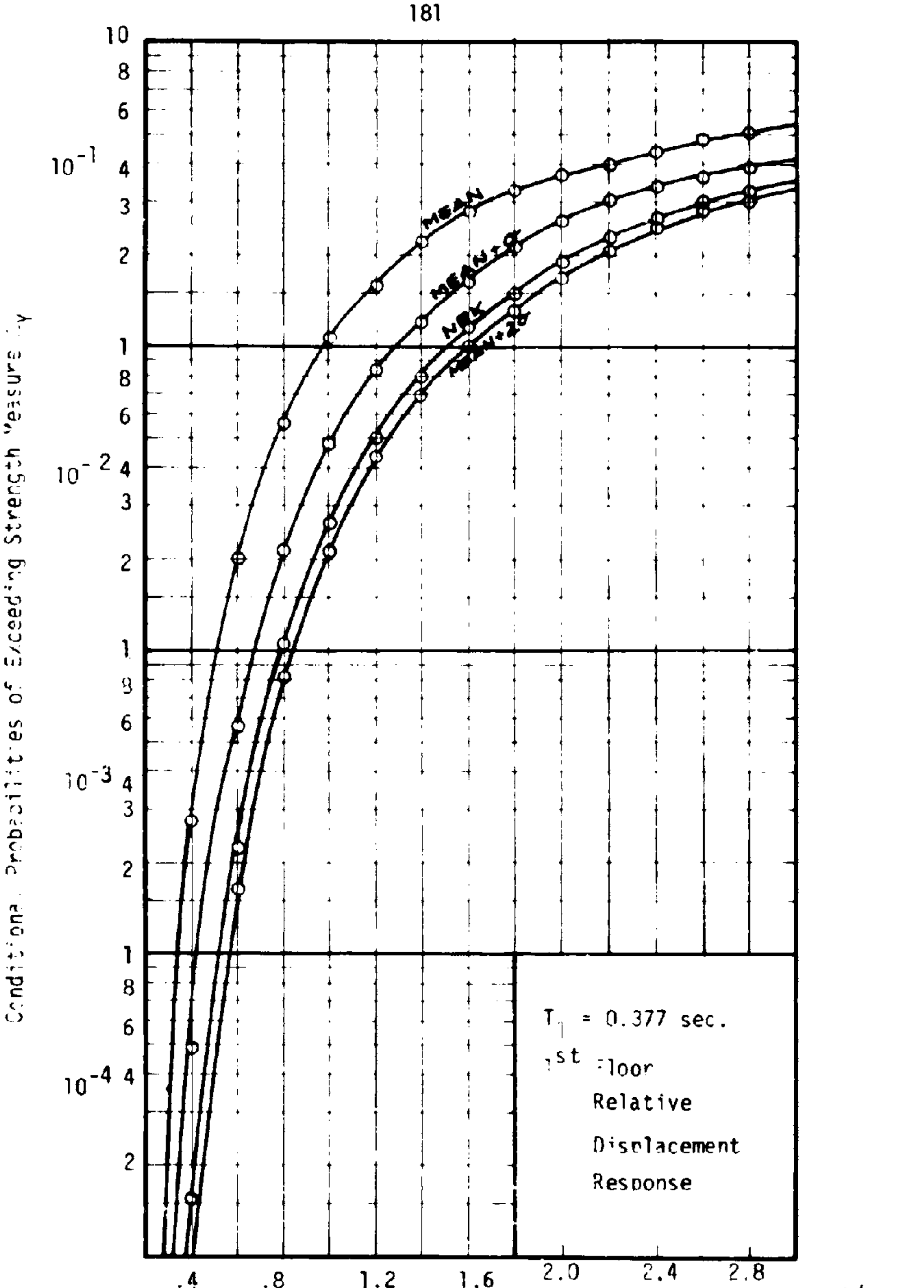

FIGURE 5.3 - CONDITIONAL FAILURE PROBABILITIES FOR DESIGNS BASED ON DIFFERENT RESPONSE SPECTRA

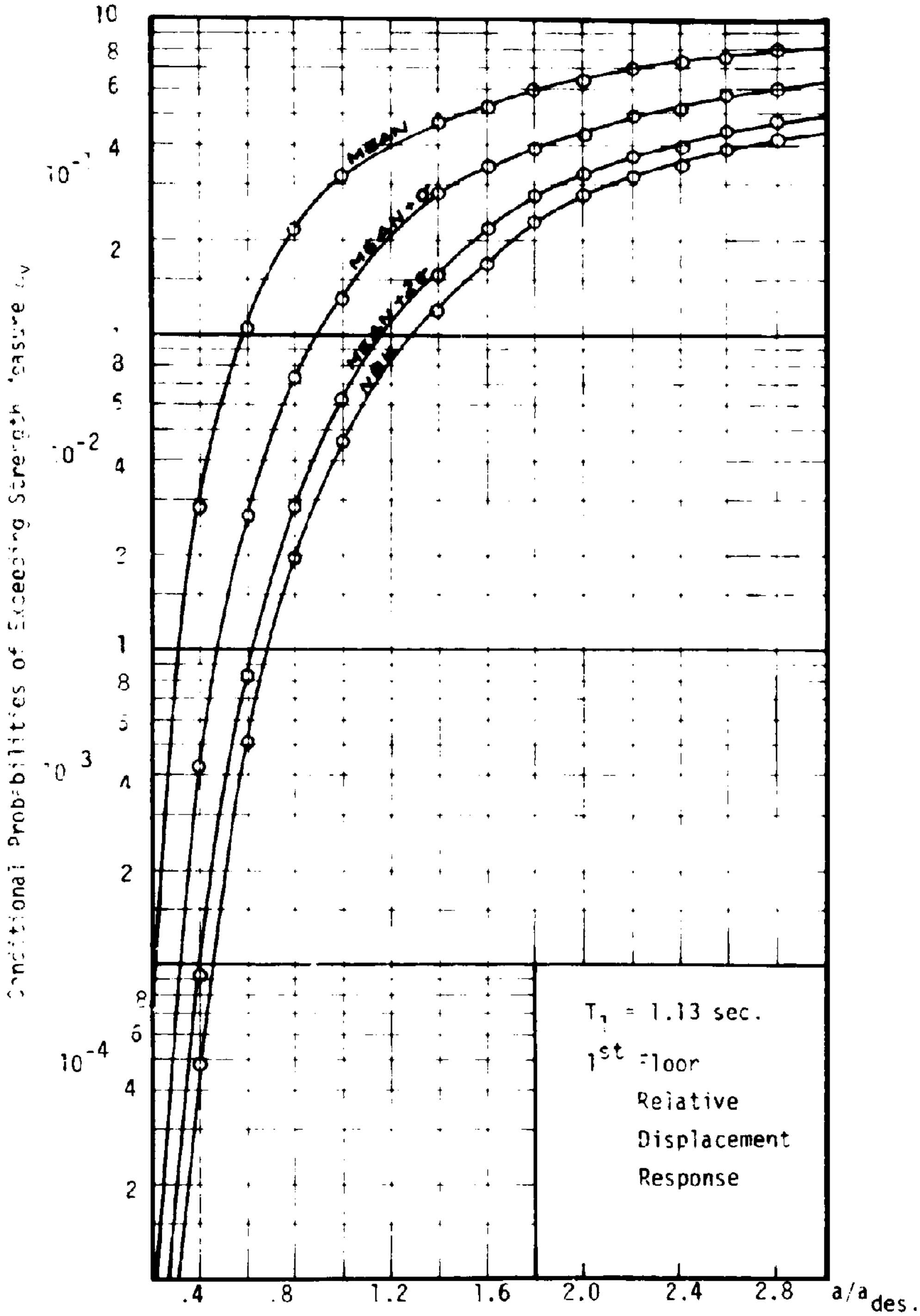

FIGURE 5.4 - CONDITIONAL FAILURE PROBABILITIES FOR DESIGNS BASED ON DIFFERENT RESPONSE SPECTRA

5.4.2 Overall Failure Probabilities

Tables 5.2 and 5.3 show overall failure probabilities for designs corresponding to each of the four spectra. Three design accelerations were used, with yearly probabilities of exceedance, as predicted by the Cornell-Merz seismic risk curve, given in Table 5.4.

a_0	$P[a \leq a_0]$
.1g	9×10^{-5}
.15g	4×10^{-5}
.20g	2×10^{-5}

TABLE 5.4 - DESIGN ACCELERATIONS AND ASSOCIATED CORNELL-MERZ EXCEEDANCE PROBABILITIES

As for conditional risks, overall failure probabilities increase as T_1 increases. Again, this is because normalization to peak ground acceleration forces all spectra to converge as $T_1 \to 0$. As expected then, the differences in resultant failure probabilities are greater for the T_1 = 1.13 sec. structure.

Alternate $a_{des.}$

For the same spectrum, an increase in $a_{des.}$ from 0.1g to 0.2g clearly decreases the resultant failure probabilities by factors ranging from ≈ 7 to ≈ 11. As expected, the decrease is generally greater for the T = 1.13 sec. structure.

Alternate Spectra

For the same design acceleration, use of a more conservative spectrum decreases failure probabilities by a factor of ≈ 10 for the T = 1.13 sec. structure and by a factor of ≈ 4 for the T = 0.377 sec. structure.

Story	NBK	m of 39	m+σ of 39	m+2σ of 39
1	1.3	4.4	2.1	1.2
2	1.2	4.1	1.9	1.1
3	1.4	4.8	2.3	1.3
4	1.7	5.7	2.6	1.5

$a_{des.} = 0.1g$

Story	NBK	m of 39	m+σ of 39	m+2σ of 39
1	.42	1.45	.69	.36
2	.38	1.36	.64	.33
3	.46	1.58	.75	.40
4	.54	1.84	.88	.47

$a_{des.} = 0.15g$

Story	NBK	m of 39	m+σ of 29	m+2σ of 39
1	.16	.63	.28	.13
2	.14	.59	.25	.12
3	.17	.69	.31	.15
4	.21	.81	.37	.18

$a_{des.} = 0.2g$

TABLE 5.2 - OVERALL FAILURE PROBABILITIES ($*10^5$) FOR ALTERNATE DESIGNS, T_1 = 0.377 sec. Model

Story	NBK	m of 39	m+σ of 39	m+2σ of 39
1	2.1	21.3	5.9	2.8
2	1.9	18.7	5.2	2.5
3	2.4	24.5	6.7	3.1
4	3.2	35.4	9.3	4.2

$a_{des.} = 0.1g$

Story	NBK	m of 39	m+σ of 39	m+2σ of 39
1	.67	6.1	1.9	.91
2	.59	5.5	1.7	.80
3	.77	7.0	2.2	1.0
4	1.1	9.8	3.0	1.4

$a_{des.} = 0.15g$

Story	NBK	m of 39	m+σ of 39	m+2σ of 39
1	.26	2.2	.82	.36
2	.22	2.0	.72	.32
3	.30	2.5	.94	.42
4	.45	3.2	1.3	.61

$a_{des.} = 0.2g$

TABLE 5.3 - OVERALL FAILURE PROBABILITIES ($*10^5$) FOR ALTERNATE DESIGNS, T_1 = 1.13 sec. Model

5.5 COMPARISON OF METHODS - REAL TIME HISTORIES

Not considering choices in the intensity or dominant frequency of an earthquake, there remains to choose the exact earthquakes used for analysis, their number and the design load effect. The relative conservatism of using 1, 2, ... n "accepted" motions (El Centro, Taft, Golden Gate, Parkfield, Helena, etc.) is likely to be a function of the nominal periods of a structure. That is, where a computed load effect due to, say, El Centro, lies in a total conditional distribution of load effects depends on the periods of the structure. Therefore the effectiveness of multiple time history analyses using specific earthquakes cannot be established a priori. Rather, one is limited to developing probabilistic statements regarding the effectivenss of using n arbitrary earthquakes.

In general, load effects from n arbitrary real earthquakes (all normalized to an intensity measure) can be viewed as a sample of n random variables assumed to be independent and identically distributed. Functions of the sample, such as the mean or the maximum value are generally called sample statistics and can be viewed for purposes stated herein as alternate design strategies. The implication of such alternate strategies in terms of the design load effect distribution and the conditional failure probabilities may be partially quantified as follows.

5.5.1 Strategy: Choose Mean of n Load Effects for Design Purposes

This is equivalent to a basic problem of statistical estimation [15]. That is, the moments of the sample mean are desired. It can be shown that, if D = Random (Demand) load effect (m_D, σ_D^2),

$$DD = \frac{1}{n} \sum_{i=1}^{n} D_i = \text{Random (Design Demand) design load effect}$$

and the D_i are mutually independent, then

$$\begin{aligned} m_{DD} &= m_D \\ \sigma^2_{DD} &= \frac{1}{n} \sigma_D^2 \end{aligned} \qquad (5.2)$$

The moments m_{DD} and σ_{DD} are independent of the form of the distribution of D. It is further noted that, if n is large, by the central limit theorem, no matter what the distribution of D, the sample mean will be approximately normally distributed. The likelihood of using a design load effect close to the actual mean load effect increases as n increases. Conversely, the probability of using extreme design load effects significantly below or above the mean decreases Figure 5.5 illustrates these points.

If D is normally distributed (and hence also DD) Table 5.5 indicates probabilities of choosing a design demand within different ranges of the load effect distribution. For example, if the mean load effect of four arbitrary earthquakes is chosen for design, there is an *a priori* probability of 0.955 that such a design demand will be within plus or minus one standard deviation of the mean of the load effect distribution.

Conditional Failure Probabilities

It is customary to express reliability, R, as

$$R = P\,[M > 0] \qquad (5.3)$$

where $$M = C\text{-}D \qquad (5.4)$$

n	$P[m_D - \frac{\sigma_D}{4} \leq DD \leq m_D + \frac{\sigma_D}{4}]$	$P[m_D - \frac{\sigma_D}{2} \leq DD \leq m_D + \frac{\sigma_D}{2}]$	$[m_D - \sigma_D \leq DD \leq m_D + \sigma_D]$	$P[m_D - 2\sigma_D \leq DD \leq m_D + 2\sigma_D]$
1	.107	.383	.683	.955
2	.277	.520	.843	.994
3	.335	.613	.917	.9994
4	.383	.683	.955	
5	.424	.734	.974	

TABLE 5.5 - A PRIORI PROBABILITIES OF DESIGNING WITHIN VARIOUS RANGES OF THE TOTAL LOAD EFFECT DISTRIBUTION

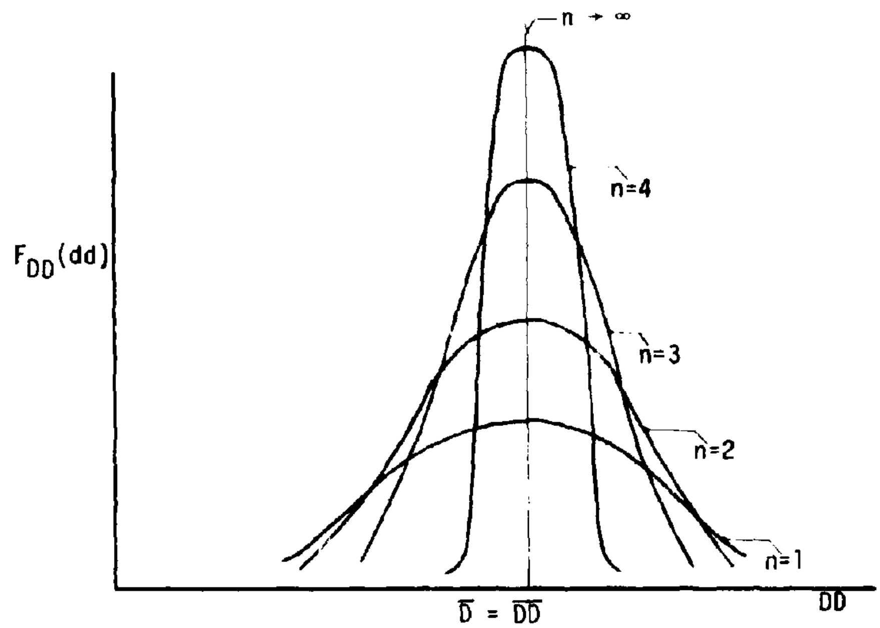

FIGURE 5.5 - DISTRIBUTIONS OF SAMPLE MEAN FOR DIFFERENT SAMPLE SIZES

and where C is the random strength or Capacity. It can be shown [3] that, if C and D are normally distributed and uncorrelated:

$$V_M = \frac{\sigma_M}{m_M} = \frac{\sqrt{\sigma_C^2 + \sigma_D^2}}{m_C - M_D} \tag{5.5}$$

and

$$P_F = F_u\left(-\frac{1}{V_m}\right) = F_u\left(\frac{m_D - m_C}{\sqrt{\sigma_C^2 + \sigma_D^2}}\right) \tag{5.6}$$

where F_u is the cumulative distribution function of the standardized normal variable U.

Given m_D, σ_D then, safety is a function of m_C and σ_C. It is here assumed that V_C is a constant and that m_C is a function of the design load effect (or Design Demand), DD. Specifically, it is assumed that

$$m_C = k * DD \tag{5.7}$$

as illustrated by Figure 5.6.

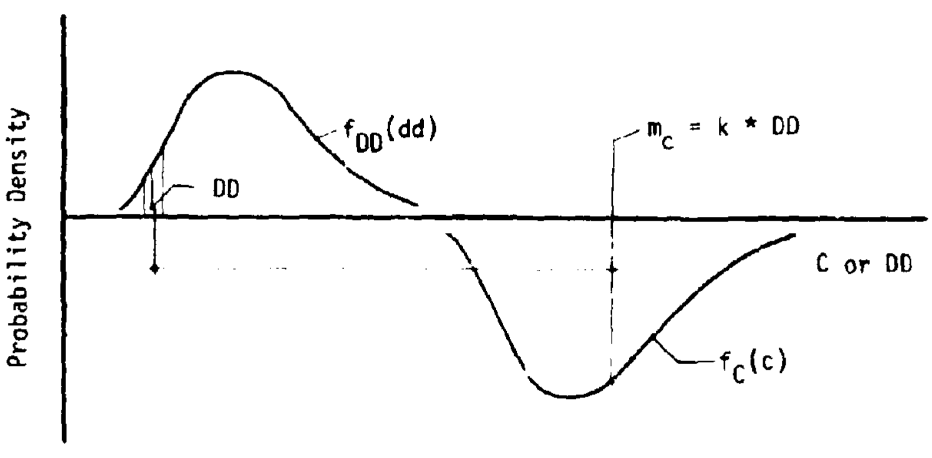

FIGURE 5.6 -STRENGTH DISTRIBUTIONS IN RELATION TO DESIGN LOAD EFFECT

The conditional probability of failure is then:

$$P_{F|DD} = F_u\left(\frac{m_D - k\ DD}{\sqrt{(k*DD*V_c)^2 + \sigma_D^2}} \right) \tag{5.8}$$

and the overall a priori probability of failure can be numerically calculated by

$$P_F = \sum_{\text{All DD}} P[DD] * P_{F|DD} \tag{5.9}$$

As an example, assuming:

$$k = 1.5$$

$$m_D = 10.0$$

$$V_D = 0.15$$

$$V_c = 0.10$$

the overall a priori probabilities of failure may be calculated for several values of n. Figure 5.7 shows the results. It can be noted that with this strategy (and under the assumptions made), even in the limit (as $n \to \infty$), the probability of failure decreases only by a factor of ≈ 5. If $n = 4$ the probability of failure is decreased by a factor of ≈ 3. However, the assumption of a normal distribution for demand may not be realistic.

5.5.2 Strategy: Choose the Maximum of n Computed Load Effects for Design Load Effect

The implications of choosing for design purposes the maximum of a sample of computed load effects may be partially quantified as follows.

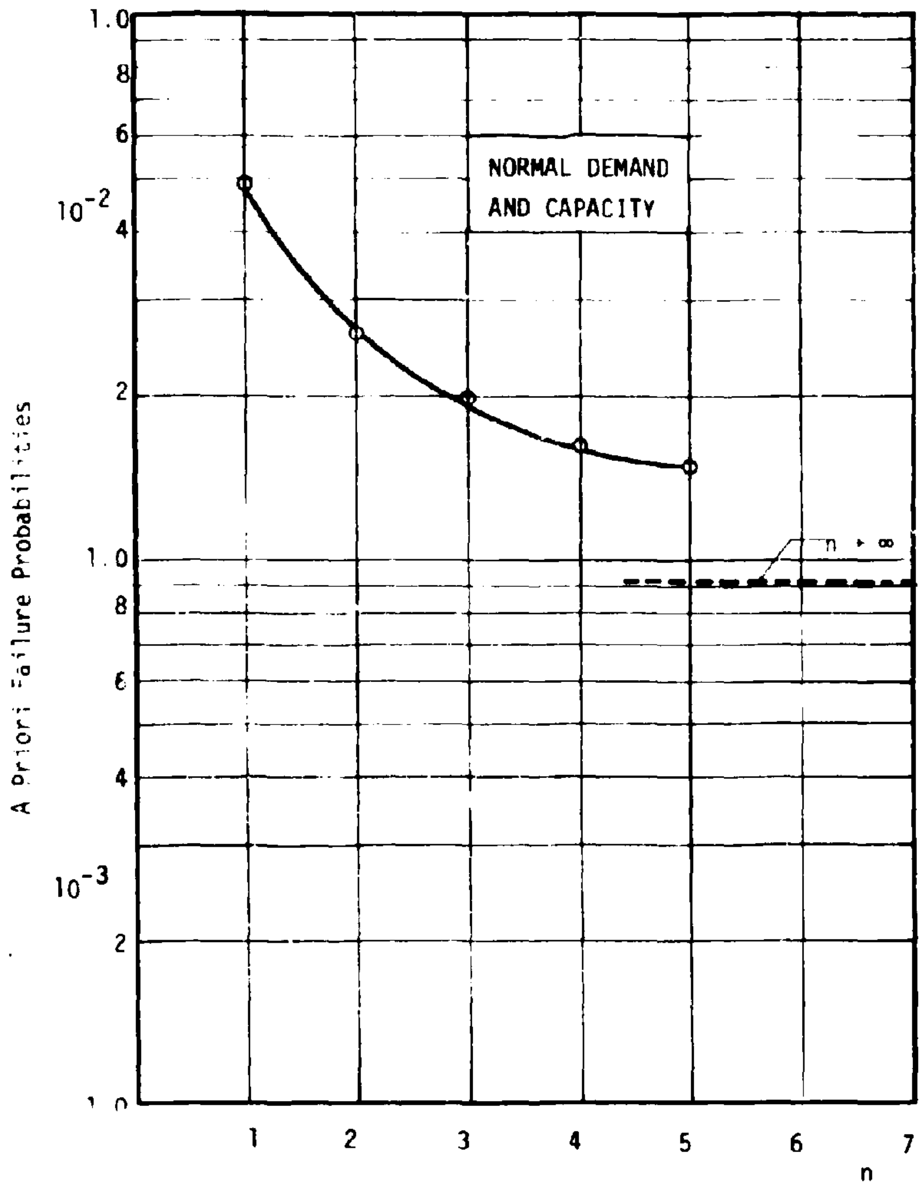

FIGURE 5.7 - VARIATION IN A PRIORI CONDITIONAL FAILURE PROBABILITIES FOR STRATEGY OF USING MEAN OF n LOAD EFFECTS

Letting

$$DD = \max_{i=1}^{n} (D_1, D_2 \ldots . D_n) \tag{5.10}$$

If all the D are independent and identically distributed random variables, then:

$$F_{DD}(dd) = (F_D(dd))^n \tag{5.11}$$

and

$$f_{DD}(dd) = n(F_D(dd))^{n-1} f_D(dd) \tag{5.12}$$

Assuming D is $N(m_D, \sigma_D^2)$, Table 5.6 shows probabilities of choosing load effect values DD in different ranges of the <u>total</u> load effect distribution for several values of n. As an example, if four arbitrary time history analyses are performed and the maximum load effect is chosen for design, the <u>a priori</u> probability is $\approx .5$ (given our assumptions) that a load effect $\geq m+\sigma$ will be chosen for design.

Assuming D is <u>lognormally</u> distributed with $V_D = 0.75$, then Table 5.7 indicates corresponding probabilities of choosing design load effects in several ranges of the D distribution. $V_D = 0.75$ is a value close to those obtained for the interstory distortion responses of the $T_1 = 0.377$ sec. and $T_1 = 1.13$ sec. models in Chapter 2. Assuming the first story relative displacement response of the $T_1 = 1.13$ sec. model (Fig. 2.16) is lognormally distributed with $m_D = 0.63$ and $V_D = 0.75$, Figure 5.8 indicates the variation in the design load effect (DD) distribution with n.

<u>Conditional Failure Probabilities</u>

Assuming both demand D and capacity C are lognormally distributed, it is convenient to let

$$F = C/D \tag{5.13}$$

n	$P[DD > m_D]$	$P[DD > m_D + \sigma_D]$	$P[DD > m_D + 2\sigma_D]$	$P[DD > m_D + 3\sigma_D]$
1	.500	.159	.0228	.00135
2	.750	.292	.0450	.00270
3	.875	.405	.0667	.00404
4	.938	.499	.0880	.00539
5	.969	.579	.109	.00673

TABLE 5.6 - A PRIORI PROBABILITIES OF DESIGNING WITHIN VARIOUS RANGES OF THE TOTAL LOAD EFFECT DISTRIBUTION; NORMALLY DISTRIBUTED DEMAND

n	$P[DD > m_D]$	$P[DD > m_D + \sigma_D]$	$P[DD > m_D + 2\sigma_D]$	$P[DD > m_D + 3\sigma_D]$
1	.369	.121	.044	.0180
2	.602	.227	.0861	.0356
3	.749	.320	.126	.0529
4	.842	.402	.165	.0700
5	.900	.474	.202	.0866

TABLE 5.7 - A PRIORI PROBABILITIES OF DESIGNING WITHIN VARIOUS RANGES OF THE TOTAL LOAD EFFECT DISTRIBUTION; LOGNORMALLY DISTRIBUTED DEMAND; $v_D = 0.75$

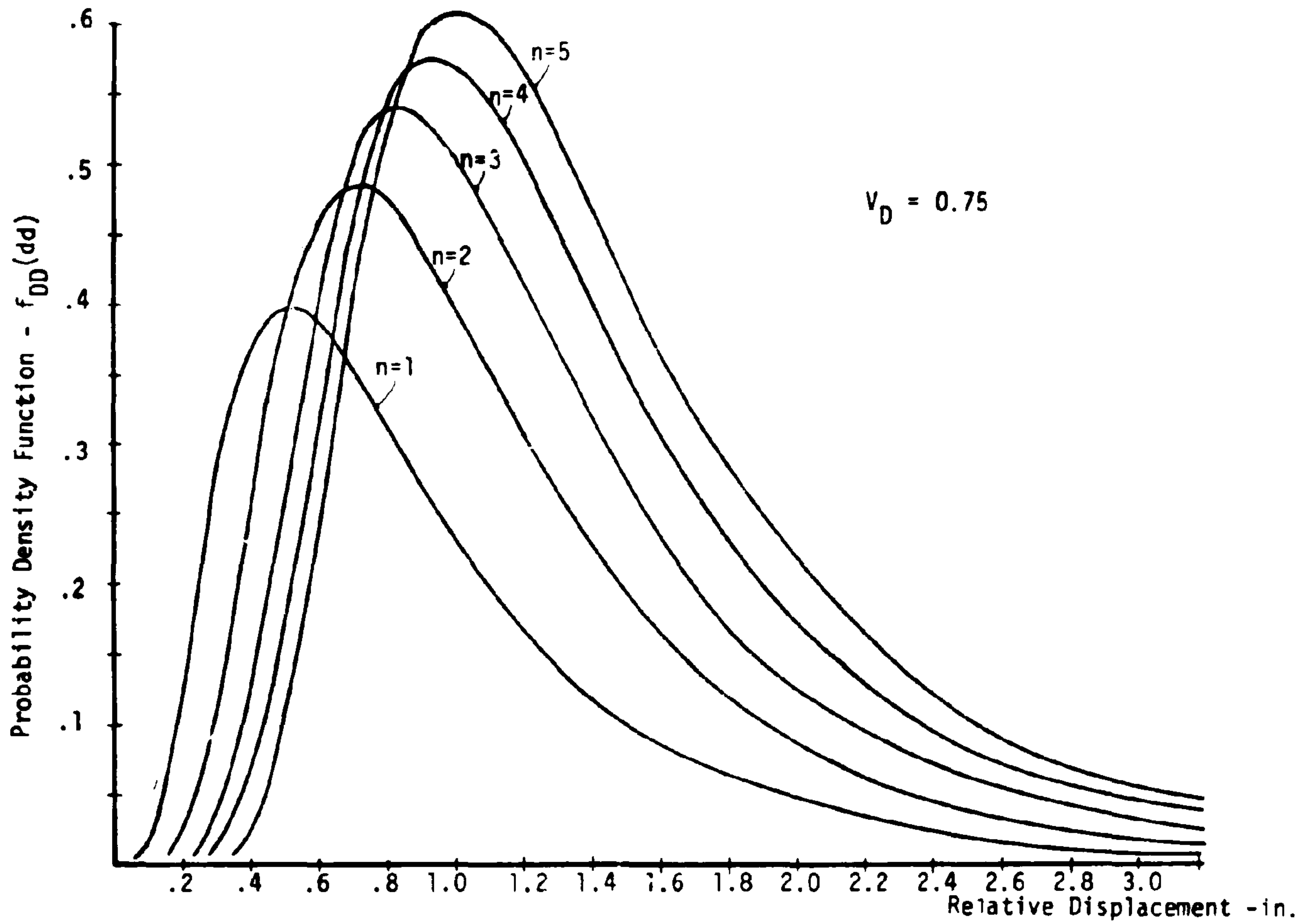

FIGURE 5.8 - VARIATION OF DESIGN LOAD EFFECT DISTRIBUTION WITH n

and then the reliability, R, may be expressed as

$$R = P[F \geq 1] = 1 - P[F < 1] \tag{5.14}$$

Then, since $\ln C$, $\ln D$, and $\ln F$ are normally distributed, the probability of failure is given by:

$$P_F = F_u\left(-\frac{1}{V_{\ln F}}\right) = F_u\left(\frac{m_{\ln D} - m_{\ln C}}{\sqrt{\sigma^2_{\ln C} + \sigma^2_{\ln D}}}\right) \tag{5.15}$$

where F_u is the CDF of the standardized normal variable. Further, since for a lognormally distributed random variable, X:

$$\sigma^2_{\ln X} = \ln(V_X^2 + 1)$$

$$m_{\ln X} = \ln m_X - \frac{1}{2}\sigma^2_{\ln X} = \ln \check{m}_X \tag{5.16}$$

equation (5.15) may be expressed as

$$P_F = F_u\left(\frac{\ln(m_D/m_C) + \frac{1}{2}\ln\left(\frac{V_C^2 + 1}{V_D^2 + 1}\right)}{\sqrt{\ln(V_D^2 + 1)(V_C^2 + 1)}}\right) \tag{5.17}$$

Making the additional assumption

$$m_C = k * DD \tag{5.18}$$

conditional a priori failure probabilities may be estimated using Equations (5.9) and (5.17). As an example, the conditional (on $a_{max} = 0.1$ g) first floor relative displacement load effect (Demand-D) of the T = 1.13 sec. model is assumed to be lognormally distributed with moments as calculated through random vibration analysis (Chapter 2, Figure 2.28.)

i.e., m_D = 0.63 in; V_D = 0.74. Strength is also assumed to be lognormal with V_C = 0.10 (therefore the distribution is very close to normal). Assuming k = 1.5 in Equation (5.18), Table 5.8a shows the variation in the resultant conditional (on a_{max} = 0.10g) a priori failure probabilities of the first floor as a function of n, if the strategy of choosing the maximum load effect of n is followed.

n	P[F|a = 0.1g]
1	.335
2	.185
3	.123
4	.0907
5	.0708

a)

Design Spectrum	P[F|a = .1g]
mean	.32
m+σ	.130
m+2σ	.062
NBK	.044

b)

TABLE 5.8 - COMPARISON OF A PRIORI FAILURE PROBABILITIES FOR VARIOUS DESIGN STRATEGIES

Accepting the above assumptions, conditional failure probabilities obtained through such a strategy may be compared with those obtained for alternate response spectrum designs as tabulated in Table 5.8b (taken from Figure 5.4). The implication is that for the model considered, choosing a maximum load effect out of 3 is a priori (on the average) approximately equivalent, in terms of resultant conditional failure probabilities, to using a m+σ design response spectrum.

5.6 COMPARISON OF METHODS - ARTIFICIAL TIME HISTORIES

The comments herein are based on earthquakes generated by the program SIMQKE [36] which are considered to be representative of current practice. Briefly, such artificial earthquakes are normally based on a $G(\omega)$ and intensity derived from a smooth target S_v; non-stationarity is simulated by a deterministic trapezoidal time envelope of intensity. Resultant spectra match, on the average, the target response spectrum. Random peak accelerations are adjusted to perfectly match the target a_{max}. The COV's of responses calculated through multiple artificial time history analyses may normally be decreased by modifying $G(\omega)$ [36].

Similar strategies to those described for real earthquakes may be followed for artificial earthquakes. Qualitatively, if the strategy is to choose the mean of n_1 artificial time history (ATH) responses, in the limit, as n_1 grows large, the design load effect and the associated probabilities of failure approach those computed for the target response spectrum design. Therefore, it is evident that the conservatism of the target spectrum determines the conservatism of such a procedure. As an example, if the target spectrum is a <u>mean</u> spectrum, and

D_1 = Random Demand Computed from Artificial Earthquakes

then

$$m_{DD} = m_{D_1} = m_D \tag{5.19}$$

$$\sigma^2_{DD} = \frac{\sigma^2_{D_1}}{n_1} = \frac{\sigma^2_D}{n_1(\sigma^2_D/\sigma^2_{D_1})} = \frac{\sigma^2_D}{n_1\,(V_D/V_{D_1})^2} \tag{5.20}$$

Therefore (see also Equation (5.2)) $n_1 = n/(V_D/V_{D_1})^2$ artificial earthquakes decrease the uncertainty in the desired mean load effect to that obtained with n real earthquakes.

Table 5.6, then, entered with $n_1 * (V_D/V_{D_1})^2$ may be used to determine a priori probabilities of choosing a design demand within different ranges of the total load effect distribution. Of course as V_{D_1} is made small (by "smoothing" [36], say) the need for multiple analyses disappears; V_{D_1} approaching zero assures that the match is "perfect" and therefore a mean (or any other target value) response will result.

Analogous arguments may be made for the strategy of choosing the maximum of n arbitrary earthquakes. However, with such a strategy one approaches the reliability associated with a somewhat higher fractile spectrum; <u>the actual fractile achieved is dependent on V_{D_1}</u>. Figure 5.9 shows schematically the use of multiple artificial earthquakes with different strategies.

5.7 COMPARISON OF METHODS - RANDOM VIBRATION

It is clear that an alternative to the prediction of design load effects by RS and TH analyses is to choose design load effects (at appropriate fractiles) from the load effect distribution predicted by random vibration. Figures 5.10 and 5.11 show such distributions conditional on $a_{max} = 0.10g$ for the first story distortion of the two models. Also superposed on the figures are the design load effects computed from the four response spectra discussed herein. It is crucial to recognize that the random vibration distributions were derived considering both the period

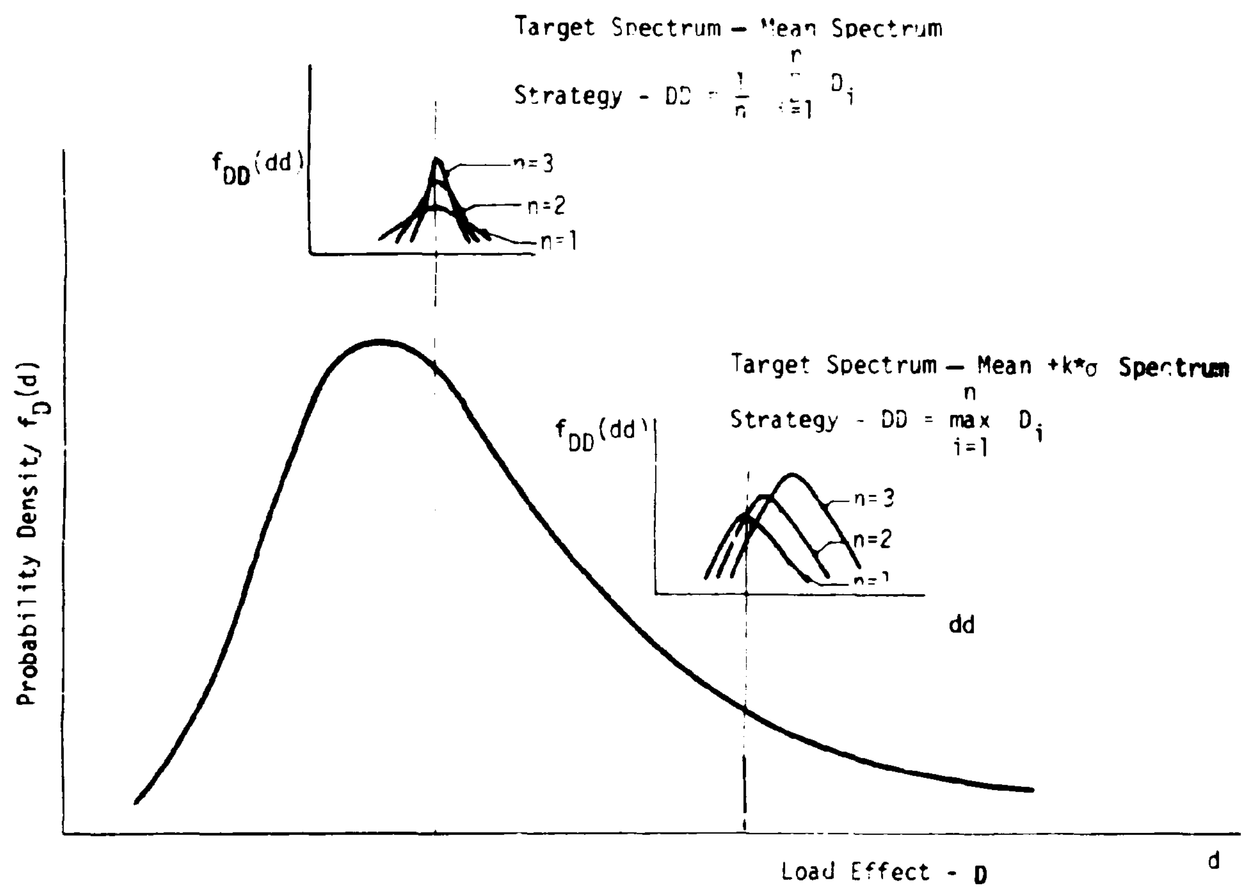

FIGURE 5.9 - VARIATION IN DESIGN LOAD EFFECT DISTRIBUTIONS; ARTIFICIAL TIME HISTORIES

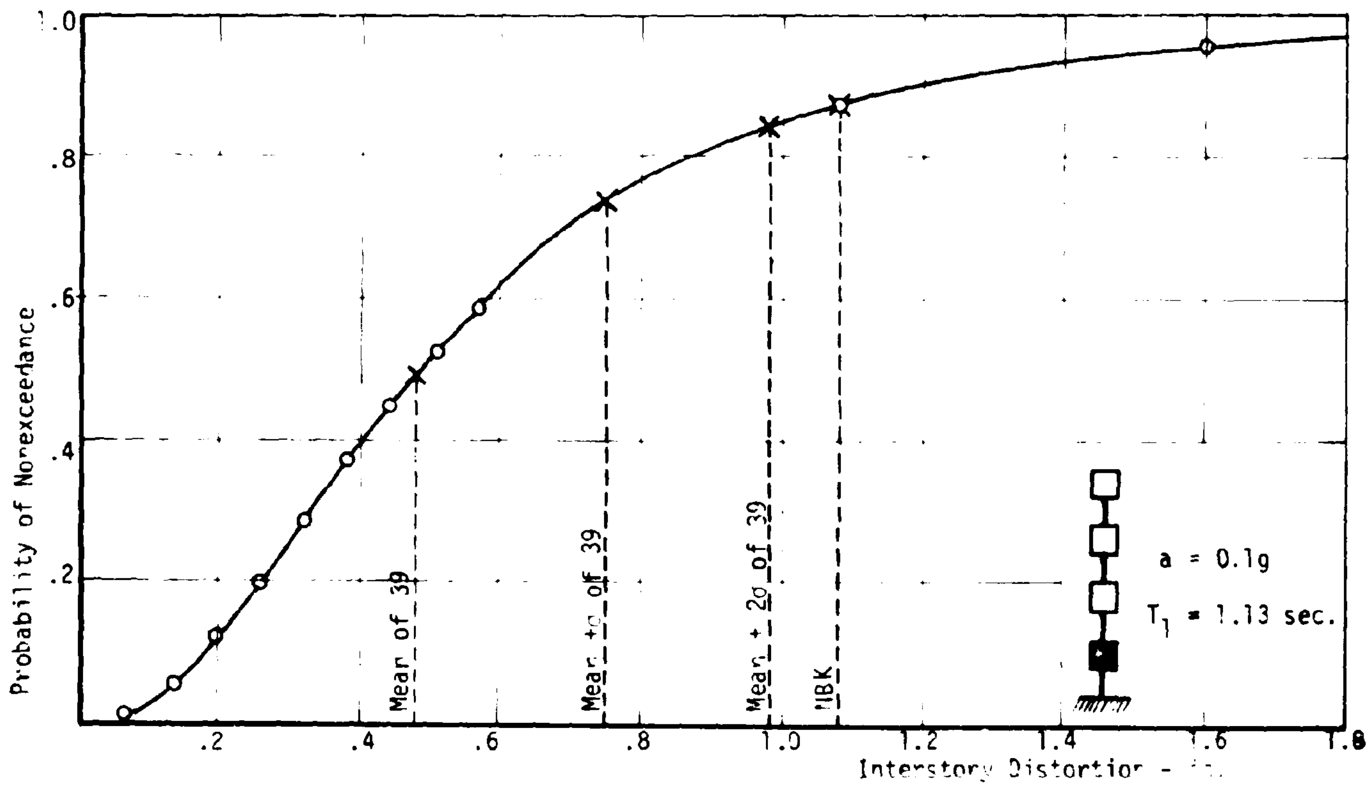

FIGURE 5.10 - DISTRIBUTION OF 1st STORY DISTORTION CONDITIONAL ON a_{max} = 0.1g WITH DESIGN LOAD EFFECTS FROM DIFFERENT STRATEGIES, T_1 = 1.13 sec. Model

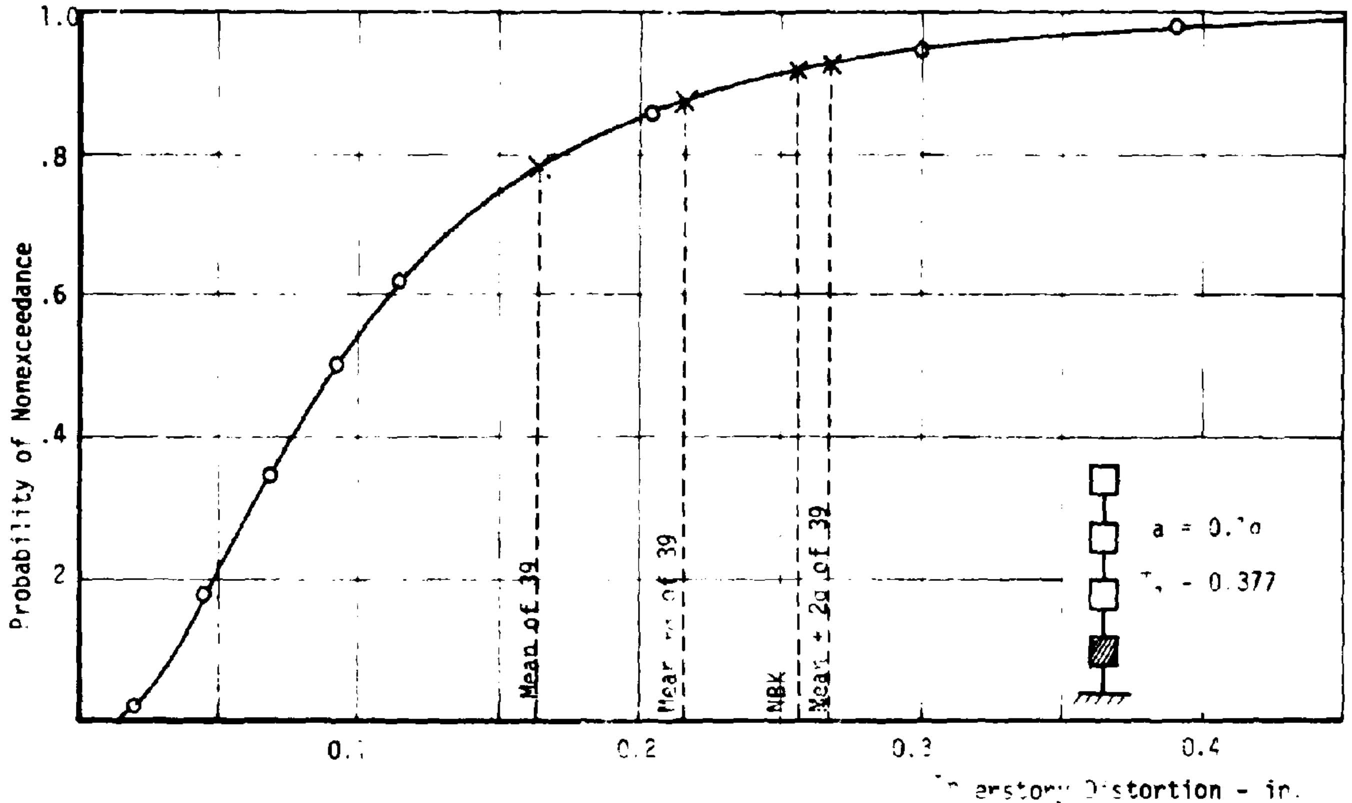

FIGURE 5.11 - DISTRIBUTION OF 1st STORY DISTORTION CONDITIONAL ON a_{max} = 0.1g WITH DESIGN LOAD EFFECTS FROM DIFFERENT STRATEGIES T_1 = 0.377 sec. Model

and damping of the structures as random variables. Hence the load effects computed from the mean response spectrum do not necessarily correspond to the means predicted by random vibration. Indeed, the random vibration distributions include the uncertainty normally accounted for by "broadening the peaks"[78] of spectra or performing time history analyses using multiple models.

It is apparent that the same conservatism in design may be achieved by: 1) specifying a lower design acceleration and choosing a high fractile of the conditional floor response distribution; 2) specifying a high design acceleration and choosing a relatively low fractile of the conditional response distribution or, 3) deriving an unconditional (incorporating the seismic risk curve) response distribution first and then choosing the design load effect corresponding to the absolute floor reliability.

5.8 SUMMARY AND CONCLUSIONS

As has been previously observed [43], reliability implied by the NBK spectrum varies with fundamental period. Analogously, the relative importance of using normalized (to a_{max}) m, m+σ, or m+2σ spectra is also a function of period. For the T_1 = 0.377 sec. model, overall story failure probability estimates vary only by a factor of 4 as the design spectrum is increased from its mean to its mean+σ value. Similar variations of design spectra for the T_1 = 1.13 sec. model cause an order of magnitude change in failure probability estimates.

Varying the design acceleration has, as expected, a relatively period-independent effect on overall failure estimates. In general an order of magnitude change in failure probabilities is noted as $a_{des.}$ is doubled from 0.1g to 0.2g.

The a-priori reliability of a design based on the mean of n load effects approaches the reliability associated with a design based on the exact mean. Assuming normally distributed capacity and demand, approximately 85% of the total possible increase in reliability with such a strategy is achieved with n=4.

Choosing for design the maximum of n arbitrary (TH) load effects is effective in increasing the a-priori conditional reliability of a structure. It was found that for the T_1 = 1.13 sec. structure (assuming lognormally distributed capacity and demand) choosing the maximum of three arbitrary time history load effects resulted in a-priori reliability approximately equal to that of a design based on an $m+\sigma$ spectrum.

Finally, it was noted that design load effects may logically be chosen at appropriate fractiles of load effect distributions predicted by random vibration theory. As such, random vibration theory constitutes a complete alternative to response spectrum or time history techniques.

CONCLUSIONS AND RECOMMENDATIONS FOR FURTHER WORK

CHAPTER 2

Multiple random vibration analyses, an associated first-passage problem solution, and the associated stationary (in frequency content) random-process model for an earthquake, offer a viable alternative for deriving distributions of elastic load effects. For the two models considered herein, such distributions (conditional on a_{max}) match distributions obtained through multiple time-history analyses.

Probabilistic models for the two (random) earthquake parameters, central frequency, ω_g, and strong motion duration, S', must be carefully defined for a site. It is likely that significant statistical uncertainty remains in such probabilistic models.

For purposes of random vibration analyses, the intensity parameter a_{max} is not a satisfactory measure of the strength of an earthquake. Predictive models for intensity measures such as σ_a and $G_a(\omega)$ or $|f_a(\omega)|$ ordinates must be developed.

The sensitivity of conditional load effect distributions to the parameters ω_g, T_0/T_c, ζ_i and S' (and their distributions) is a function of the nominal fundamental period of a structure and the response of interest. The methodology presented herein offers a feasible way to quantify such sensitivity for any particular model of interest.

Statistical correlations among the parameters (ω_g, S', $T_0/T_c/\zeta_i$) as well as correlations of the parameters with earthquake intensity need to be quantified.

CHAPTER 3

Stiffness and strength properties of shear beam models must be examined further. Studies to quantify the uncertainty in strength measures due to uncertain failure mechanisms and to individual members' strength interaction diagrams remain to be performed.

For the simple structure designed (by NRC-like design criteria and for NBK-SSE seismic load levels) in Chapter 3, the ratios of the mean story strengths to the design interstory shears was computed to be between 1.5 and 2.0. The coefficients of variation of the story strength measures, due solely to uncertain member strengths (M_p), were $\simeq$ 0.04. The assumption was made that strengths (M_p) of different members in a story were uncorrelated; hence such a coefficient of variation is not meaningful for reinforced concrete frames. It is likely that the actual coefficient of variation for a story strength measure is considerably larger due to uncertainty in the failure mechanism.

CHAPTER 4

Given the design of a structure by NRC-like seismic design criteria, story failure probabilities given the occurrence of the design intensity were found to be $\simeq$ 2 - 6%. Because of normalization of distributions to a_{max}, such conditional failure probabilities increase as the nominal fundamental period of the structure, T_1, increases.

The coefficient of variation of strength becomes an important parameter when computing conditional failure probabilities due to small intensity levels. Proper evaluation of the mean of the strength measure is crucial in determining conditional failure probabilities for the entire intensity range. Alternate design damping values, $\zeta_{des.}$, in effect imply a shift in the strength distribution in relation to the conditional load effect distribution (assuming that the distribution of actual ζ values remains the same.

Seismic risk input, as expected, has the most significant influence in determining overall story reliabilities. For a structure designed by NRC-like seismic design criteria (for $a_{SSE} = 0.2g$), use of a seismic risk curve for Boston [6] firm ground sites yielded story failure probabilities between 1.0 to 5.0×10^{-6}. If load effects have greater dispersion than resistance measures, modal (or story) safety margins tend to be highly correlated, implying that the system failure probability is close to its lower bound.

Failure estimates derived herein cannot be directly interpreted as indicators of NPP seismic safety. Insofar as inelastic structural behavior implies uncertainty in the performance of critical systems, the failure estimates may be related to the mean rate of accident initiation (by seismic forces) in a specific mode in a NPP.

CHAPTER 5

Given normalization of design spectra to a_{max}, the relative importance (in terms of overall story reliabilities) of using the mean, mean + σ, mean + 2σ or any other response spectra (e.g., NBK) is clearly dependent on T_1. For the $T_1 = 0.377$ sec. structure examined herein, overall failure probabilities decreased by a factor $\simeq 4$ if the mean + σ

rather than the mean spectrum was used for design; for the T_1 = 1.13 sec. structure an order of magnitude decrease was noted. An order of magnitude change in story failure probabilities (for the two models) also results if the design intensity is doubled.

Designing for the mean load effect of n arbitrary real earthquakes is likely not to significantly decrease a priori conditional story failure probabilities from those associated with just using one arbitrary real earthquake. In the limit, as n grows large, one merely approaches the reliability of using the "mean earthquake." Designing for the maximum load effect of n arbitrary real earthquakes is effective in reducing a priori story failure probabilities. For the T_1 = 1.13 sec. structure (assuming lognormal demand and capacity distributions), the a priori reliability of a story designed for the maximum of three arbitrary earthquakes is approximately equivalent to the reliability obtained by using the $m+\sigma$ design response spectrum.

The story reliabilities associated with designing for either the mean or the maximum load effect of n arbitrary artificial earthquakes is primarily a function of the target response spectrum used to generate the motion and the inherent variability of responses from statistically similar earthquakes. The need for multiple artificial time history (ATH) analyses is precluded if: one, the reliability of a design based on the target response spectrum is satisfactory and, two, the motions are sufficiently "smoothed"[36] to provide very close spectral matches.

Of course if the strategy is to choose the maximum load effect of n ATH analyses, the increase in reliability over that associated with the target response spectrum is an inverse function of the variability of responses from statistically similar artificial earthquakes, i.e., it is not reasonable to: one, extensively smooth each artificial earthquake, and two, choose the maximum load effect of n ATH analyses.

Random vibration analyses constitute a complete alternative (for elastic systems) to response spectrum and real or artificial time history analyses. Conservatism may be directly achieved by: 1) choosing a design load effect at a fractile of a response distribution conditional on an intensity, or 2) deriving distributions of responses incorporating seismic risk data and then choosing a design load effect associated with the desired probability of nonexceedance.

LIMITATIONS

Only elastic systems were considered herein. To obtain reliability estimates consistent with UBC-like seismic design criteria, inelastic random vibration procedures must be developed. The methodology described becomes increasingly expensive as the number of discrete combinations of the parameters used in the random vibration analysis increases or as the number of responses for which distribution are required increases.

Finally, additional conservatism inherent in the treatment of design spectra or earthquakes as components has not been quantified herein.

REFERENCES

1. Cramer, H., and Leadbetter, M.R., Stationary and Related Stochastic Processes, Wiley, New York, 1967.

2. Crandall, S.H., Chandiramani, K.L., and Cook, R.G., "Some First Passage Problems in Random Vibration," Journal of Applied Mechanics, Vol. 33; Trans. ASME, Vol. 88, Series E, 1966.

3. Ang, A.H.S., and Cornell, C.A., "Reliability Basis of Structural Safety and Design," Journal of The Structural Division, ASCE, September 1974.

4. Corotis, R., and Vanmarcke, E.H., "First Passage of Nonstationary Random Processes," Journal of the Engineering Mechanics Division, ASCE, April 1972.

5. Bryson, A.E., and Ho, Y-C., Applied Optimal Control, Ginn and Co., Waltham, Massachusetts, 1969.

6. Cornell, C.A., and Merz, A Seismic Risk Analysis of Boston, M.I.T. Dept. of Civil Engineering Research Report R74-2, April 1974.

7. Corotis, R., and Vanmarcke, E.H., "Time-Dependent Spectral Content of System Response," Journal of the Engineering Mechanics Division, ASCE, October, 1975.

8. Berrill, J.B., "A Study of High-Frequency Strong Ground Motions from the San Fernando Earthquake," California Institute of Technology Ph.D. Thesis, March 1975.

9. Committee on Reactor Licensing and Safety, AIF Workshop on Reactor Licensing and Safety, Atomic Industrial Forum, Inc., 475 Park Avenue South, New York, N.Y., 10016, May 1975.

10. Cornell, C.A., "Bounds on the Reliability of Structural Systems," Journal of the Structural Division, ASCE, Vol. 93, No. ST1, February 1971.

11. Biggs, J. M., and Grace, P., Seismic Response of Buildings Designed by Code for Different Earthquake Intensities, M.I.T. Dept. of Civil Engineering Research Report R73-7, January 1973.

12. Aziz, T.S.A., "Inelastic Dynamic Analysis of Building Frames," Sc.D. Thesis, Dept. of Civil Engineering, M.I.T., September 1974.

13. Donovan, N.C., Valera, J.E., and Beresford, P.J., "Statistical Uncertainty of Design Based on Smooth Response Spectra," 1st U.S. National Conference on Earthquake Engineering, Ann Arbor, Michigan, June 1975.

14. CERL, Guidelines for Developing Design Earthquake Response Spectra, Technical Report M-114, June 1975.

15. Benjamin, J.R., and Cornell, C.A., Probability Statistics and Decision for Civil Engineers, McGraw-Hill, 1970.

16. ATC-2, An Evaluation of A Response Spectrum Approach to Seismic Design of Buildings, Applied Technology Council, San Francisco, Calif., September 1974.

17. Donovan, N.C., "Site Response Procedures for Major Buildings," Dames & Moore EE73-1 (ASCE National Structural Engineering Meeting, April 1973).

18. Alpsten, G.A., "Variations in Mechanical and Cross-Sectional Properties of Steel," Planning and Design of Tall Buildings, Vol. 1b, International Conference on Planning and Design of Tall Buildings, Lehigh University, August 1972.

19. Baker, M.J., "Variability in the Strength of Structural Steels--a Study in Structural Safety," Technical Note 44, Construction Industry Research and Information Association, September 1972.

20. ATC-3-04, "Working Draft of Recommended Comprehensive Seismic Design Provisions for Buildings," Applied Technology Council, San Francisco, Calif., January 1976.

21. Dietrich, J.H., "A Deterministic Near Field Source Model," Proceedings of the 5th World Conference on Earthquake Engineering, Rome, Italy, 1973.

22. Blume, J.A., "The Motion and Damping of Buildings Relative to Seismic Response Spectra," Bulletin of the Seismological Society of America, Vol. 60, No. 1, February 1970.

23. Distefano, N., and Pena-Pardo, Bonifacio, "System Identification of Frames Under Seismic Loads," Journal of the Applied Mechanics Division, ASCE, April 1976.

24. Cornell, C.A., "Engineering Seismic Risk Analysis," Bulletin of the Seismological Society of America, Vol. 58, No. 5, October 1968.

25. Cramer, H., and Leadbetter, M.R., Stationary and Related Stochastic Processes, Wiley, New York, 1967.

26. Crandall, S.H., "First Crossing Probabilities of the Linear Oscillator," Journal of Sound and Vibration, Vol. 12, No. (3), 1970.

28. Arnold, P., "The Influence of Site Azimuth and Local Soil Conditions on Earthquake Ground Motion Spectra," thesis presented to the Department of Civil Engineering in partial fulfillment for the requirements for the degree of Civil Engineer, January 1975.

29. Anagnostopoulos, S.A., Nonlinear Dynamic Response and Ductility Requirements of Building Structures Subject to Earthquakes, M.I.T. Department of Civil Engineering Research Report R72-54, September 1972.

30. Hou, S.N., Earthquake Simulation Models and their Application, M.I.T. Department of Civil Engineering Research Report R68-17, May 1968.

31. Esteva, L., and Rosenblueth, E., "Use of Reliability Theory in Building Codes," Proceedings of the First International Conference on Applications of Statistics and Probability to Soil and Structural Engineering, Hong Kong, September 1971.

32. Gazetas, G., "Random Vibration Analysis of Inelastic Multi-Degree-of-Freedom-Systems," Ph.D. thesis, M.I.T. Department of Civil Engineering, August 1976.

33. Ferry-Borges, J., and Castanheta, M., Structural Safety, Laboratorio Nacional de Engenharia Civil, Lisbon, March 1971.

34. Haviland, R., A Study of the Uncertainties in the Fundamental Translational Periods and Damping Values for Real Buildings, M.I.T. Dept. of Civil Engineering Research Report R76-12, February 1976.

35. Hart, G.C., and Hasselman, T.K., "Modal Analysis of Random Structural Systems," Journal of the Engineering Mechanics Division, ASCE, June 1972.

36. Gasparini, D.A., and Vanmarcke, E.H., Simulated Earthquake Motions Compatible with Prescribed Response Spectra, M.I.T. Department of Civil Engineering Research Report R76-4, January 1976.

37. Jennings, P., and Guzman, , "Seismic Design Criteria for Nuclear Power Plants," U.S. National Conference on Earthquake Engineering, Ann Arbor, Michigan, 1975.

38. Liu, S.C., "Evolutionary Power Spectral Density of Strong Motion Earthquakes," Bulletin of Seismological Society of America, Vol. 60, No. 3, 189-900, 1970.

39. Kanai, K., "An Empirical Formula for the Spectrum of Strong Earthquake Motions," Bulletin Earthquake Research Institute, University of Tokyo, Vol. 39, 85-95, Tokyo, Japan, 1961.

40. Luyties, W.H., Anagnostopoulos, S.A., and Biggs, J.M., Studies on the Inelastic Dynamic Analysis and Design of Multi-Story Frames, M.I.T. Department of Civil Engineering Research Report R76-29, July 1976.

41. Roberts, J.B., "The Covariance Response of Linear Systems to Non-stationary Random Excitation," Journal Sound and Vibration, 14 (3), 385-400, 1971.

42. Priestley, M.B., "Power Spectral Analysis of Nonstationary Random Processes," Journal Sound and Vibration, Vol. 6, 1967.

43. McGuire, R.K., "Seismic Structural Response Risk Analysis, Incorporating Peak Response Regressions on Earthquake Magnitude and Distance," Ph.D. Thesis, M.I.T. Department of Civil Engineering, August 1974.

45. Newmark, N., Blume, J., and Kapur, K.K., "Design Response Spectra for Nuclear Power Plants," ASCE Structural Engineering Meeting, San Francisco, Calif., April 1973.

44. Newmark, N.M., "Overview of Seismic Design Margins," AIF Workshop on Reactor Licensing Safety, Vol. 21, No. 1, May 1975.

46. Newmark, N.M., "Probability of Predicted Seismic Damage in Relation to Nuclear Reactor Facility Design," (Draft), September 1975.

47. N.R.C., Reactor Safety Study: An Assessment of Accident Risks in U.S. Commercial Nuclear Power Plants, Main Report, WASH-1400 (NUREG-75/014), October 1975.

48. Piqué, J., "On the Use of Simple Models in Nonlinear Dynamic Analysis," Ph.D. thesis, M.I.T. Department of Civil Engineering, September 1976.

49. Stevenson, J., and Moses, F., "Reliability Analysis of Frame Structures," Journal of the Structural Division, ASCE, Vol. 98, No. ST.11, November 1970.

50. Shinozuka, M., "Safety Against Dynamic Forces," Journal of the Structural Division, ASCE, September, 1974.

51. Stevenson, et al., Structural Analysis and Design of Nuclear Plant Facilities, Editing Board of Task Group of the Committee on Nuclear Structures and Materials of the Structural Division of the ASCE, 1976.

52. Randall, M.J., "The Spectral Theory of Seismic Sources," Bulletin of Seismological Society of America, Vol. 63, No. 3, pp. 1133-1144, June 1973.

53. Roesset, J., APPLE PIE: A Program for Elastic Dynamic Analysis of Structures, M.I.T. Dept. of Civil Engineering.

54. Structural Engineers' Association of California, Recommended Lateral Force Requirements and Commentary, 1974.

55. Sixsmith, E., and Roesset, J., Statistical Properties of Strong Motion Earthquakes, M.I.T. Department of Civil Engineering Research Report R70-7, January 1970.

56. Roesset,J., Private Communication

57. Roesset, J., Whitman, R.V., and Dobry, R., "Modal Analysis for Structures with Foundation Interaction," Journal of the Structural Division, ASCE, March 1973.

58. Rice, S.O., "Mathematical Analysis of Random Noise," Bell System Technical Journal, Vol. 23, 1944; Vol. 24, 1945.

59. Sexsmith, R.G., Reliability Analysis of Concrete Members," ACI Journal, May 1969.

60. Vanmarcke, E.H., "First Passage and Other Failure Criteria in Narrow Band Random Vibration: A Discrete State Approach," Ph.D. thesis, Dept. of Civil Engineering, M.I.T., Cambridge, Massachusetts, February 1970.

61. Vanmarcke, E.H., "On the Distribution of the First Passage Time for Normal Stationary Random Processes," Journal of Applied Mechanics, March, 1975.

62. Veneziano, D., Contributions to Second Moment Reliability Theory, M.I.T. Department of Civil Engineering Research Report R74-33, April, 1974.

63. Vanmarcke, E.H., "Matrix Formulation of Reliability Analysis and Reliability-Based Design," International Journal of Computers and Structures, Vol. 3, No. 4, July 1973.

64. Vanmarcke, E.H., Chapter 8 of Seismic Risk and Engineering Decisions, edited by C. Lomnitz and E. Rosenblueth, Elsevier Publ. (to be published).

65. Veneziano, D., Probabilistic and Statistical Models for Seismic Risk Analysis, M.I.T. Dept. of Civil Engineering,Research Report R75-34 July 1975.

66. Trifunac and Brady, "A Study on the Duration of Strong Earthquake Ground Motions," Bulletin of the Seismological Society of America, June 1975.

67. Veneziano, D., "Statistical Estimation of Prediction in Probabilistic Models, with Application to Structural Reliability," Ph.D. thesis, Dept. of Civil Engineering, M.I.T., Cambridge, Mass., September 1974.

68. Trifunac, M.D., "Analysis of Strong Earthquake Ground Motion for Prediction of Response Spectra," Earthquake Engineering and Structural Dynamics, Vol. 2, July-Sept., 1973.

69. Uniform Building Code, 1976 ed., International Conference of Building Officials, Pasadena, California, 1976.

70. Veneziano, D., "Probabilistic Response Spectra for Nonstationary White Noise," Unpublished Draft of proposed paper, M.I.T. Department of Civil Engineering, Cambridge, Massachusetts.

71. Trifunac, M.D., and Brady, A.G., "A Study on the Distribution of Strong Earthquake Ground Motion," Bulletin of the Seismological Society of America, Vol. 65, No. 3, June 1975.

72. Vanmarcke, E.H., Biggs, J.M., et al., Comparison of Seismic Analysis Procedures for Elastic Multi-Degree-of-Freedom Systems, M.I.T. Department of Civil Engineering Research Report R76-5, January 1976.

73. Vanmarcke, E.H., and Cornell, C.A., "Seismic Risk and Design Response Spectra," Specialty Conference on Safety and Reliability of Metal Structures, Pittsburgh, Pa., November 1972.

74. Vanmarcke, E.H., "Properties of Spectral Moments with Applications to Random Vibration," Journal of the Engineering Mechanics Division, ASCE, April 1972.

75. Yao, J.T.P., "Formulation of Structural Reliability," Journal of the Structural Division, ASCE, December 1969.

76. Tang, J.P., and Yao, J.T.P., Probability of Fatigue Failure under Earthquake Loads, University of New Mexico Bureau of Engineering Research.

77. Yao, J.T.P., "Fatigue Reliability and Design," Journal of the Structural Division, ASCE, September 1974.

78. Zar, M., Evaluation of Seismic Design of Nuclear Power Plants, AIF Workshop on Reactor Licensing and Safety Program Report, Vol. 2, No. 1, May 1975.

79. Shibata, A., Sozen, M.A., The Substitute Structure Method for Earthquake-Resistant Design of Reinforced Concrete Frames, University of Illinois, Urbana, ENG. 74-2027.

80. Jacobs, O.L.R., Introduction to Control Theory, Clarendon Press, Oxford, 1974.

81. ACI-ASME Joint Technical Committee, Code for Concrete Reactor Vessels and Containments, ASME Boiler and Pressure Vessel Code Section III - Division 2 and ACI Standard 359-74, 1975.

82. Hammond, J.K., "On the Response of Single and Multi-degree-of Freedom System to Non-Stationary Random Excitation," Journal Sound and Vibration 7(3), 393-416, 1968.

83. Veneziano, D., Unpublished Course Notes for 1.184, Applied Random Processes, M.I.T., Cambridge, Massachusetts 1975.

84. Penzien, J., and Liu, S.C., "Nondeterministic Analysis of Nonlinear Structures Subjected to Earthquake Excitations," Proceedings of the 4th World Conference on Earthquake Engineering, Santiago, Chile, 1969.